November 2014

Development of a Support Structure for Multi-Rotor Wind Turbines

Gaurav Murlidhar Mate
University of Massachusetts Amherst

Development of a Support Structure for Multi-Rotor Wind Turbines

A Thesis Presented

by

GAURAV MATE

Submitted to the Graduate School of the
University of Massachusetts Amherst in partial fulfillment
of the requirements for the degree of

MASTER OF SCIENCE IN MECHANICAL ENGINEERING

September 2014

Mechanical and Industrial Engineering

Development of a Support Structure for Multi-Rotor Wind Turbines

A Thesis Presented

by

GAURAV MATE

Approved as to style and content by:

Matthew A. Lackner, Co-chair

James F. Manwell, Co-chair

Sergio F. Breña, Member

Donald L. Fisher, Department Head

Department of Mechanical and Industrial Engineering

ACKNOWLEDGEMENTS

First and foremost, I take this opportunity to thank Dr. Matthew A. Lackner for his motivation and support. I also thank him for being my mentor during my graduate studies at the University of Massachusetts Amherst. I would also like to express my sincere gratitude to Dr. James F. Manwell for his guidance and support. This thesis would not have been possible without their insightful expertise in Wind Energy. My special thanks to Dr. Sergio F. Breña for his valuable advice on Structural Analysis.

This work has been supported by the Armstrong Fund for Science grant awarded for encouraging transformative research conducted at University of Massachusetts Amherst. Therefore, I would like to express my deepest gratitude to the benefactors Dr. John Armstrong and Dr. Elizabeth Armstrong for this grant.

I dedicate this thesis to my late father Mr. Murlidhar V. Mate and my late mother Mrs. Madhavi Mate, whose blessings have helped me to achieve success in my life. I also thank my elder sisters Madhura and Mugdha for their moral support and my deepest thanks to my brother-in-law Santosh who has encouraged me to attain my goals throughout my graduate studies. I would also like to express my heartfelt thanks to my friends and lab mates.

I am also grateful to all the professors who inspired interest in the courses I chose and made it a unique learning experience for me during my Masters at the University of Massachusetts Amherst.

ABSTRACT

DEVELOPMENT OF A SUPPORT STRUCTURE FOR MULTI-ROTOR WIND TURBINES

SEPTEMBER 2014

GAURAV MATE

B.S.M.E., COLLEGE OF ENGINEERING PUNE, INDIA

M.S.M.E., UNIVERSITY OF MASSACHUSETTS AMHERST

Directed by: Professor Matthew A. Lackner and Professor James F. Manwell

The earliest design of a wind power system with multiple rotors on a single support structure dates back to the late 1800s. Such a system called a Multi-Rotor Wind Turbine (MRWT) was proposed by several researchers due to its perceived advantages over a single-rotor wind turbine. As turbine size increases, power produced by a rotor tends to scale up as the square of its diameter, as opposed to rotor weight which varies as its cube. So, several smaller rotors will weigh and cost less than one large rotor producing the same power. MRWTs offer several advantages such as better distribution of loads, better logistics of the components and scope for standardization. The MRWT system can also continue operation even if some of the rotors fail. However, MRWTs require a complex support structure to connect the rotors to the tower and an arrangement to yaw them into the wind. A recent study involving a scaling model for a three-rotor MRWT system estimates a cost saving of 13.1% as compared to the NREL 5 MW single-rotor model. A triangular truss type support structure for the MRWT model is designed and its preliminary static analysis is performed in that study. This thesis is a continuation of that study where the scaling model is extended to include MRWT systems

having two to seven rotors. A systematic design method is developed for modeling any MRWT support structure for two to seven rotors for the given 5 MW configuration. The structure consists of frames and cables and the design constraints for the static analysis are stress, deflection and buckling. A dynamic analysis of the MRWT solution is also carried out to verify that the structure can withstand loads induced at varying wind conditions and design load cases – especially steady, turbulent and extreme wind conditions. Some special cases for the three-rotor MRWT system, such as use of two-bladed rotors, direct-drive machines, analysis for zero wind loads, load analysis for each of the assembly stages are also discussed. Finally, as the support structure design for the three and seven-rotor models is the main focus of the thesis, the scaling model is validated by comparing these models with similar turbines having rated power corresponding to the rotors used in the models.

TABLE OF CONTENTS

Page

LIST OF TABLES

Table Page

LIST OF FIGURES

Figure Page

CHAPTER 1

INTRODUCTION

Wind power is emerging as a promising alternative to conventional energy sources. Wind energy is abundant, renewable and pollution-free. There has been a considerable worldwide awareness about environmental concerns such as fossil fuel depletion as well as climate change. Wind energy is one such source of renewable energy that provides a solution.

As of 2011, the global wind power production totaled 459.9 TWh [1] while the installed capacity stood at 238 GW [2]. The U.S. leads global wind power production at 120 TWh while having the second largest wind power installed capacity at 46.9 GW. In order to boost the global installed capacity, wind turbines with high rated power have been developed. Currently, the Enercon E-126 [3] is the largest wind turbine with a capacity of 7.5 MW while the 20 MW UpWind project [4] funded by the EU is in the conceptual design stage.

With the increase in the size of wind turbines, it is important to consider the limitations of the current designs. The fundamental assumptions of these designs may not be valid for very large wind turbines. So, it may be necessary to develop new architectures and to consider the advantages offered over the current approaches.

This thesis investigates one such concept that involves multiple rotors supported by a single tower. A background of the Multi-rotor concept as proposed by several researchers is provided. Next, a detailed design and analysis of two Multi-rotor concepts is conducted, and the resulting designs are compared to a baseline conventional single rotor design. The

concepts are analyzed in terms of the total system mass and cost. Some special cases for one concept are also discussed to determine whether the system can be made more cost-effective and efficient. Finally, a dynamic analysis of that concept is performed in this thesis at various wind conditions.

1.1. Basics of Wind Turbines

Wind turbines convert the kinetic energy of the flowing wind into electrical energy. Wind turbine blades are made of airfoil sections [5] which produce the aerodynamic lift forces that generate torque and therefore mechanical power, which is further converted to electric power in a generator.

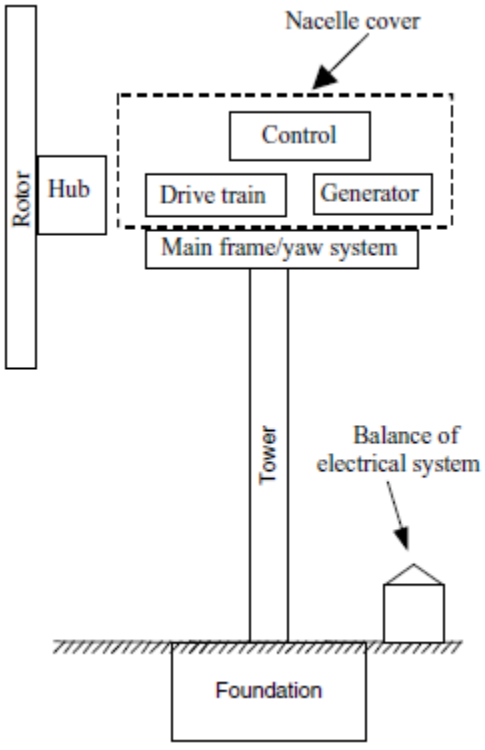

Figure 1. Major Components of a HAWT [5]

The most common type – Horizontal Axis Wind Turbines (HAWTs) [5] – consist of the rotor rotation about a horizontal axis parallel to the ground, usually with two or mostly three rotor

blades attached to the hub. The rotor-nacelle assembly (RNA) consists of a rotor, hub, drive train, generator and a controller as shown in Figure 1. The tower, foundation and electrical system are the other major components. The yaw system allows the RNA to rotate about the tower axis into the wind direction for maximizing the power output.

The rotor of a HAWT may be facing the wind on the windward side of the tower or it may be placed on the downwind side. Depending on this rotor orientation, HAWTs are either upwind or downwind [5]. Some downwind turbines have had free yaw, but almost all modern turbines have controlled yaw. For downwind turbines, the tower shadow has an effect on the dynamics, causing power fluctuations and noise and so, these turbines are less common.

The simplest model used to quantify the interaction between the rotor and the wind [5] is the one-dimensional momentum theory. The rotor of radius R can be considered as an actuator disc enclosed in a control volume. The power P produced by the rotor at rated wind speed U and air density ρ is given by Eq. (1.1).

$$P = \frac{1}{2}\rho C_p \pi R^2 U^3 \tag{1.1}$$

The power coefficient C_p is a measure of the rotor performance and its theoretical value cannot exceed 0.593 which is called the Betz limit. Practically it is even less than this value primarily due to non-linear aerodynamic effects like wake rotation and drag.

Power produced at varying wind speeds follows a power curve. The cut-in wind speed is the lowest speed at which power production begins. Rated power is produced at rated wind speed while the turbine does not produce power above the cut-out wind speed due to safety and design factors.

Wind turbines are classified as land-based or onshore turbines and offshore turbines. Originally, all wind turbines were land-based. The offshore concept is relatively new and as the name implies, these turbines are installed off the coast. Offshore turbines [5] vary in terms of the method used to support the tower, design factors, electrical connections and environmental issues. These turbines benefit from the availability of steady and generally high wind speed, but face several challenges like high installation costs, difficulties in maintenance and corrosive environmental conditions.

1.2. Scaling Relations

Scaling relations are formulae used to estimate the design parameters of a wind turbine of a particular size, subject to certain assumptions. 'Upscaling' refers to the process of designing a large wind turbine based on a smaller turbine. The exact opposite is 'downscaling'. The assumptions for scaling are as follows.

1. The tip speed ratio i.e. the ratio of the blade tip speed to the free stream wind speed is constant.
2. The number of blades, airfoils and blade material are the same.
3. Geometric similarity is maintained to the extent possible.

The most important scaling relations considered for this thesis are those of the rotor power and the rotor weight [5]. Power, P_i, generated by the rotor varies as the square of its radius R_i while rotor weight W_i varies as the cube of R_i. So, the square-cube law is given by Eq. (1.2) and Eq. (1.3).

$$P_1/P_2 = (R_1/R_2)^2 \tag{1.2}$$

$$W_1/W_2 = (R_1/R_2)^3 \tag{1.3}$$

There are several other scaling equations that relate other parameters like forces, moments, stresses and natural frequencies. These relations are the theoretical or 'Simple' scaling relations as they do not consider other non-linear effects like wind shear and boundary layer effects related to the blades [10].

Data from actual wind turbines do not follow these simple scaling relations and so, several empirical models have been proposed based on observed trends. The empirical relations used for this research are the 'Advanced' and the 'Baseline' scaling relations, and these are discussed later in section 2.4.

1.3. Limitations of Upscaling

According to the square-cube law, as wind turbines continue to be upscaled, the weight of the rotor and other components increases faster than the power produced for a given wind turbine design. So, at some point, increasing the turbine size becomes uneconomical. The 20 MW wind turbine of the UpWind project has been upscaled [4] from the NREL 5 MW baseline turbine, but with certain design modifications. The airfoils are changed so that they are suitable for high Reynolds' number and stronger materials have been proposed. Upscaling in the multi-megawatt range also has several disadvantages [12] as discussed below.

1. Large turbines have large blades and components leading to difficulty and high cost involved in their manufacturing, logistics and assembly.
2. For upwind turbines, longer blades have a higher deflection and may cause blade collision with the tower.
3. Longer blades experience a greater difference in wind loading due to wind shear, which increases the chances of fatigue failure.

4. Rotor blades are commonly made of composites. There is a high statistical probability of material defects for large blades and the defects may propagate and cause failure.

1.4. NREL 5 MW Baseline Turbine

The 5 MW Baseline Wind Turbine model developed by NREL [7] for research is used as a benchmark for this thesis. It is a three-bladed, upwind, variable-speed, variable blade-pitch-to-feather-controlled turbine having a high speed multi-stage gearbox. It is chosen as the benchmark as it represents most of the current utility-scale turbines and has detailed design information available. The basic specifications of the NREL 5 MW baseline turbine are given in Table 1.

Table 1. NREL 5 MW baseline turbine – Basic configuration [7]

Turbine Configuration	5 MW, Upwind, 3-bladed turbine
Control	Variable-speed, Collective Pitch
Drivetrain	High speed, Multi-stage Gearbox
Rotor, Hub Radius	63 m, 1.5 m
Hub Height	90 m
Cut-in, Rated, Cut-out wind speed	3 m/s, 11.4 m/s, 25 m/s
Cut-in, Rated RPM	6.9 rpm, 12.1 rpm

1.5. Multi-Rotor Wind Turbines

One approach to overcome the drawbacks of upscaling is to develop Multi-Rotor Wind Turbines (MRWTs). As the name suggests, these are wind power systems with multiple rotors on a single support structure. The advantages and design challenges faced by MRWTs are given below.

1.5.1. Advantages

1. MRWTs take advantage of the square-cube law. As a large rotor is downscaled to several small rotors producing the same total power, the weight of the components reduces. This fact is explained mathematically by Jamieson et al. [10] and it is shown

that the smaller rotors are $1/\sqrt{n}$ times lighter than the large rotor, where n is the number of smaller rotors, and so, they are likely less expensive.

2. The loads acting on a MRWT are better distributed than the loads that are concentrated at a point for a single large rotor. According to the square-cube law, some total loads on a MRWT – the total rotor torque, total rotor weight and the total nacelle weight - are also reduced. This is assuming simple scaling, which is discussed later in the thesis.
3. When one or more rotors fail, the other rotors of a MRWT system may continue to produce power. In such cases, a symmetrical set of rotors may be turned off to prevent unbalanced forces acting on the structure until the failed rotors are restored.
4. If the rotors in a MRWT are of the same rating, their cost can be reduced substantially by standardization [10] and mass production.
5. As smaller blades are used in MRWTs, their transportation and assembly is easier.
6. Reliability, which is a function of turbine size [13], is improved in the case of MRWTs as these systems use smaller rotors. This reliability is associated with the probability of defects as a smaller blade size would mean less chance of defects in the components.

1.5.2. Limitations

1. MRWTs need a complex support structure to join the rotors to the tower.
2. An entirely different yaw system consisting of one or more yaw bearings is required to orient the rotors into the wind.
3. The support structure causes the structural dynamic response of the system to be even more complex.

4. The fact that MRWT systems have a higher number of total components than a single-rotor turbine could increase the possibility of failure.

1.6. Objective and Scope of Thesis

This thesis is a continuation of the work by Verma [32], which examines the feasibility of the MRWT concept by first developing a scaling model, followed by a preliminary design of a support structure for a three-rotor MRWT model. Therefore, the key objectives of this thesis are to extend the scaling model for two to seven-rotor MRWT systems, to develop support structures for three-rotor and seven-rotor models, and to perform dynamic analysis for the three-rotor model. The specific objectives are as given below.

1. To modify the scaling model such that it can estimate the total mass and total cost of a MRWT system having two to seven rotors.
2. To calculate cost/mass ratios, for the individual components in the scaling model based on the NREL 5 MW baseline turbine, which determine the component costs based on the mass values already calculated from the scaling model, for any MRWT configuration and for different numbers of rotors using simple, baseline and advanced scaling relations.
3. To develop a support structure for a three-rotor 5 MW MRWT with a novel method different from the one implemented by Verma [32], such that the design steps can also be used to develop a support structure for a seven-rotor 5 MW MRWT. These two support structures consider different configurations and make use of cables in addition to steel frames.
4. To determine whether each of the above two designed structures satisfy the basic structural requirements of stress, deflection and buckling as well as to reduce the total

mass and total cost to the extent possible, such that these two quantities are less than those of a single-rotor 5 MW system. In other words, determining whether the MRWT structures are economically viable.

5. To present a yaw system that will orient the multiple rotors into the wind.
6. To analyze the dynamic performance of the three-rotor MRWT structure at varying wind conditions such as steady, turbulent and extreme conditions and to evaluate the resonant frequencies that should be avoided by the system.
7. To validate the scaling model by comparing each of the individual rotors – the 1.67 MW for the three-rotor model and the 0.71 MW for the seven-rotor model, with two turbines of similar power rating – the WindPACT 1.5 MW turbine (a conceptual turbine) and the Vestas V47 0.66 MW (an actual turbine).
8. To discuss some special cases for the three-rotor MRWT system, such as the use of two-bladed rotors, direct-drive machines, analysis for zero wind loads and load analysis for each of the assembly stages.

CHAPTER 2

LITERATURE REVIEW

The idea of MRWTs [15] emerged because manufacturing very large rotor blades made of steel was not feasible. With time, materials with high strength-to-weight ratio like fiber reinforced polymer were developed and the multi-rotor concept was considered too complex and unnecessary.

2.1. History of MRWTs

An extensive review of literature on the previous MRWT design propositions has already been done by Verma [32]. A brief summary of the same follows here. For more specific details, one should refer to the document [32].

The earliest design of Multi-rotor systems dates back to 1873 in Denmark [34] where Danish twin mills, as shown in Figure 2, were being used for containment and drying projects.

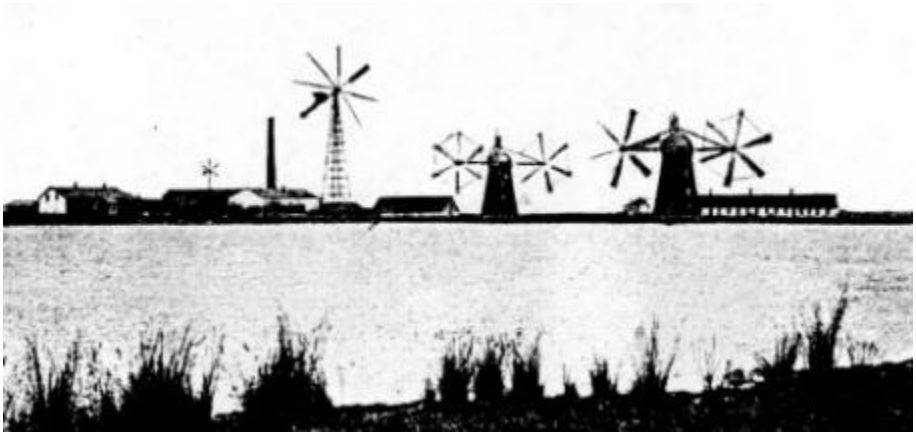

Figure 2. Danish twin-mills, 1873 [34]

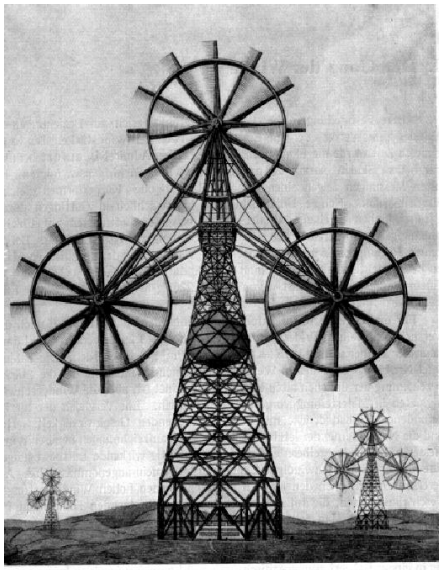

Abb. 1. Ansicht des normalen Einheitswindkraftwerkes

Figure 3. Multi-rotor concept by Hermann Honnef (1930) [15]

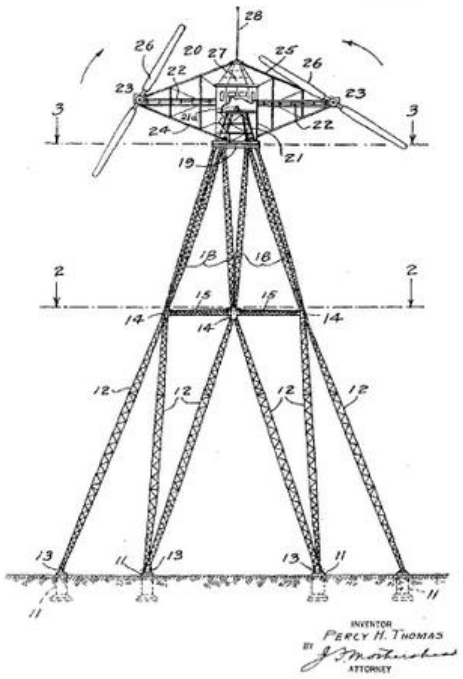

Figure 4. The Aerogenerator Tower [17]

In 1930, German engineer Hermann Honnef proposed a multi-rotor concept that involved a 430 m high tower with three contra-rotating rotors intended to generate 20 MW as shown in Figure 3.

The Aerogenerator Tower model proposed in 1950 by Percy Thomas [17] was the next multi-rotor model consisting of hingedly mounted elements as shown in Figure 4.

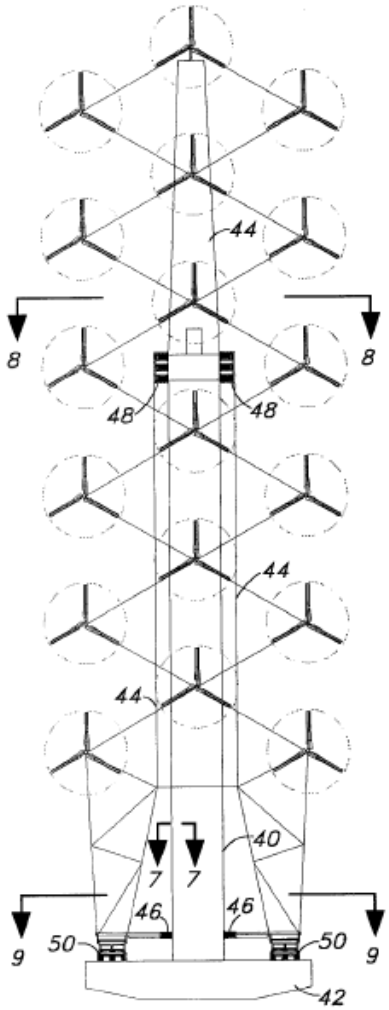

Figure 5. 18-rotor array by Heronemus [12]

In the 1970s, Capt. William Heronemus proposed several configurations of multi-rotor arrays [12]. In most of them, each rotor was designed for the wind speed it faced at its height to

extract maximum energy out of the wind. Also, for a multi-rotor array of 18 rotors shown in Figure 5, the entire structure including the tower would rotate about a bearing mounted at the base. Pneumatic tires riding on a yaw track would be attached to that yaw bearing to support such a large load. There would be additional yaw bearings at the mid portion of the tower to support the yaw motion and the loads on top.

In the Netherlands, in the 1980s, Henk Lagerweij of Lagerwey Wind built the Sixmaster [19], the Quadro [20] and the Twinmaster [21] which had 6, 4 and 2 rotors respectively on a single tower as shown in Figure 6. Each rotor had a rating of 75 kW and later faced vibration or control system issues due to which they were brought down.

Figure 6. (Left to right) Twinmaster [21], Quadro [20] and Sixmaster [19] built by Lagerwey Wind

Most MRWTs proposed in the past have not been implemented in practice. MRWT designs either involved co-planar or co-axial rotors and this thesis focuses only on the co-planar designs of HAWTs.

2.2. Effect of Rotor Interaction in MRWTs

Wind tunnel tests have been conducted by some researchers to determine whether the interaction between rotors affected the overall performance. A brief description of some tests conducted is given below.

1. Smulders et al. [8] showed through wind tunnel tests that the performance of a two-rotor system is improved if the spacing between them is small – about 2.5% of the rotor diameter. This was attributed to the vortex wake interactions. The rotor diameter was 20 cm and so the results were yet to be validated for larger arrays of rotors.

2. Another study was conducted by the Southwest Research Institute (SwRI) [9] in the NASA Langley Full scale Wind Tunnel (LFST) on a seven-rotor array to determine the effect on the aerodynamic performance of these rotors when situated close to each other. These tests were conducted on larger size rotors each having a diameter of 43 inches, and the rotor spacing was varied from 2% to 16%. These tests also maintained the fact that there is no negative effect on the power produced by the rotor array.

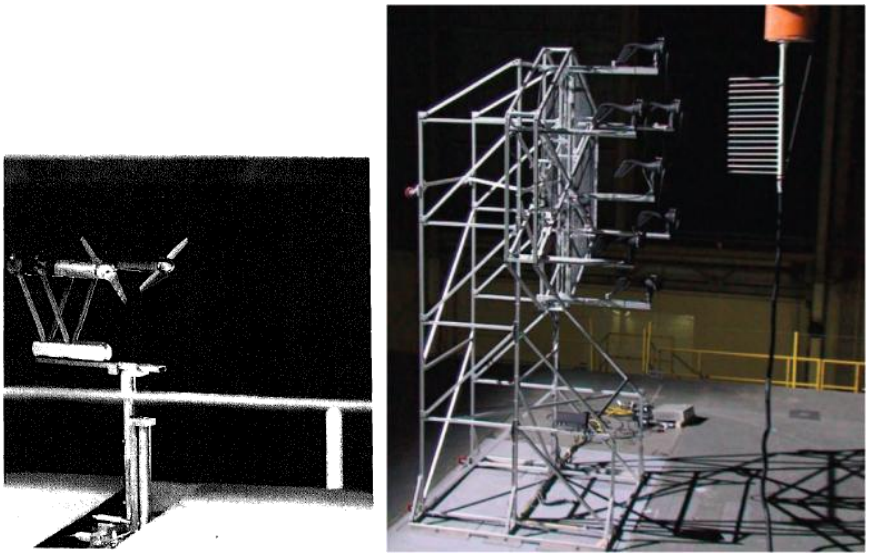

Figure 7. Wind Tunnel Tests (left) Smulders et al.[8], (right) Technology Today 2009 [9]

2.3. Recent Work by Jamieson

The main advantage of MRWTs is related to the square-cube law between the rotor power and the rotor weight. Jamieson et al. [10] introduced a mathematical derivation relating the rotor mass of a MRWT with the rotor mass of an equivalent single-rotor turbine having the same swept area. Also, a 20 MW wind turbine was compared with two MRWT configurations: a 4-rotor x 5MW MRWT structure and a 45-rotor x 444kW MRWT structure.

2.3.1. Mathematical Formulation

For a large rotor with diameter *D* and mass *M* having the same swept area as *n* smaller rotors of diameter *d* and mass *m*, Eq. (2.1) is obtained.

$$D^2 = nd^2 \tag{2.1}$$

As the power produced is proportional to the swept area, both configurations produce the same power. The rotor masses vary as the volume and hence are proportional to the third power of their respective diameters.

$$\frac{m}{M} = \frac{d^3}{D^3} \tag{2.2}$$

So, the ratio of the mass of the *n* rotors to that of the large rotor is given by Eq. (2.3).

$$\frac{nm}{M} = n\left(\frac{d}{D}\right)^3 = \frac{1}{\sqrt{n}} \tag{2.3}$$

Therefore, the smaller rotors would be $1/\sqrt{n}$ times lighter than the large rotor and thus less expensive. In practice, this weight deficit might be slightly different as ‘simple’ scaling is not followed by actual turbines as discussed before.

2.3.2. Support Structure Considerations

In the recent paper by Jamieson et al. [10], a 20 MW wind turbine was compared with two MRWT configurations: a 4-rotor x 5MW case and a 45-rotor x 444kW case. A lifetime cost analysis has been performed. It was estimated that the cost of the 4-rotor model is 20% less and the 45-rotor model is 30% less as compared to the single rotor 20 MW model.

A space frame design was suggested for the support structure joining the 45 rotors with two yaw bearings. The cost of the supplementary yaw bearing was simply assumed as equal to that of the first yaw bearing. The cost of the tower and support structure for the MRWT was assumed as twice the cost of the single-rotor tower. There has been no detailed analysis to find the mass and cost of the support structure.

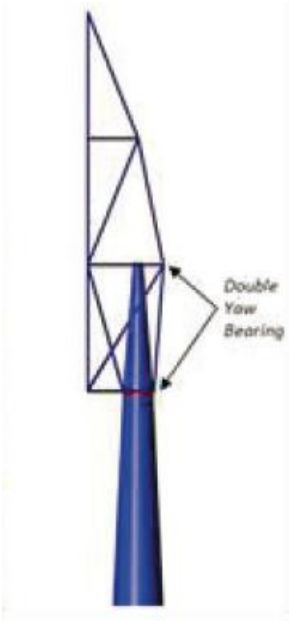

Figure 8. Double yaw bearing suggested in [10]

2.4. Recent Work by Verma

As discussed before, this thesis is a continuation of the work by Verma [32] and therefore, a short summary is provided here. Again, it is encouraged to refer to that work for more details. The work discusses the economic feasibility of the three-rotor MRWT through the scaling model and the structural feasibility by means of the support structure design.

2.4.1. Scaling Model

As previously stated, scaling relations estimate the design parameters for a given wind turbine in terms of the rotor dimensions. Scaling is required for designing MRWTs because a large rotor is downscaled to multiple small rotor sizes. Also, as data from actually constructed turbines does not match theoretical scaling relations, several empirical scaling relations have been proposed. Verma [32] prepared a scaling model using these empirical relations to estimate the total cost of a single and three-rotor system. The following section explains the three types of scaling relations used in the model – baseline, advanced and simple scaling relations.

2.4.1.1. Empirical Scaling Trends

Fingersh et al. [6] studied the recent trends in the mass and the cost of wind turbine components in the industry with respect to the rotor size. These trends are a direct function of the rotor diameter, power rating and tower height, and are discussed in this section.

2.4.1.2. Rotor Blades

For the rotor blades, the study identifies two types of empirical relations.

1. Baseline – based on data obtained from the WindPACT (Wind Partnerships for Advanced Component Technology) designs.

2. Advanced – related to the LM Glasfiber advanced blade design.

These two relations differ from the theoretical 'simple' scaling relations. Based on [6], Verma prepared a scaling model that provides the mass and cost data for a downscaled turbine for a three-rotor system using these simple and empirical relations.

The blade mass relations in terms of rotor radius *R* are given by Eq. (2.4) and Eq. (2.5).

$$\text{Baseline: } Blade\ mass = 0.1452 * R^{2.9158} \tag{2.4}$$

$$\text{Advanced: } Blade\ mass = 0.4948 * R^{2.53} \tag{2.5}$$

The graphs for trends in the blade mass and cost [6] are shown in Figures 9 and 10.

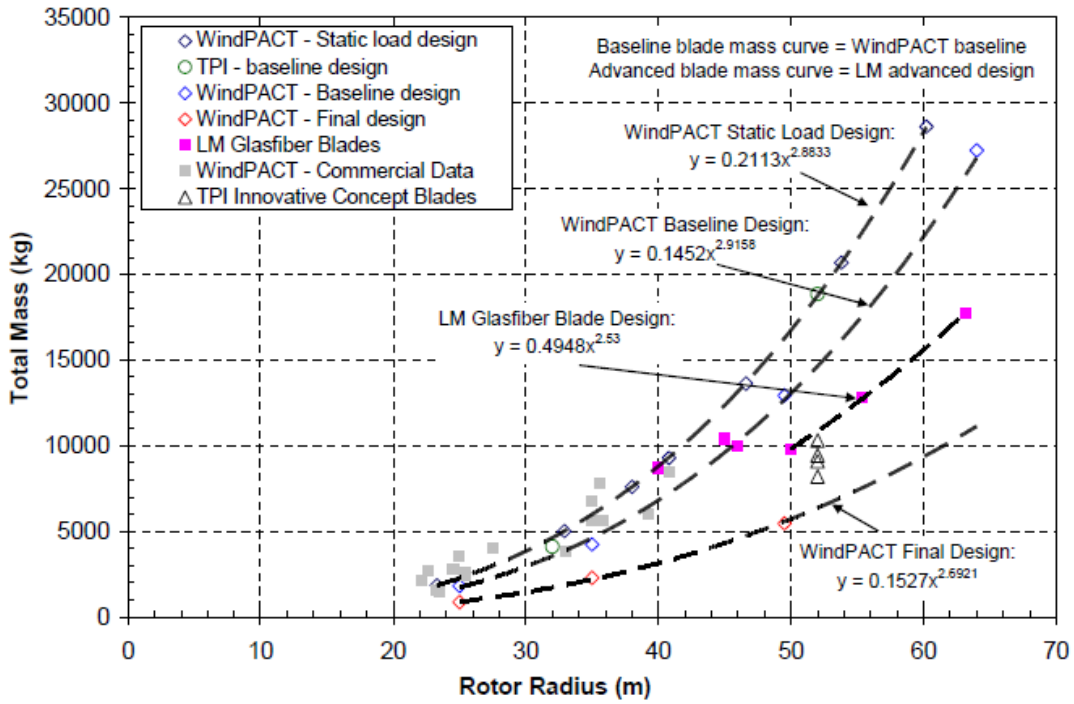

Figure 9. Scaling relations for blade mass [6]

2.4.1.3 Hub

The mass and cost of the hub was scaled according to the blade and therefore, the hub was also classified as per the advanced and baseline relations.

$$Hub\ mass = 0.954 * (blade\ mass) + 5680.3 \quad (2.6)$$

$$Hub\ cost = Hub\ mass * 4.25 \quad (2.7)$$

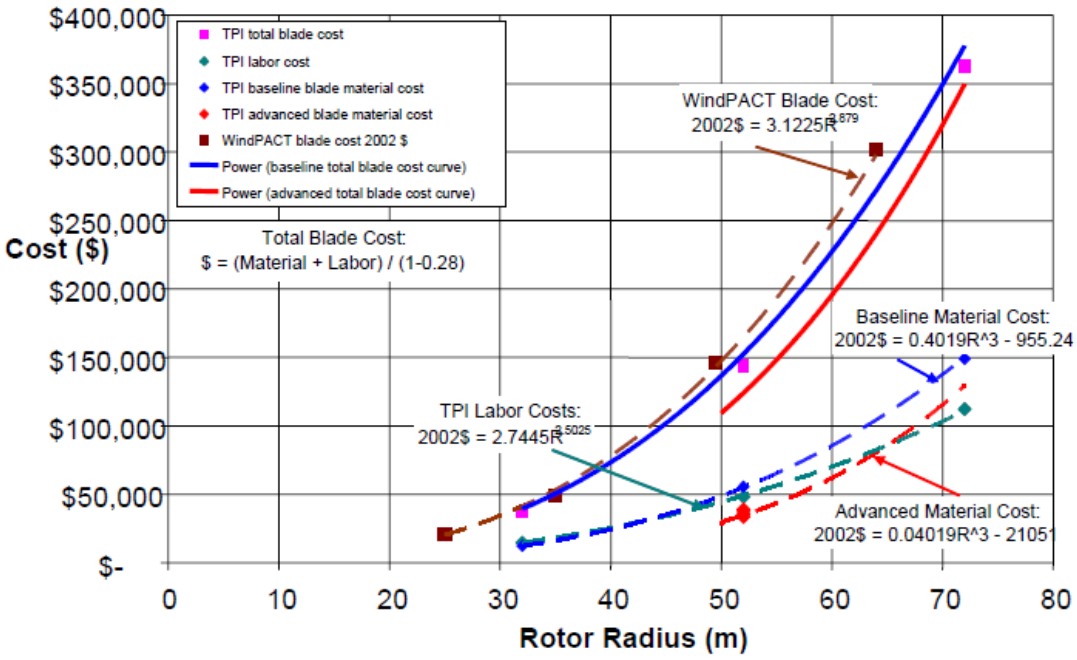

Figure 10. Scaling relations for blade cost [6]

2.4.1.4. Nacelle and Tower

The components included in the nacelle were scaled [32] according to the empirical scaling relations given in [6] called 'General' scaling in this thesis. The gearbox, generator, mainframe, platform and railing are classified as either 'Single-stage', 'Three-stage', 'Multi-path' or 'Direct drive'. The NREL 5 MW turbine has a multiple stage planetary gearbox [7] and so, the Three-stage case was chosen. As regards the tower, the same tower mass and cost is considered for 5 MW MRWTs and so, the tower was not downscaled.

2.4.1.5 Baseline Model

Out of the two models, Verma [32] used the baseline model because:

1. The baseline relations shown in Figures 9 and 10 are valid for rotor radii ranging from 25 to 63 m while the advanced relations are only valid for radii from 50 to 63 m.
2. The NREL 5 MW turbine [7] has a rotor radius of 63 m which downscales to a radius of 36.37 m for a three-rotor MRWT. Thus, only the baseline relations can be used.

Also, in this thesis, while extending the scaling model to 2 to 7 rotors; it is found that the advanced scaling relations for five or more number of rotors give negative values for the cost of some components, which is not logical. Thus the model finally chosen for the analysis in this thesis is the 'baseline, three-stage' model as the NREL 5 MW turbine has a three-stage planetary gearbox [7].

2.4.1.6 Results of the Scaling Model

Using the baseline scaling model, Verma [32] obtained the following results when a single-rotor 5 MW turbine was compared with a three-rotor 5 MW MRWT with each rotor producing 1.67 MW. These results did not consider the mass and the cost of the support structure, which was designed in a later section in Verma's work [32]. Figure 11 shows the values for each component of both systems and the total values and Figure 12 shows the results for the total mass and total cost obtained after considering the WindPACT scaling curve nacelle mass.

Thus, Verma concluded that the three-rotor 5 MW MRWT is 37% lighter and 25% cheaper than the single-rotor 5 MW turbine without considering the support structure.

	Component	Cost Summary ($)		Weight Summary (kg)	
		Single-rotor	Multi-Rotor	Single-Rotor	Multi-Rotor
Rotor	Blades	778,745	506,086	76,843	46,473
	Hub	127,995	135,232	30,116	31,819
	Pitch	183,552	127,907	14,423	11,615
	Nose	10,084	13,792	1,811	2,476
	Total	1,100,375	783,017	123,193	92,383
Nacelle	Shaft	11,582	7,116	16,526	10,148
	Bearing	95,050	41,094	5,401	2,335
	Gearbox	685,772	521,777	36,608	31,201
	Brake	9,947	9,949	995	995
	Generator	325,000	325,065	16,690	18,181
	Power Electronics	395,000	395,079		
	Yaw System	113,954	113,954	13,152	13,152
	Electrical Systems	200,000	200,040		
	Hydraulics	60,000	60,012	400	400
	Nacelle cover	61,535	69,246	6,153	6,925
	Mainframe/Railing	150,732	154,690	31,773	32,608
	Total	2,108,570	1,898,020	127,699	115,944
Total RNA		3,208,945	2,681,037	250,891	208,327

Figure 11. Scaling Model results by Verma [32] – Comparison between single-rotor 5 MW and three-rotor 5 MW MRWT without the support structure

	Cost Summary ($)		Weight Summary (kg)	
	Single-rotor	Multi-Rotor	Single-Rotor	Multi-Rotor
Total rotor	1,100,375	783,017	123,193	92,383
Total nacelle	2,108,570	1,629,376	234,608	132,526
Total RNA	3,208,945	2,412,393	357,801	224,918

Figure 12. Revised Scaling Model results by Verma [32]

2.4.2. Structural Analysis

A preliminary structural analysis was performed by Verma [32] on a 5 MW MRWT system employing three-rotors. The first structure analyzed was a three-arm truss-type support frame

to support the rotors as shown in Figure 13. Since this design did not satisfy the deflection criterion of 1 m maximum and was 28.2% heavier, it was discarded.

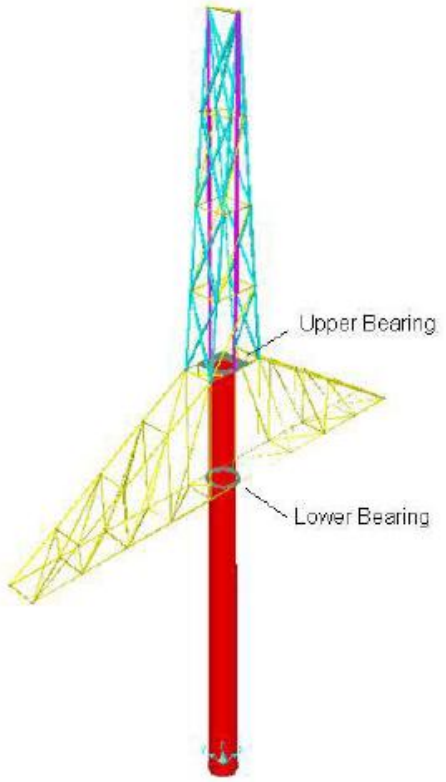

Figure 13. Three arm truss-type support frame [32]

A triangular truss type space frame shown in Figure 14 was then considered, which satisfied the conditions. It was only 5.13% heavier than the single-rotor NREL 5 MW turbine but comparing the overall cost, it was 13.1% cheaper. The design used slew bearings for the yaw system, which are also adopted in this thesis. The mass of this support structure was 135,600 kg and cost was $203,400, while the mass of the yaw bearings was 11,000 kg and cost was $130,000.

The material considered for both the support frames was structural steel ASTM A992 with minimum yield strength of 345 MPa. The support structure was analyzed for rated wind conditions for maximum deflection and stress in SAP2000.

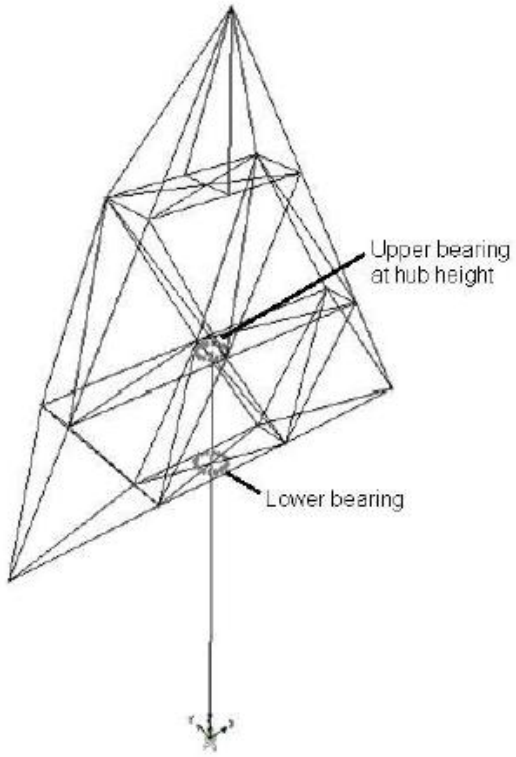

Figure 14. Triangular truss type support frame [32]

The goal of this thesis is to extend the scaling model developed by Verma and to reduce the total mass and cost of a MRWT system by continuously improving the design and considering other configurations such as those using cables. Also, the dynamic analysis of the system and its response to the different load cases is implemented in this thesis. Finally, a seven-rotor MRWT case for the same 5 MW configuration is considered by designing the support structure with the same approach. This model is analyzed and then compared with the three-rotor MRWT and the single-rotor models. The result will be useful in creating a method to determine the optimum number of rotors for turbines with a given power rating.

2.5. Additional Material

Certain other references are used for designing the support structure developed in this thesis for a three-rotor model.

1. A supplementary yaw bearing provides an extra point from where the structure can be rotated to orient itself in the wind direction and to support the loads. This bearing located at a tower section should be of a larger diameter. Therefore, a catalogue of slew bearings published by Kaydon Corp. [33] is used for reference.
2. A product catalogue of cables by Ronstan Tensile Architecture [23] is referred to for designing cables required for the support structure.
3. The support structure primarily consists of I-beam sections. The data for these comes from a catalogue issued by Agate Inc. [24] and it is a catalogue issued by the American Institute of Steel Construction (AISC).

CHAPTER 3

EXTENDED SCALING MODEL

This chapter presents the scaling model that is developed to be able to consider MRWT systems employing 2 to 7 rotors. Note that the initial scaling model developed by Verma was used only for obtaining the parameters of the three-rotor model. For extending the scaling model, the 'cost per unit mass' ratios are obtained for each component of the NREL 5 MW baseline turbine. Finally, after the scaling model is developed, the scaling trends for total system mass and cost of 2 to 7 rotor MRWT models are presented which are unique to this thesis.

3.1. Inputs for the Scaling Model

The total power rating is fixed at 5 MW for this thesis. The model could also be used for MRWTs with any other rating. It is assumed that the basic operational parameters for the MRWTs are equal to the values for a single-rotor turbine as given in Table 2.

Table 2. NREL 5 MW turbine - basic operational characteristics

Variable	Value
Tip speed ratio	7
Cut-in wind speed	3 m/s
Rated wind speed	11.4 m/s
Cut-off wind speed	25 m/s

The required variables, such as number of blades, maximum tip speed and rated generator speed etc., and their default inputs for a 5 MW turbine are fixed for a single-rotor. The formulae pertaining to scaling and multi-rotors are as below.

1. The total power P produced by the MRWT system consisting of n rotors is related to the power p produced by each rotor assuming equal distribution among the n rotors.

This step is unique to this thesis and was not included in the work by Verma.

$$p = \frac{P}{n} \tag{3.1}$$

2. As the radius of the NREL 5 MW turbine is 63 m, the radius *r* of each rotor is given by Eq. (3.2).

$$r = 63\ m * \left(\frac{p}{5\ MW}\right)^{1/2} \tag{3.2}$$

3. The scale factor *S* is the ratio of the rotor radius *r* with the baseline rotor radius.

$$S = \frac{r}{63\ m} \tag{3.3}$$

4. The hub radius r_h for each rotor is given by Eq. (3.4).

$$r_h = S * (1.5\ m) \tag{3.4}$$

Table 3. Model Inputs for the General model

DESIGN PARAMETERS	**VALUE**	**UNIT**
Total Power of the wind turbine system	5.00	MW
Number of rotors	**1**	
Number of blades	**3**	
Power produced by each wind turbine	5.00	MW
Radius of each rotor	63	m
Maximum Tip speed	**80**	m/s
Generator efficiency	**94.4**	%
Scale factor	1.00	
Rated rotor speed	12.13	rpm
Hub radius of the rotor	1.5	m
Blade length	61.5	m
BCE[1] & GDPE[2]	**1**	
Direct Drive	**False**	
Generator Speed at rated	**1174**	rpm
Gearbox ratio	96.79	
Rated Mechanical power	5.30	MW
Generator Torque	43,094	Nm
Rotor Aerodynamic Torque	4,171,081	Nm
Air Density	**1.23**	kg/m^2
Coefficient of Thrust	**0.73**	
Rated Wind speed	**11.4**	m/s

[1] Blade material cost Escalator [2] Labor Cost Escalator [6]

5. The rated rotor speed, blade length, rated mechanical power, generator and rotor torque are obtained using standard formulae as given in [5]. The quantities in bold in Table 3 are the inputs while the others are fixed or evaluated from the inputs.

The maximum tip speed is not allowed to exceed 80 m/s due to noise issues. This conforms to the value of tip speed *TS* calculated from the tip speed ratio λ and rated wind speed *U*.

$$TS = \lambda * U = 7 * 11.4 = 79.8\, m/s \tag{3.5}$$

The value for 'direct drive' controls the gearbox and the generator calculations in the model. A value of False implies calculation of gearbox mass and cost while a value of True makes the gearbox mass and cost zero. The additional cost of a direct drive generator can be obtained since the generator speed is smaller and in this case equal to the rotor speed.

While downscaling a system with a gearbox, the generator speed is kept constant and close to either 1200 or 1800 rpm. This corresponds to a 60 Hz operating frequency with 3 or 2 pole pairs respectively. Typically a value of 1174 rpm is used in the NREL baseline machine at rated conditions [7]. With a constant generator speed, the gearbox ratio is then varied accordingly.

The thrust coefficient of 0.73 is obtained by considering the rated thrust value of F_T equal to 724.55 kN from results using the FAST code [29] obtained along with those in section 4.2.3.1.

$$F_T = \frac{1}{2}\rho\pi(R)^2(U)^2C_T = \frac{1}{2} * 1.225 * \pi * (63)^2 * (11.4)^2 * 0.73 = 724.55\, kN \tag{3.6}$$

3.2. Cost per Unit Mass

The model results are slightly inconsistent for the cost of certain components for five or more rotors. The mass values are more accurate than the cost values because they are directly related to the rotor radius. This anomaly is corrected by using cost/mass ratios.

Consider the case of NREL 5 MW turbine with a single-rotor [7]. The cost per unit mass of all the components is calculated. These ratios of $/kg as shown in Table 4 are then fed into the model and multiplied by the corresponding mass of the component, for any downscaled design.

Table 4. Cost per unit mass of components for an NREL 5 MW turbine

($/kg)	**Cost/ mass for NREL 5 MW single-rotor 3-bladed turbine**			
Scaling Relations	**General**	**Baseline**	**Advanced**	
Blade		10.13	13.13	
Hub		4.25	4.25	
Pitch system	12.73			
Nose cone	5.57			
Low Speed shaft	6.99			
Main bearing	35.2			
VSE & electrical	Negligible mass			
Yaw system	8.66			
Brake coupling	10			
Hydraulic / cooling	150			
Nacelle cover	10			
Tower	1.5			
Drive Train	**Single-stage**	**Three-stage**	**Multi-path**	**Direct Drive**
Gearbox	6.38	16.66	6.92	0
Generator	10.09	19.47	17.43	10.31
Mainframe	3.23	4.25	2.68	2.46
Platform + railing	8.7	8.7	8.7	8.7

3.3. General and Baseline Models

The values for cost per unit mass from Table 4 are used in the model to develop a general model to find the cost of the components from the mass.

$$Cost = \left(\frac{Cost}{kg}\right) * (Mass) \tag{3.7}$$

Table 5. General Model

Single rotor 5 MW	**Mass(kg)**				**Cost($)**			
Components	**Baseline**		**Advanced**	**Simple**	**Baseline**		**Advanced**	
Blades	76,843		52,952	53,220	778,421		695,260	
Hub	30,116		22,519	56,780	127,995		95,706	
Pitch System	*14,423*				*183,551*			
Nose Cone	*1,810*				*10,085*			
Low speed shaft	*16,526*				*115,670*			
Main bearing	*5,400*				*95,050*			
Variable speed electronics	-				*395,000*			
Yaw system	*13,152*				*113,896*			
Brake & coupling	*994*				*9,946*			
Electrical system	-				*200,000*			
Hydraulic & Cooling sys.	*400*			*240,000*	*60,000*			
Nacelle Cover	*6,154*				*61,535*			
Drive Train	**Single-stage**	**Three-stage**	**Multi-path**	**Direct Drive**	**Single-stage**	**Three-stage**	**Multi-path**	**Direct Drive**
Gearbox	*55,974*	*39,688*	*88,560*	*0*	*357,112*	*661,203*	*612,835*	*0*
Generator	*27,113*	*16,690*	*13,775*	*6,469*	*273,561*	*324,960*	*240,104*	*66,693*
Mainframe, Platform & Railing	*18,427*	*31,773*	*21,767*	*17,473*	*70,717*	*150,748*	*82,008*	*55,100*
Tower	347,460				521,190			

The ‘General’ spreadsheet model is shown in Table 5. An If-condition is set to ‘True’ for obtaining the direct drive case and ‘False’ for the gearbox cases. The values in the column of simple scaling are basically the values of the NREL 5 MW turbine model [7]. The nacelle

mass of the NREL 5 MW turbine is higher than the total nacelle mass for baseline and advanced three-stage scaling, which is 144,310 kg. So, while using the weight of the nacelle as a load in the structural model, the higher value is used i.e. 240,000 kg or 2354.4 kN. The pitch system cost is obtained from the equation given in Fingersh et al. [6]. The cost of simple scaling cannot be found as only empirical cost relations are provided in [6]. Ultimately, with the baseline scaling relations modified as per section 3.4 and 3.5, the general model is changed to the baseline model as obtained in Table 6. This model uses a three-stage drive.

Table 6. Baseline Model

BASELINE	**Single rotor 5 MW Model**	
Components	**Mass(kg)**	**Cost($)**
Blades	76,843	778,421
Hub	30,116	127,995
Pitch System	*14,423*	*183,551*
Nose Cone	*1,810*	*10,085*
Low speed shaft	*16,526*	*115,670*
Main bearing	*5,400*	*95,050*
Variable speed electronics	-	*395,000*
Yaw system	*13,152*	*113,896*
Brake & coupling	*994*	*9,946*
Electrical system	-	*200,000*
Hydraulic & Cooling system	*400*	*60,000*
Nacelle Cover	*6,154*	*61,535*
Gearbox	*39,688*	*661,203*
Generator	*16,690*	*324,960*
Mainframe, Platform & Railing	*31,773*	*150,748*
Tower	347,460	521,190
TOTAL	**601,429**	**3,809,250**

Thus, the total system mass and cost for a single-rotor 5 MW turbine considering a baseline, three-stage drive model is 601,429 kg and $3,809,250 as shown in Table 6. This table is later compared with an equivalent 5 MW MRWT system with three-rotors.

3.4. Number of rotors

In the general model, with all other inputs in Table 3 i.e. quantities in bold being the same, the number of rotors are now varied from 1 to 7. This gives us a general trend of the cost reduction achieved by using MRWTs but without considering the required support structure. The other input properties that change with the number of rotors are shown in Table 7. It should be noted that the generator speed and the total power remain the same.

Table 7. Variation in General Model input properties with number of rotors

5 MW Turbine	**Number of rotors**						
Properties	1	2	3	4	5	6	7
Rotor Radius (m)	63	44.55	36.37	31.5	28.17	25.72	23.81
Power per rotor (MW)	5	2.5	1.67	1.25	1	0.833	0.71
Scale Factor	1	0.71	0.58	0.5	0.45	0.41	0.38
Rotor speed (rpm)	12.13	17.15	21	24.25	27.11	29.7	32.08
Hub radius (m)	1.5	1.06	0.87	0.75	0.67	0.61	0.57
Blade length (m)	61.5	43.49	35.51	30.75	27.5	25.11	23.24
Generator speed (rpm)	1174	1174	1174	1174	1174	1174	1174
Gearbox Ratio	96.79	68.44	55.88	48.4	43.29	39.51	36.58
Rated Mechanical power per rotor (MW)	5.3	2.65	1.77	1.32	1.06	0.88	0.76
Total Mechanical power (MW)	5.3	5.3	5.3	5.3	5.3	5.3	5.3
Generator Torque (kNm)	43.09	21.55	14.36	10.77	8.62	7.18	6.16

With these different input properties, the values of the total mass and the total cost for different number of rotors are calculated. A series of general models finding the total system mass and cost are obtained and plotted in Figures 15 and 16, from which we may infer that:

1. As the number of rotors increases, the total mass decreases rapidly for the simple scaling relations.
2. Based on the mass, the optimum number of rotors is five for baseline scaling and four for advanced scaling. This analysis does not consider the mass of the support structure.

3. Seven rotor wind turbines would cost the least, but again without considering the cost of the support structure.

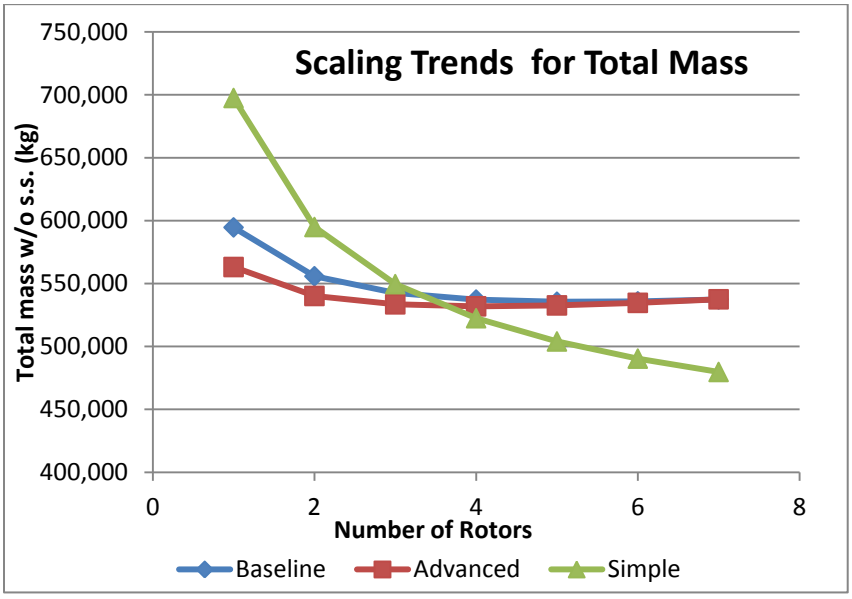

Figure 15. Total Mass of General Model vs. number of rotors

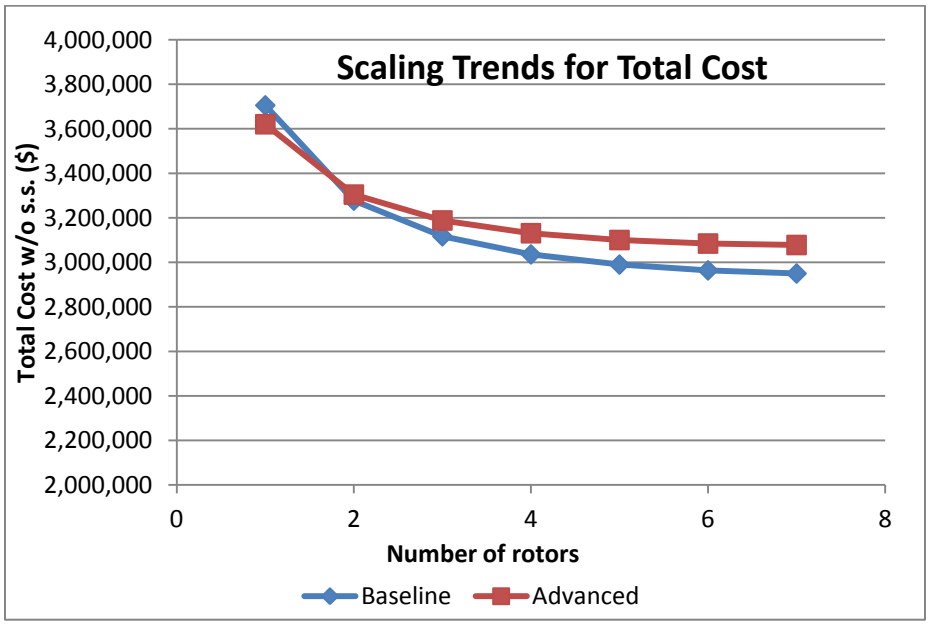

Figure 16. Total Cost of General Model vs. number of rotors

The mass and cost are then normalized based on the simple scaling mass and baseline cost respectively to easily compare the results.

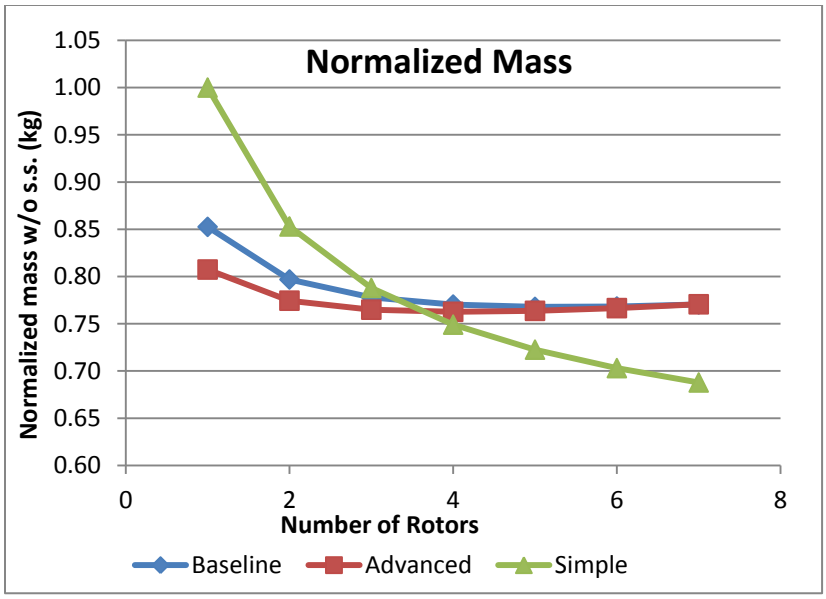

Figure 17. Normalized Mass of General Model vs. number of rotors

A mass reduction of 15% can be achieved with two rotor MRWTs producing the same power based on simple scaling. Even more reduction of up to 30% can be attained with seven rotors. Note that the baseline and advanced values for a single-rotor do not match those of the NREL 5 MW turbine, since these scaling methods are different from simple scaling. Cost reductions of up to 20% are possible with 7 rotors.

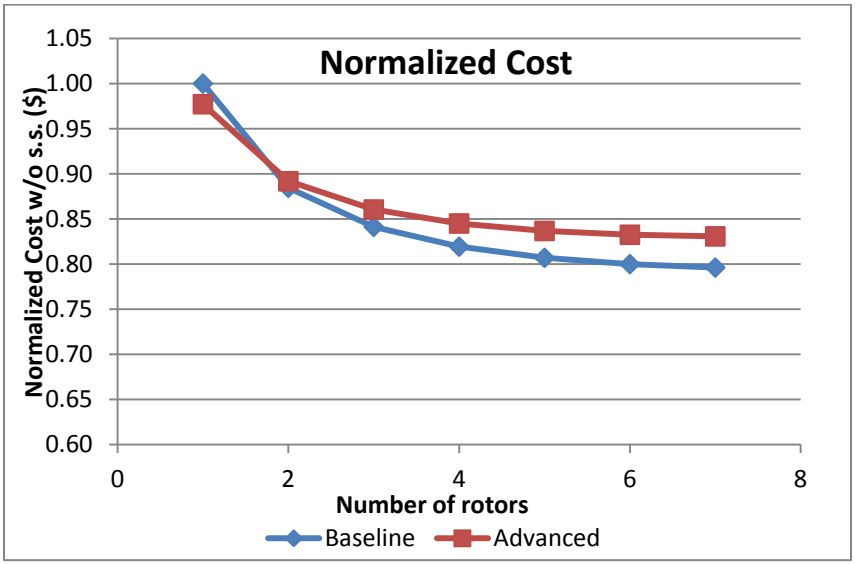

Figure 18. Normalized Cost of General Model vs. number of rotors

The masses are then converted to weights, and along with the downscaled torque and thrust, Table 8 is created.

Table 8. Variation in loads with number of rotors

5 MW MRWT	**Number of rotors**						
Loads per rotor	1	2	3	4	5	6	7
Weight of nacelle (kN)	2354.4	832.41	453.1	294.3	210.58	160.2	127.13
Weight of hub (kN)	557.01	154.05	112.14	93.82	83.79	77.54	73.31
Weight of blades (kN)	522.09	274.41	151.94	99.89	72.15	55.31	44.18
Tower self-weight (kN)	3408.6	3408.6	3408.6	3408.6	3408.6	3408.6	3408.6
Thrust force (kN)	724.55	362.28	241.52	181.14	144.91	120.76	103.51
Rotor torque (kNm)	4171.08	1474.7	802.72	521.39	373.07	283.81	225.22

From Table 8, as the number of rotors in a MRWT increases, the loads are more well-distributed about the entire structure. Some of the loads such as the total component weights and the total rotor torque for the MRWT system (2 or more rotors) are also reduced in comparison with the single-rotor case. Note that the tower self-weight remains the same.

CHAPTER 4

SINGLE-ROTOR ANALYSIS

This chapter describes the structural analysis of a single rotor model utilizing the software, SAP2000 v14. The objective is to create and analyze a single-rotor model first before exploring MRWT models.

4.1. SAP2000 Modeling Environment

SAP2000 is a software package developed by Computers and Structures, Inc. for structural analysis of general structures [28]. The software is specialized for applications in civil engineering for modeling, analysis, design and optimization of structures. Object-based modeling in SAP2000 allows automatic mesh generation. Although meshing could also be performed or refined by the user, automatic meshing simplifies the analysis. Unless otherwise specified, the units used for this thesis are kN and m (meters).

The single and multi-rotor models are developed in SAP2000 with the help of joints at the fundamental level and frame elements - the building blocks. Frame elements are line objects used to model beams, columns, braces and trusses [28]. The tower is also modeled using frames of hollow pipe sections. Cables, which are similar to frames, are also used.

4.2. Single-Rotor Model

The model of the NREL 5 MW baseline single-rotor turbine structure consists of the tower and two frames joining the tower top to the center of mass (C.M.) locations of the hub and the nacelle. The key aspects of the design of this model are given below.

4.2.1 Model Geometry

1. The tower base serves as the origin and is a fixed support, with restraints in all 6 DOFs.

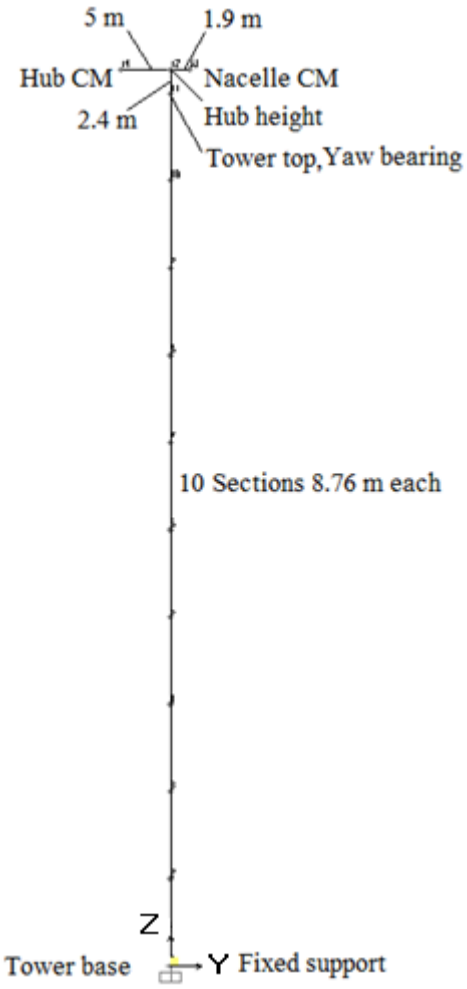

Figure 19. Single-rotor model – features

2. The tower is conical and consists of a set of 11 hollow pipe sections tapering towards the top. SAP2000 cannot define a conical section for a frame so cylindrical sections are used. The thickness of each section is increased by 30% as per [7]. The tower dimensions are based on [7] as given in Table 9 and another frame of length 2.4 m extends from the tower top to the hub height. The tower properties at intermediate locations i.e. the diameter and thickness are obtained by interpolation.

Table 9. Tower Section Properties

Section Name	Location (z-axis)	Outside Diameter (m)	Thickness (m)
SEC1	0 m – 8.76 m	6	0.0351
SEC2	8.76 m – 17.52 m	5.787	0.0338
SEC3	17.52 m – 26.28 m	5.574	0.0325
SEC4	26.28 m – 35.04 m	5.361	0.0312
SEC5	35.04 m – 43.8 m	5.148	0.0299
SEC6	43.8 m – 52.56 m	4.935	0.02925
SEC7	52.56 m – 61.32 m	4.722	0.02808
SEC8	61.32 m – 70.08 m	4.509	0.0273
SEC9	70.08 m – 78.84 m	4.296	0.026
SEC10	78.84 m – 87.6 m	4.083	0.0247
SEC11	87.6 m – 90 m	3.87	0.0247

3. The two frames emerging from the tower top are assumed to have I-beam sections and the dimensions are used from [7]. The length of each frame is the distance of the C.M. of the hub, which is 5 m in the upwind direction and the C.M. of the nacelle, which is 1.9 m in the downwind direction, from a point 2.4 m above the tower top. Loads are then applied at these ends as discussed in section 4.2.2.

4. The material used is structural steel ASTM A992Fy50 with a yield strength of 344 MPa minimum specified, 379 MPa effective, and a density of 8500 kg/m^3 as in [7] to account for bolts, flanges and welds.

The front and side view of the model after extrusion is shown in Figure 20. It clearly shows the taper of the tower and the two frames joined to the tower top.

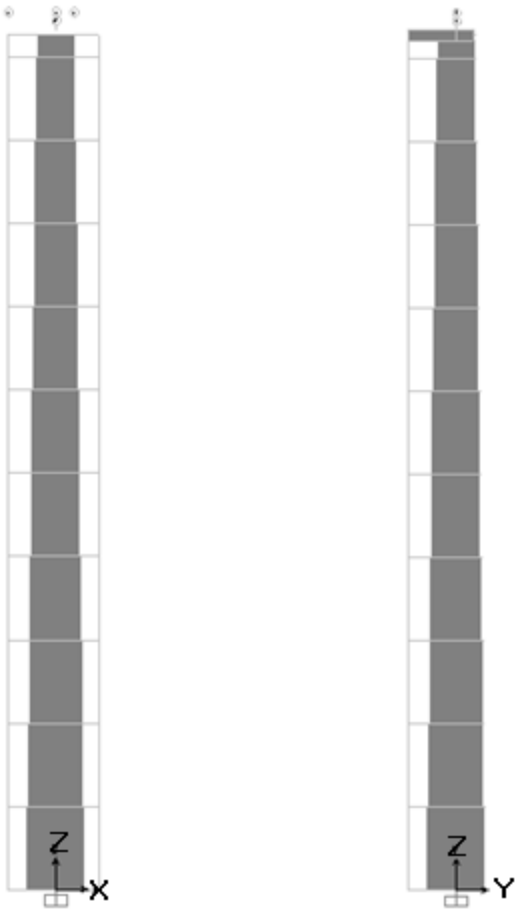

Figure 20. Tower Front and Side View for single-rotor model in SAP2000

4.2.2. Model Loads

After defining the single rotor model, the loads are applied. A load pattern in SAP2000 [27] is a classification of loads defined at the fundamental level e.g. live and dead loads, whereas a load case specifies how a load pattern or a combination of load patterns are applied e.g. static and buckling load cases.

On the basis of the mass values from the General model in the previous chapter, the weights are calculated and shown in Table 10. The loads are then applied in SAP2000 for structural analysis of the single-rotor model.

Table 10. Load values used in SAP2000 model according to different scaling relations

Load Name	Baseline Scaling	Advanced Scaling	NREL 5 MW model
Thrust per rotor	724.55 kN	724.55 kN	**724.55 kN**
Aerodynamic Torque	4,171.08 kNm	4,171.08 kNm	**4,171.08 kNm**
Weight of blades per rotor	753.83 kN	519.46 kN	**522.09 kN**
Weight of hub	313.20 kN	238.67 kN	**557.01 kN**
Weight of nacelle	1,385.38 kN	1,424.42 kN	**2,354.40 kN**
Weight of tower	3,408.58 kN	3,408.58 kN	**3,408.58 kN**

Most loads for a single-rotor model are selected from the NREL 5 MW model because:

1. Scaling i.e. upscaling or downscaling is referenced to these values, which are real values of the NREL 5 MW baseline turbine.
2. The load values for a NREL 5 MW model are higher so the model is designed for a higher safety factor.

Table 11. Load patterns for Static load case

Load pattern	Type	Position	Value	Direction
Weight of the nacelle	Point Load	Nacelle CM downwind	2354.4 kN	Z axis downwards
Weight of the hub	Point Load	Hub CM upwind	557.01 kN	Z axis downwards
Weight of the rotor blades	Point Load	Hub CM upwind	522.09 kN	Z axis downwards
Self-weight of the tower	Distributed Load	Along tower	3408.58 kN (total)	Z axis downwards
Thrust force due to wind	Point Load	Hub CM upwind	724.55 kN	Y axis downwind
Aerodynamic Torque	Point Load	Nacelle CM downwind	4171.08 kNm	@ Y axis CCW
Self-weight of frames	Distributed Load	Along frames	Value varies with frame	Z axis downwards

A static load case, consisting of all the load patterns, is defined first. The thrust force is considered to act at the center of the swept area which is the hub C.M. The 'self-weight of frames' represents the self-weight loads for all the frames of the support structure for MRWTs. For a single-rotor case, this is the self-weight of the two frames joining the C.M.s of the hub and the nacelle. The value of aerodynamic torque is taken from the Table 3 and each torque is applied to the C.M. of the nacelles of each of the rotors located downwind.

The loads in Table 11 are applied near the tower top as shown. The self-weights are not visible.

In addition to the static load case, the modal and buckling load cases are defined taking into account all the load patterns. The modal load case produces the first 5 mode shapes and uses Ritz vectors while the buckling load case produces 5 buckling mode shapes.

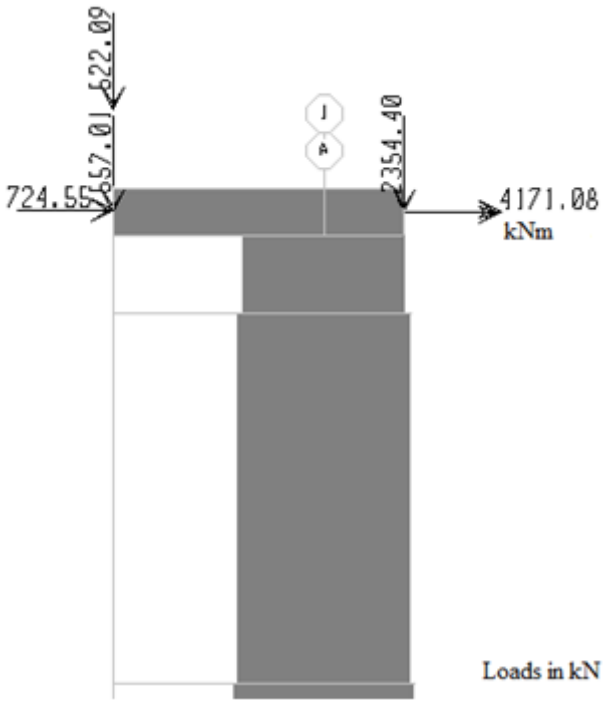

Figure 21. Location of Loads

4.2.3. Model Results

The three load cases are then run in SAP2000 using the "Analyze" menu. The advanced solver is used as default and the design code used is AISC-LRFD93. The maximum deflection of all nodes of the entire structure is constrained to be less than 1 m. Stress and buckling are the other design criteria. Stresses could be axial, shear or bending stresses. Usually SAP2000 considers the maximum of these stresses for the frame elements. The Stress ratio for a given element is defined as Eq. (4.1).

$$Stress\ ratio = \frac{Stress\ value}{Allowable\ stress} \tag{4.1}$$

Buckling is the instability of a component, especially a structural column, leading to sudden failure under high compressive load and is related to the dimensions of the component. The buckling criterion is that the compressive load on an element should be less than the critical buckling load. The critical buckling load depends on the slenderness ratio given by Eq. (4.2).

$$Slenderness\ ratio = \frac{kl}{r} \tag{4.2}$$

Where, k is the column effective length factor depending on how the component is restrained at the ends, l is the unsupported length of component, and r is the radius of gyration of the component.

The stress ratio for all elements should be less than 0.95 and the slenderness ratio of all elements should be less than 200 to satisfy the above criteria. This check is done by the software and the results are shown in table 12. All the elements satisfy the buckling criterion i.e. the axial load does not exceed the critical buckling load calculated according to the code equations.

Table 12. Single-rotor Model Results

Design Criterion	**Results**		
Deflection	Maximum	0.40973 m	Located at Hub CM
	Minimum	-0.02428 m	Located at Nacelle CM
Stress	Stress ratio of all components < 0.95		
Buckling	Slenderness ratio of all components < 200		

4.2.4. Verification of SAP2000 with FAST

The rated power operation for the single-rotor 5 MW model is then simulated in the FAST code [29] and the results are compared with those obtained from SAP2000 for a constant wind speed of 11.4 m/s to ascertain that the SAP2000 model is appropriate.

The inputs in the FAST file are based on those in [7]. The FAST input files are already provided in [7] and are directly used with minor changes.

The values for angular deflection in FAST are converted from degrees to radians. FAST output values, after achieving steady state, are compared with SAP2000 values in Table 13.

Table 13. Comparison of FAST and SAP2000 results-Single Rotor 5 MW Turbine Model at Rated speed operation

1. Tower Base Reactions				
Output	**Notation**	**FAST results**	**SAP2000 results**	
Shear Force x-direction	Fx	2.62 kN	0 kN	
Shear Force y-direction	Fy	726.10 kN	724.55 kN	
Shear Force z-direction	Fz	6847 kN	6991.85 kNm	
Bending Moment @ X-axis	Mx	66060 kNm	64241.25 kNm	
Bending Moment @ Y-axis	My	4262 kNm	4171.082 kNm	
Bending Moment @ Z-axis	Mz	0 kNm	0 kNm	
2. Tower top Deflection				
Output	**FAST results**		**SAP2000 results**	
	Notation	**Value**	**Notation**	**Value**
Fore-aft deflection (x-direction)	TTDspFA	0.39 m	U1	0.4099 m
Side-to-side deflection (y-direction)	TTDspSS	0.04839 m	U2	0.0462 m
Axial deflection (z-direction)	TTDspAx	0.00181 m	U3	0.0045 m
Roll deflection (angular @ x-axis)	TTDspRoll	0.00132 rad	R1	0.0045 rad
Pitch deflection (angular @ y-axis)	TTDspPtch	0.00744 rad	R2	0.00786 rad
Twist deflection (angular @ z-axis)	TTDspTwst	0 rad	R3	0 rad

The model degrees of freedom (DOFs) that are active in FAST are:

1. First flapwise blade mode DOF

2. First edgewise blade mode DOF

3. First fore-aft tower bending mode DOF

4. First side-to-side tower bending mode DOF

5. Compute aerodynamic forces

Table 13 demonstrates that the reaction forces and moments at the tower base are accurate to within 3% of the FAST values and the tower top deflections are accurate to within 5%.

Important stress values that are checked are the bending stresses at the tower base. The tower base has a diameter of 6 m and thickness 0.035 m. The inner diameter is therefore 5.965 m. The distance *y* of the load point from the neutral axis (in this case the tower axis) is half the base outer diameter. If the bending moment value M_b is used from Table 13, then the bending stress σ_b is calculated in Eq. (4.3). *I* is the moment of inertia about the neutral axis.

$$\sigma_b = \frac{M_b y}{I} = \frac{(64241.25*10^{-3})(\frac{6}{2})}{(\frac{\pi}{32}*(6^4-5.9649^4))} = 65.3\ MPa \tag{4.3}$$

This shows that the stresses are within the limits of the minimum specified yield strength of steel, which is 344 MPa, and that the NREL baseline machine has been designed with a safety factor of approximately 5. Also, the design is not governed by allowable stress but perhaps by serviceability i.e. deflections or buckling.

CHAPTER 5

THREE-ROTOR ANALYSIS

After the SAP2000 model of the single-rotor NREL 5 MW baseline turbine is validated with the FAST code [29], a three-rotor model is designed with each rotor producing 1.67 MW. This procedure is similar to the one followed by Verma [32] with some exceptions such as using a downwind rotor, cables, and different arrangement of steel frames in the structure. The goal is to develop a MRWT system that is lighter in weight as well as costs less than a comparable single-rotor system.

5.1. Two rotors vs. three rotors

The reasons for choosing a three-rotor model over a two-rotor model are as follows:

1. A three-rotor model is the model with the minimum number of rotors to take advantage of some of the benefits of MRWTs. This is because the rotors are at different heights above the ground in order to optimize space and cost.
2. The three-rotor model has a reduced mass of components than a two-rotor model in the downscaling analysis.

On the other hand, a two-rotor model can be designed with just one yaw bearing placed at the same height as that of the tower top of a single-rotor model i.e. 87.6 m. However, an additional yaw bearing is required for the three-rotor model at a lower height.

5.2. Baseline Three-Rotor Model

The number of rotors in the baseline model is changed to three rotors. This model has a three-stage gearbox and uses the same tower used in the single-rotor model. The tower is not

downscaled since it has to withstand the same loads. The mass and cost values for a three-rotor model are as shown in Table 14. The single-rotor baseline model is also shown for comparison.

Table 14. Three-rotor model and equivalent single-rotor model

BASELINE	**Single rotor 5 MW**		**Three rotor 5 MW, 1.67 MW**	
Components	**Mass(kg)**	**Cost($)**	**Mass(kg)**	**Cost($)**
Rotor	76,843	778,421	46,466	470,696
Hub	30,116	127,995	31,817	135,222
Pitch System	14,423	183,551	11,613	147,798
Nose Cone	1,810	10,085	2,476	13,791
Low speed shaft	16,526	115,670	10,147	71,020
Main bearing	5,400	95,050	2,334	41,086
Variable speed electronics	-	395,000	-	395,000
Yaw system	13,152	113,896	17,098	120,896
Brake & coupling	994	9,946	995	9,946
Electrical system	-	200,000	-	200,000
Hydraulic & Cooling system	400	60,000	400	60,000
Nacelle Cover	6,154	61,535	6,923	69,234
Gearbox	39,688	661,203	34,086	567,876
Generator	16,690	324,960	18,178	353,918
Mainframe, Platform &	31,773	150,748	32,605	154,690
Tower	347,460	521,190	347,460	521,190
TOTAL	**601,429**	**3,809,250**	**562,598**	**3,332,363**

The mass and cost of the 2 yaw bearings for the three-rotor model are discussed in section 5.5.6. The main yaw bearing at the rotor centroid (hub height of 90 m) is the same as the single-rotor model, whereas the second yaw bearing only provides stability to the yawing motion and only supports a fraction of the weight.

The reduction in total mass of 38,831 kg and total cost of $476,887 is due to the square-cube law discussed in section 1.2. The cost reduction is attributed to the following individual reductions.

Table 15. Contribution of Cost Reduction per Component

Component	Cost Reduction	Percentage Contribution
Rotor	$307,725	57.47%
Pitch system	$35,753	6.7%
Low speed shaft	$44,650	8.33%
Main bearing	$53,964	10.08%
Gearbox	$93,327	17.43%
Total	**$535,419**	**100%**

Most other components either do not contribute or cause a slight increase in the cost. This is of course, without considering the additional mass of the support structure.

5.3. Arrangement of Rotors

Some general considerations for the arrangement of rotors include:

1. While designing a multi-rotor system with *n* rotors, the center of their collective swept area should correspond to the hub height of the NREL 5 MW single-rotor turbine which is 90 m [7], since we are comparing rotor scenarios producing the same power and therefore having the same average elevation.
2. For multi-rotor offshore turbines, the wave height should be used to determine the limit of the lowest rotor location. A distance of 15 m from the tower base, which is half the blade tip clearance of 30 m for the NREL 5 MW single-rotor turbine [7] is chosen for the MRWT rotor configuration.
3. The rotors should be symmetric but to an extent that the stresses due to gravity are minimized.

5.3.1. Rotor Spacing

For rotors placed close to each other, it was shown through experimentation [8] that the spacing between rotors measured in terms of the dimensionless quantity *t* should be between 1.025 and 1.4, with *t* defined in Eq. (5.1) and *s* is the distance between rotor axes and *R* is the rotor radius.

$$t = \frac{s}{2R} \tag{5.1}$$

The size of these rotors was as small as 20 cm diameter and with a tip speed ratio of 4. These results were supported by another study conducted by the SwRI [9], which included CFD simulation in addition to experimental testing on a seven rotor array. The spacing between the rotors for this thesis is chosen as 5% of rotor diameter, so ***t* = 1.05**.

5.3.2. Rotor Locations

With the criteria from sections 5.1 through 5.3, the rotor coordinates for a three-rotor system are calculated. While comparing two different MRWT arrangements with centroids at 90 m [32], the configuration with two rotors below the hub height results in reduced gravity loads. In this configuration, the rotor tips are sufficiently far away from the mean sea level (M.S.L.). These values are shown in Eq. (5.2) and (5.3).

$$Height\ of\ lower\ rotors = 67.95\ m \tag{5.2}$$

$$Distance\ between\ lower\ rotor\ tip\ and\ M.S.L. = 67.95\ m - 36.37\ m = 31.58\ m \tag{5.3}$$

This distance of 31.58 m is greater than 15 m as per [7] and hence acceptable. The rotor spacing is selected as 5% of the rotor diameter which is 72.74 m.

$$Rotor\ spacing = 0.05 * \ 72.74 = 3.637\ m \tag{5.4}$$

The distance between the centers of the rotors is given by Eq. (5.5)

$$s = 72.74 + 3.637 = 76.377\ m \tag{5.5}$$

The rotor arrangement is an equilateral triangle with 76.377 m long sides. From the geometry shown in Figure 22, the co-ordinates of the rotor centers are:

$$\text{Top rotor} = (0, 0, 134.1)\ \text{m} \tag{5.6}$$

$$\text{Lower left rotor} = (-38.192, 0, 67.95)\ \text{m} \tag{5.7}$$

$$\text{Lower right rotor} = (38.192, 0, 67.95)\ \text{m} \tag{5.8}$$

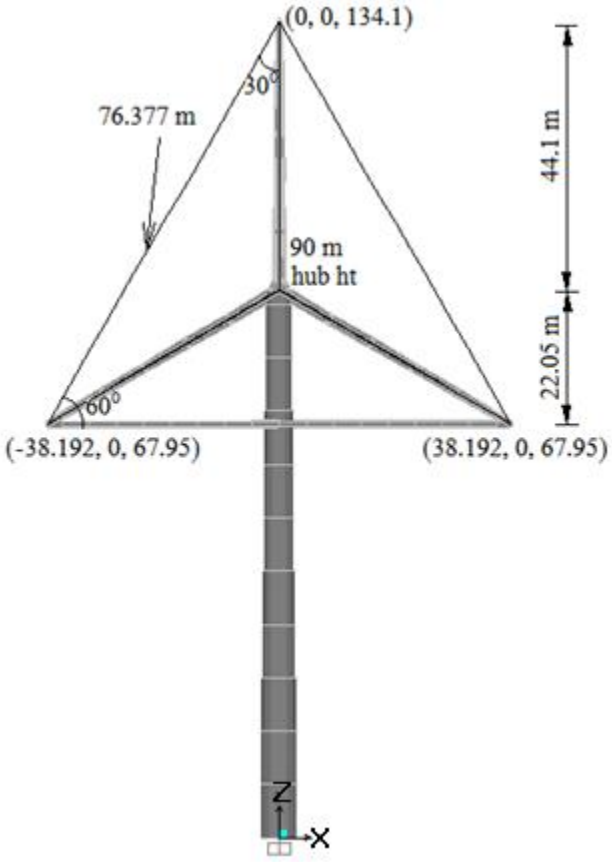

Figure 22. Calculation of rotor locations

In the single-rotor model, there are two frames near the rotor location – one joining a point 2.4 m above the tower top to the C.M. of the hub located upwind and, the other joining the former point to the C.M. of the nacelle located downwind. The lengths of these frames as per

Chapter 4 are 5 m upwind and 1.9 m downwind, respectively, and are shown on the left side of Figure 23.

In the three-rotor model, there are two frames at each of the three rotor locations. The lengths of these frames are downscaled because the hub and the nacelle masses are also downscaled.

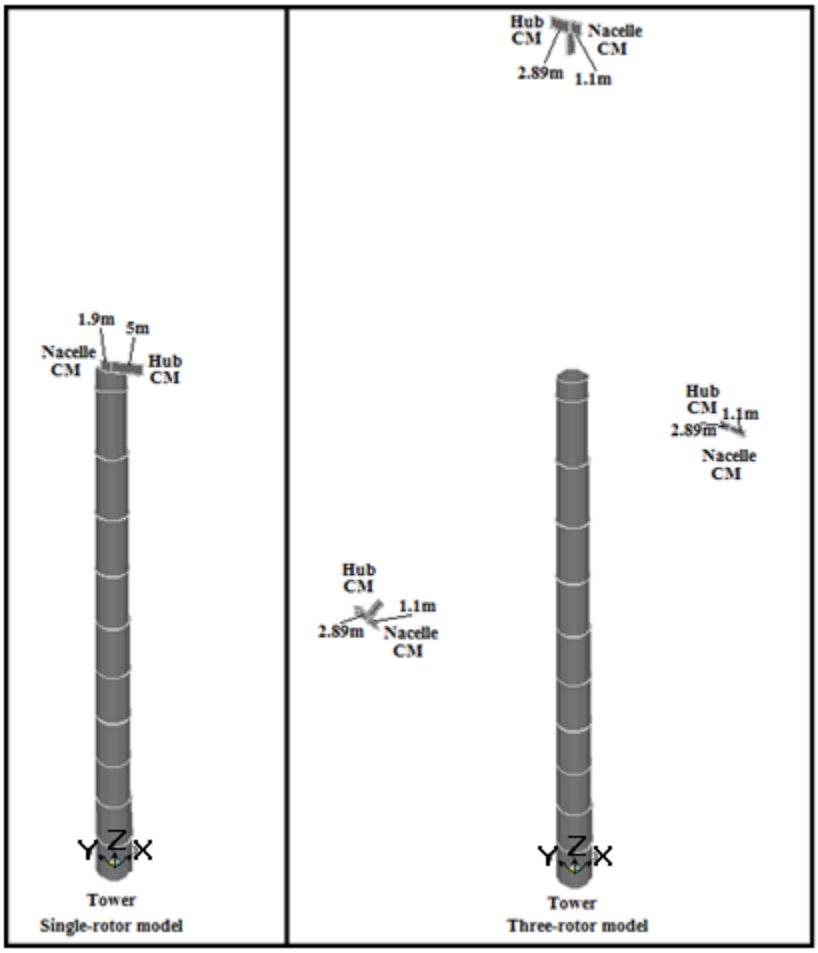

Figure 23. Downscaling of Hub and Nacelle CM (before support structure design)

As mass is a product of density and volume, and the volume is proportional to the cube of length dimensions, these C.M. lengths are downscaled as the cube root of the masses.

$$New\ Hub\ CM\ dist = 5 * \left(\frac{1\ hub\ mass\ (3-rotor)}{hub\ mass\ (1-rotor)}\right)^{\frac{1}{3}} = 5 * \left(\frac{10927}{56780}\right)^{\frac{1}{3}} = 2.89\ m \qquad (5.9)$$

$$New\ Nacelle\ CM = 1.9 * \left(\frac{1\ nacelle\ mass\ (3-rotor)}{nacelle\ mass\ (1-rotor)}\right)^{\frac{1}{3}} = 1.9 * \left(\frac{46188}{240000}\right)^{\frac{1}{3}} = 1.1\ m \quad (5.10)$$

Also, a downwind rotor is used for the three-rotor case. So, the lengths of these frames in the three-rotor model is 2.89 m downwind for the hub C.M., and 1.1 m upwind for the nacelle C.M. These lengths are shown on the right side of Figure 23.

5.4. Preliminary Considerations for Support Structure

1. The support structure for connecting the three rotors of a MRWT is made of steel and consists of frames and cables. Steel is the preferred material as it is widely used in the industry and also less expensive than composites.
2. The structure contains spars directly connecting the hub of a rotor to the tower. This requires less material than the case when there are horizontal and vertical frames connecting the rotors. These spars are 3D trusses that provide stiffness in the downwind direction and resist the thrust load.
3. Diagonal bracing may or may not be used depending on the dimensions.

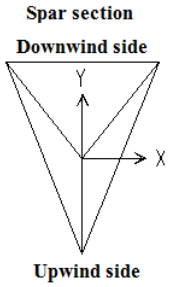

Figure 24. Spar section design

4. The spar section is triangular with one vertex in the upwind direction as shown in Figure 24. This reduces the wind resistance of the structure and is a good design against bending. Also, it uses less material than a square section.

5. A space frame, being shaped like a matrix to support symmetrically situated rotors, would be suitable for a large number of rotors [10]. For the number of rotors between 3 and 7, the most cost effective structure would be the one directly joining the rotors together and so, the space frame is unnecessary.

5.5. Model Geometry

After calculating the rotor co-ordinates and finding the distance of the C.M.s from these co-ordinates, the rest of the model is constructed in SAP2000.

5.5.1. Downwind Rotors

The rotors are oriented downwind for the three-rotor model so that the cables can be used to resist the downwind deflection, by connecting the cables to a jib located upwind. The point of using cables is to minimize the number of frames required, by making use of the tensile forces that the cables support.

5.5.2. Frames

The structure is made of steel and consists of frames and cables. I-beam sections, also sometimes called wide flange sections, are primarily chosen for the frames as they are the most efficient shape for carrying both bending and shear loads in the plane of the web [30].

A group of frames joining the tower top to the rotor center is the spar, and these spars are of triangular sections as shown in Figure 24. Therefore, the spar as shown in Figure 25, consists of I-beam frames, which are joined together to form the triangular sections.

The very large number of frames makes this structure difficult to analyze, and necessitates the use of the SAP2000 package. In SAP2000, an I-beam section is specified by its flange and web dimensions. A standard catalogue [24] is referred to for I-sections – the Steel Data

from Agate Inc. certified by the AISC. This catalogue is selected because of the wide range of dimensions of the sections.

In the course of achieving the final design, several different I-beam sections are tested for the frames. SAP2000 can select I-beams automatically by using its built-in database called "Auto-select" lists, to minimize deflection and stresses. In this thesis, some I-beams from the Agate catalogue are custom selected and entered in that database. Some other considerations for designing frames are already provided in Section 5.4.

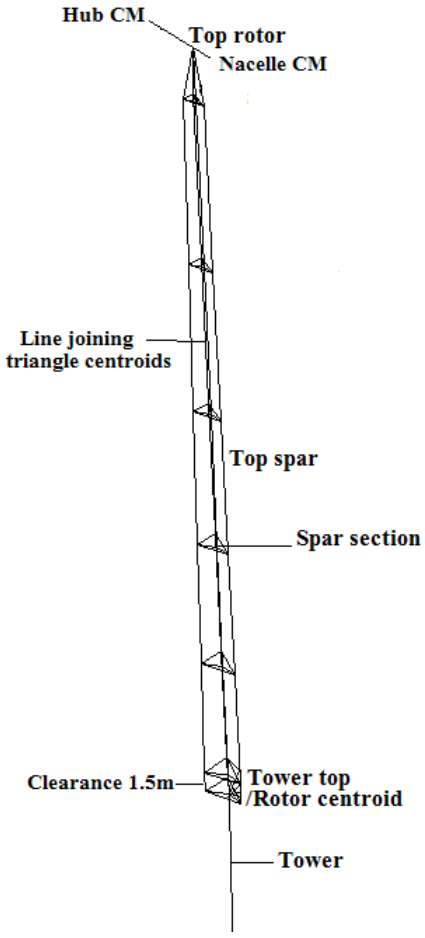

Figure 25. Construction of Top spar

5.5.3. Spars

Spars are the links made of frames connecting the rotors to the rotor centroid and are tapered towards the rotor ends to reduce the bending stresses at the rotor centroid. The procedure for constructing the spars is as follows:

1. A spar section consisting of I-beam frames near the topmost rotor is constructed. This section is triangular as discussed in 5.4. with the vertex upwind. The vertices are joined to the centroid of the triangle as shown in Figure 24.
2. Starting from the topmost section, tapering sections with increasing triangle dimensions towards the rotor centroid are created as shown in Figure 25. These sections end near the centroid with a clearance of 1.5 m. The centroids of each section are connected by straight frames. This completes one spar connecting the topmost rotor.
3. A triangular section connecting the rotor centroid to the point 1.5 m above it is created. This provides clearance for joining the spars to each other.
4. The spar is rotated by 120° twice with the axis of rotation parallel to the y-axis as shown in Figure 26. The intersection of the line of rotation with XZ plane is *x=0, z=90*. Now the three spars are created.
5. The spars are attached to each other at the rotor centroid after rotating as shown in Figure 26. In practice, these three spars could be mass produced to reduce cost.
6. The number of spar sections is arbitrarily decided as 5 as shown in Figure 25. If several frames undergo buckling then the number of sections should be increased.

The dimensions of the spar for the final design are shown in the Table 16. The isosceles triangle referred to in the table is shown in Figure 24.

Table 16. Dimensions of triangle for top spar sections

Height above ground level (m)	Dimensions of Triangle (Isosceles)	
	Base	**Height**
131.7	0.6 m	1 m
123.66	0.8 m	1.2 m
115.62	1 m	1.4 m
107.58	1.2 m	1.6 m
99.54	1.4 m	1.8 m
91.5	1.6 m	2 m
90	1.6 m	2 m

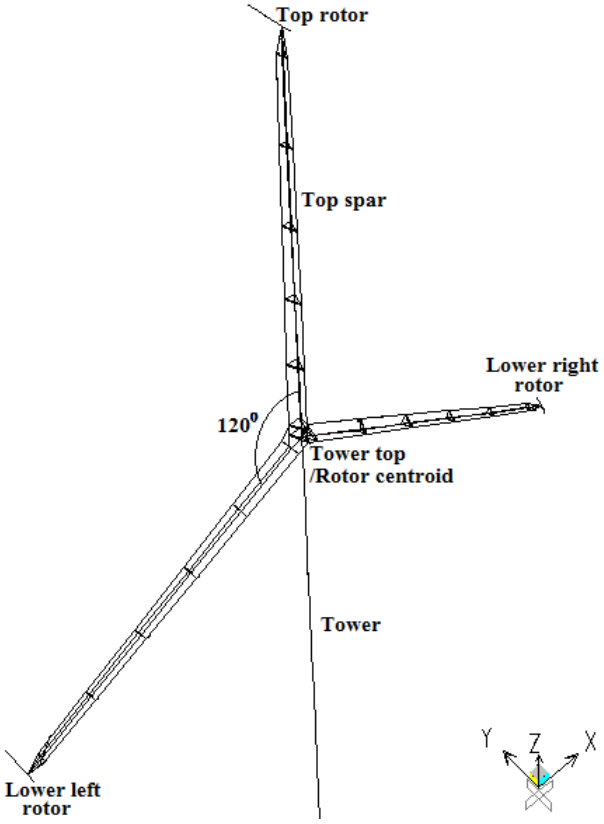

Figure 26. Construction of spars

5.5.4. Cables

Cables can resist high tensile forces and obviate the need to use a large number of frames for reducing the deflection. Therefore, cables are used with downwind rotors, by connecting them to a jib located upwind. The load carrying capacity of the frames supported by the

cables can be controlled by increasing the pre-tension applied to the cables, thereby controlling the deflections and increasing the stiffness of the structure.

Three different cable types are used in the support structure depending on the loads they support. Following are the cable types and locations:

1) Cables of Type 1 are located upwind and join the spar ends to the jib.
2) Cables of Type 2 are located upwind and join the top rotor to each of the lower rotors
3) Cables of Type 3 are located downwind and join the top rotor to each of the lower rotors

A standard catalogue [23] issued by Ronstan Tensile Architecture (Table on pg. 9 in reference [23]) is consulted for the design of cables as it contains data for the VVS type of cables, which have very large diameters of up to 140 mm. The design steps to calculate the pre-tension T in the cable, cross section area A of the cable, and its material density ρ are explained in sections 5.5.4.1 through 5.5.4.3.

5.5.4.1. Cables of Type 1

These cables resist the thrust force on each rotor. The configurations involving more than one cable of type 1 being attached to the jib have lesser total deflection and stress levels.

The magnitude of the thrust force on one rotor is 241.52 kN. There are five cables of type 1, attached to the top spar from a horizontal jib located upwind as shown in Figure 27. The cables oppose the thrust force, as shown in Equation 5.11.

$$Thrust = \sum T \sin\theta \tag{5.11}$$

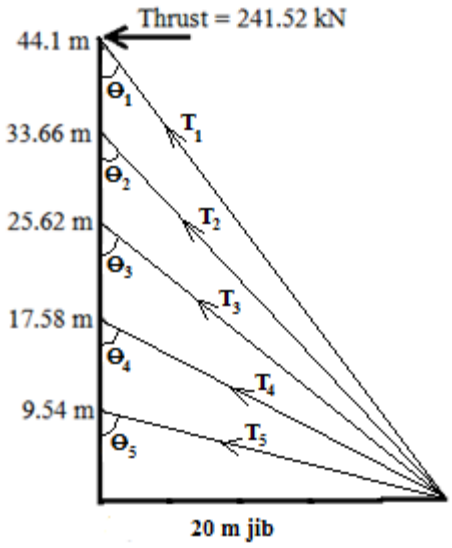

Figure 27. Cables of Type 1 (upwind)

To simplify the analysis, we assume $T_1 = T_2 = T_3 = T_4 = T_5 = T$

$$241.52\ kN = T \sum \sin\theta \tag{5.12}$$

Calculating the angle θ_1 from the geometry,

$$\theta_1 = \tan^{-1}\frac{20}{44.1} = 24.4° \tag{5.13}$$

Similarly, finding the other angles, the pre-tension T is equal to the value in Eq. (5.14).

$$\boldsymbol{T = 75.64\ kN} \tag{5.14}$$

Now, the allowable stress σ^* in the cable, related to the yield stress σ_y of the cable material, is used to find the cross-sectional area A of the cable. The safety factor is denoted by *s.f.*

$$\sigma^* = \frac{\sigma_y}{s.f.} = \frac{T}{A} \tag{5.15}$$

$$\sigma^* = \frac{379.2\ MPa}{2} = \frac{75.64\ kN}{A} \tag{5.16}$$

$$A = 398.9\ mm^2 \tag{5.17}$$

Choosing a cable of diameter d = 26 mm from the catalogue [23],

$$\boldsymbol{A \cong 430\ mm^2} \tag{5.18}$$

The cable is made of multi-strand steel cords wrapped together. The effective density is thus calculated from the mass per unit length *m/l* obtained from [23] and the area *A*.

$$\rho = \frac{m/l}{A} = \frac{3.6\ kg/m}{4.3*10^{-4}\ m^2} \tag{5.19}$$

$$\boldsymbol{\rho = 8372.09\ kg/m^3} \tag{5.20}$$

5.5.4.2. Cables of Type 2

These cables support the weight of the nacelle associated with each of the lower two rotors. The nacelle load per rotor is 453.1 kN. One of the two cables of type 2 is in Figure 28.

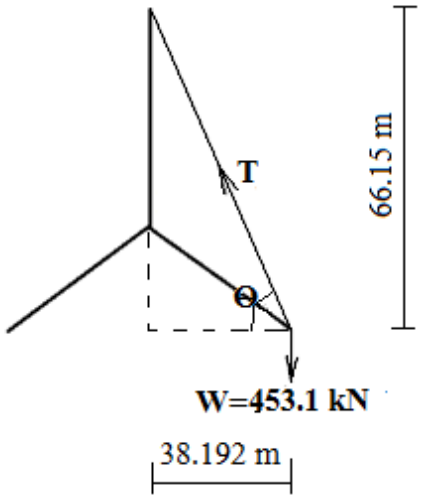

Figure 28. Cable of Type 2 (upwind)

There are two cables of this type, each joining the nacelle C.M. of a lower rotor to the nacelle C.M. of the top rotor. As the opposing load is *W* equal to 453.1 kN,

$$W = T \sin\theta \tag{5.21}$$

Calculating θ from the geometry,

$$\theta = \tan^{-1}\frac{66.15}{38.192} = 60° \tag{5.22}$$

$$453.1\ kN = T \sin 60° \tag{5.23}$$

$$\boldsymbol{T = 523.2\ kN} \tag{5.24}$$

Following the same procedure as cables of type 1,

$$\sigma^* = \frac{\sigma_y}{s.f.} = \frac{T}{A} \tag{5.25}$$

$$\sigma^* = \frac{379.2\ MPa}{2} = \frac{523.2\ kN}{A} \tag{5.26}$$

$$A = 2760\ mm^2 \tag{5.27}$$

Choosing a cable of diameter *d* = 65 mm from the catalogue [23],

$$\boldsymbol{A \cong 2920\ mm^2} \tag{5.28}$$

$$\rho = \frac{m/l}{A} = \frac{24.1\ kg/m}{2.92{*}10^{-3}\ m^2} \tag{5.29}$$

$$\boldsymbol{\rho = 8253.42\ kg/m^3} \tag{5.30}$$

5.5.4.3. Cables of Type 3

These cables support the weight of the rotor and the hub. The sum total of these loads per rotor is 112.14 + 151.94 = 264.1 kN. One of the two cables of type 3 is shown in Figure 29.

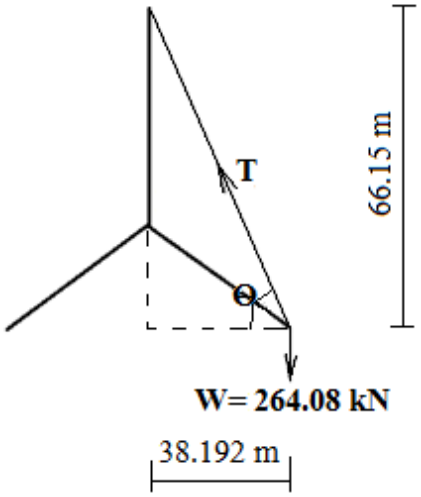

Figure 29. Cable of Type 3 (downwind)

These are two cables of this type each joining the C.M. of a lower rotor to the C.M. of the top rotor. As the opposing load is *W* equal to 264.08 kN,

$$W = T \sin\theta \tag{5.31}$$

Calculating θ from the geometry,

$$\theta = \tan^{-1}\frac{66.15}{38.192} = 60° \tag{5.32}$$

$$264.08\ kN = T \sin 60° \tag{5.33}$$

$$\boldsymbol{T = 304.93\ kN} \tag{5.34}$$

Following the same procedure as cables of type 1,

$$\sigma^* = \frac{\sigma_y}{s.f.} = \frac{T}{A} \tag{5.35}$$

$$\sigma^* = \frac{379.2\ MPa}{2} = \frac{304.93\ kN}{A} \tag{5.36}$$

$$A = 1608\ mm^2 \tag{5.37}$$

Choosing a cable of diameter d = 50 mm from the catalogue [23],

$$\boldsymbol{A \cong 1650\ mm^2} \tag{5.38}$$

$$\rho = \frac{m/l}{A} = \frac{13.8\ kg/m}{1.65{*}10^{-3}\ m^2} \tag{5.39}$$

$$\boldsymbol{\rho = 8363.6\ kg/m^3} \tag{5.40}$$

The density of each cable type is fed into the material properties of the cables in SAP2000 along with the modulus of elasticity of 160 GPa and the effective yield strength of 379 MPa. The cross-section area is fed into the section properties and the pre-tension values are used to define the individual cables in the model. A cable can also be defined by its length before and after deformation, which is calculated from the pre-tension. The self-weight of each of the cables is also applied as a load.

5.5.5. Yaw bearing and Lower link

Two options are considered while designing the yaw system for orienting all three rotors together into the wind. Their pros and cons are given in Table 17.

Table 17. Options for the Yaw System

No.	Yaw system at top near the rotor centroid	Yaw system at the bottom of the tower
1.	In this case, the yaw system is closer to all the rotors. Thus, the deflection & the stresses in the elements in general would be less.	For this case, the yaw system is too far away from rotors and therefore, this would result in high stresses and deflections in general.
2.	This system would involve faster yawing & less yaw torque would be required.	This system would involve slower yawing and larger yaw torque would be required.
3.	The rotors can be joined by trusses with a tubular tower; simpler yaw bearings such as roller and slew bearings would be used.	The structure would be complex as the yawing of the entire system would need bogey wheels running on yaw tracks as suggested in [12].

Option 1 is selected i.e. the yaw system is located at the tower top near the centroid. Two yaw bearings are required for this option because:

1. One yaw bearing is at a height of 87.6 m (upper yaw bearing) supporting most of the weight of the support structure as it is located right above the tower top. The design of this yaw bearing is exactly the same as the one used in a single-rotor system – NREL 5 MW turbine. Therefore, its mass is 13,152 kg and cost is $113,896.
2. The other yaw bearing is located between the lower two rotors at a height of 67.95 m. The purpose of this yaw bearing is only to direct the lower rotors and so, the mass and the cost of this yaw bearing would be less. This yaw bearing however has a large diameter and so, a slew bearing should be designed.

The lower link refers to the group of frames connecting the two rotors to the tower at 67.95 m above ground level, which is also the point where the second yaw bearing is located.

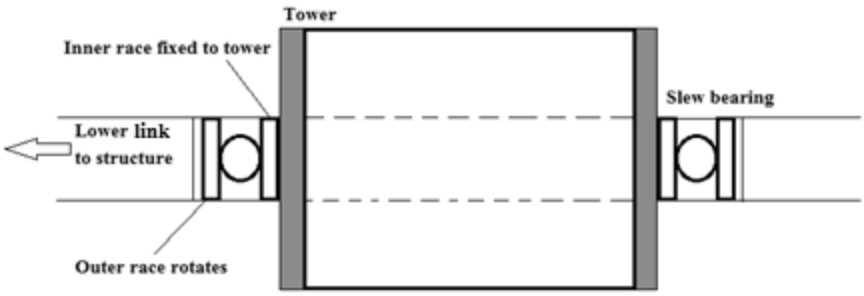

Figure 30. Second yaw bearing (slew bearing) fitted to tower

The inner race of the second yaw bearing - a slew bearing, fitted to the outer surface of the tower, is fixed. The outer race, connected to the lower link, rotates to cause the yaw motion as shown in Figure 30.

For the lower yaw bearing, the inner diameter must be greater than or equal to 4.5 m – the tower section diameter at that height. This is a simple low-cost slew bearing. The catalogue [33] issued by Kaydon Corporation includes the specifications of a XT series bearing. The cost of the slew bearing from a manufacturer Luoyang Huagong Heavy Machine Manufacturing Co. of a similar size (6 m OD) [16] is $7,000. Therefore, the total yaw system mass is 13,152 + 3,946 = 17,098 kg. Also, the total cost is 113,896 + 7,000 = $120,896.

Table 18. Specifications for Lower yaw bearing

Yaw bearing	**Details**
Type	External gear (XT series)
Part Number	16317001
Outer diameter	218.26” (5.54 m)
Inner diameter	197.24” (5 m)
Width	5.51” (0.14 m)
Mass	8,700 lb (3,946 kg)
Cost	$7,000

The lower link is a simple 3D tapered truss connecting the two rotors through the yaw bearing at the tower axis. The taper is given to reduce the bending moments at the center. It consists of a group of sections to prevent sag due to gravity loads, and to prevent buckling.

The lower link, with a total length of 76.384 m, is found to reduce deflections and stresses for the entire structure.

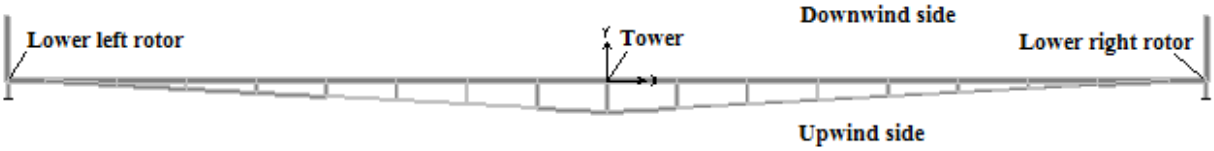

Figure 31. Lower link- Top view

5.5.6. Jib

The jib is a structural frame extending in the upwind direction that provides an attachment point for the cables. The design iterations involve a variation in the length, the number of jib sections and the cross-section of the jib.

With increasing jib length,

1. The weight of the jib increases.
2. The number of overstressed members decreases and the deflection decreases.
3. The weight of the cables increases faster so that the total weight of the system slightly increases.
4. Buckling is more likely, so the number of sections required is higher.

After modeling all the components, the final structure before the analysis is as shown in Figure 32.

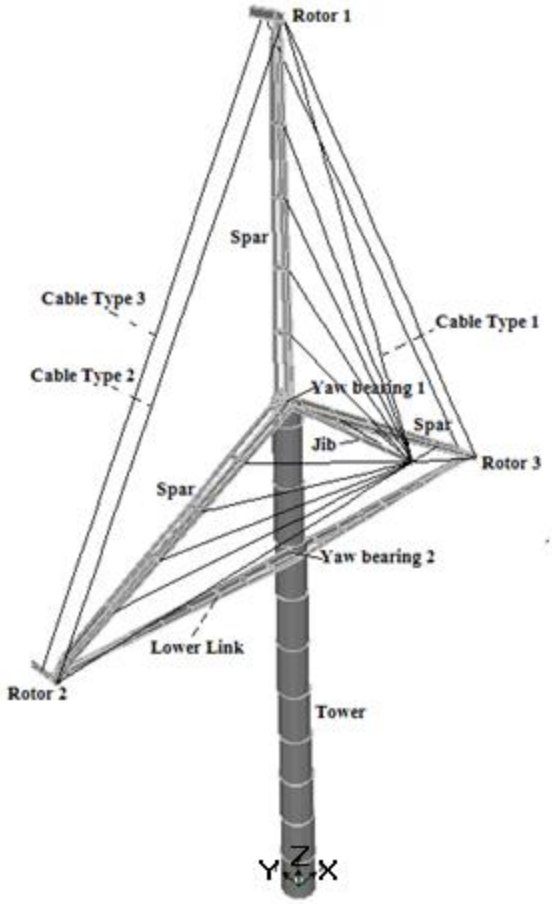

Figure 32. Model Geometry

5.6. Model Loads

Table 18 is similar to the table for single-rotor loads (Table 11), except that since the rotor is downwind, the position of upwind loads are downwind and vice versa. Also, the point loads are located near each of the three rotors. Although the rotors face different wind speeds due to wind shear, the controller changes the thrust coefficient such that the thrust force is the same i.e. 241.52 kN for all the three rotors, in order to optimize power output. The self-weight is also applied to cables similar to frames.

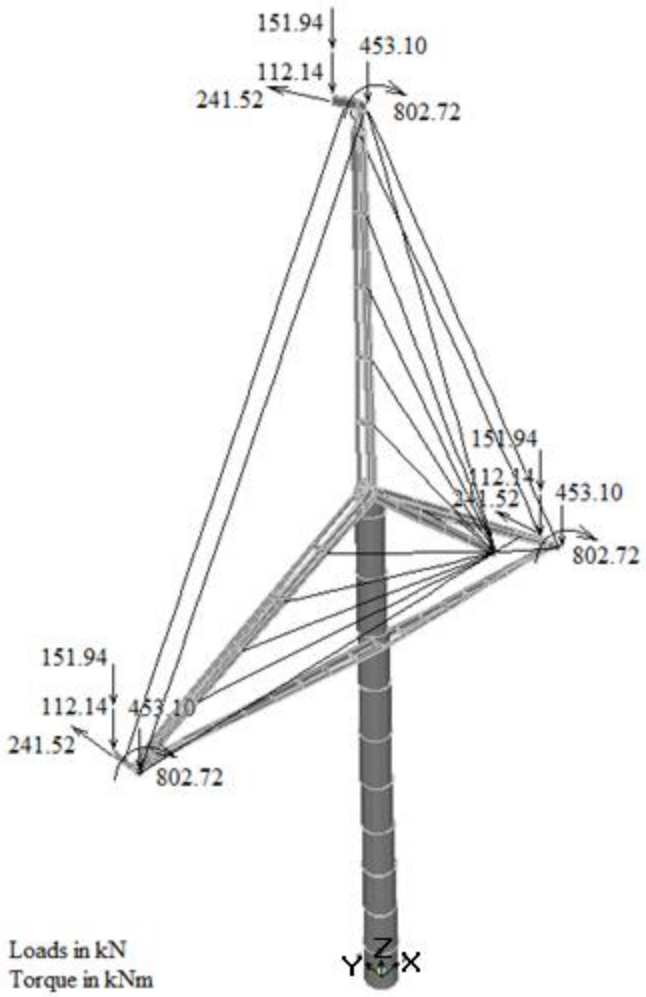

Figure 33. Loads for a Three Rotor Model

Table 19. Loads for a Three Rotor Model

Load pattern	Type	Position	Value	Direction
Weight of the nacelle	Point Load at 3 points	Nacelle CM upwind	453.1 kN	Z axis downwards
Weight of the hub	Point Load at 3 points	Hub CM downwind	112.14 kN	Z axis downwards
Weight of the rotor blades	Point Load at 3 points	Hub CM downwind	151.94 kN	Z axis downwards
Self-weight of the tower	Distributed Load	Along tower	3408.58 kN (total)	Z axis downwards
Thrust force due to wind	Point Load at 3 points	Hub CM downwind	241.52 kN	Y axis downwind
Aerodynamic Torque	Point Load at 3 points	Nacelle CM upwind	802.72 kNm	@ Y axis CCW
Self-weight of frames and cables	Distributed Load	Along frames and cables	Value varies with elements	Z axis downwards

Apart from the static load case, the modal and buckling load cases are defined similar to a single rotor model and the analysis is performed. The design process is iterated to satisfy some design constraints discussed in the next section.

5.7. Model Optimization Methods

The model is optimized subject to the constraints below:

1. The maximum deflection of all nodes of the entire structure should be less than 1 m.
2. All the elements of the support structure should satisfy the stress and buckling criteria i.e. stress ratio < 0.95 and slenderness ratio < 200. This is defined in the SAP2000 Design Code which is AISC-LRFD93. The buckling criterion doesn't apply to the cables since they are tension-only elements. There can be more criteria to improve the design but these are first used to avoid having extremely slender members.
3. The mass of the support structure should be less than 38,831 kg. But, this requirement is flexible as the cost constraint is more important than mass.
4. The cost of the support structure should be less than $476,887

5.7.1. Methods to reduce mass of the support structure

The mass of each element of the support structure is calculated using Eq. (5.44).

$$Mass = \Sigma\ [\rho\ A\ (\Sigma L)] \tag{5.44}$$

Where, ρ is the density of the material of the element, A is the cross section area of the element, and ΣL is the total length of all elements of the same type.

The mass of the support structure can be reduced in the following ways:

1. The number of elements in the model and the dimensions of the spar sections i.e. the base and height of the triangle section can be reduced to reduce the total length of elements ΣL to the extent possible.

2. Smaller I-beam sections with reduced cross-section area *A* can be used. By using I-sections with a lower range of areas *A*, the mass can be further reduced.

5.7.2. Methods to reduce deflection

1. An "Auto-select" list is used as mentioned previously. There is an option in SAP2000 to set a target minimum deflection for a point and then run the analysis. SAP2000 tries to reduce the deflection at that point to the target value.
2. Diagonal bracing is used between frame elements of the spar.
3. The addition of elements at a point in the structure, where the deflection is high, also reduces deflection. However, adding many elements increase the stresses at other points such as the rotor centroid.
4. Increasing the pre-tension in the cables can reduce deflection.
5. The cables are attached closest to the loading point to reduce deflection.
6. Increasing the length of the jib starting from 2 m to 10-20 m and even more reduces the deflection. Using a heavier jib or attaching multiple cables to the jib, are other methods.
7. Bottom up and top down approaches are used to construct the model. The bottom up approach involves starting with the smallest and thinnest structure that exceeds the deflection limit but satisfies the mass limit, and then increasing the dimensions until the optimum point. The top down approach is the reverse.

Although mass and deflection are reduced below the limit, the number of overstressed and buckled members turns out to be high. So to make the structure stiffer, the priority is given to the cost limit instead of the mass limit.

5.7.3. Methods to reduce stress and prevent buckling

1. The same Auto-select list as mentioned in the previous sections is used, and it also satisfies the desired stress and buckling criteria.
2. Dividing elements in general into sections, makes them less susceptible to buckling failure. This applies to the spars and the jib.
3. Use of an I-beam section with a larger cross-section area reduces the stress and prevents buckling.

5.8. Model Solutions

The solution obtained for the three-rotor system is just one of several solutions that could be obtained for designing a support structure subject to the required constraints. The main objective of having a total cost of the three-rotor system less than that of a single-rotor system is satisfied. Different jib and cable configurations are considered such as:

1. Jib lengths of 5 m, 10 m, 15 m and 20 m.
2. Cables of type 1: single cable or multiple cables per spar attached to the jib

The design with multiple cables of type 1 gives better results. The results for the final optimized structure for a configuration of 5 cables of type 1 attached from each spar to the jib are given in Table 19. The pre-tension in cables of type 2 and 3 is each made three times to reduce deflection. Figure 34 provides a front and side view of the final design. As of September 2012, the cost of steel of wide-flange shapes is $790/ton and this is 30% of the fabricated cost [31]. So, the cost of fabricated steel considered here, is $2600/ton.

Table 20. Three-rotor Model Results

Design Criterion	**Results**		
Deflection (downwind side & y-direction)	Top Rotor	0.9855 m (maximum)	
	Left Rotor	0.6101 m	
	Right Rotor	0.6218 m	
	Tower top	0.4043 m	
Stress	Stress ratio of all components < 0.95		
Buckling	Slenderness ratio of all components < 200		
Mass and cost of the support structure	**Component**	**Mass (kg)**	**Cost ($)**
	Jib	1,932	5,023
	Cable 1	1,830	4,758
	Cable 2	3,682	9,572
	Cable 3	2,108	5,481
	Lower link	37,975	98,735
	Spars	67,364	175,145
	Total	**114,891**	**298,714**

The total mass in Table 19 is greater than the target mass of 38,831 kg. But the total cost is less than the target cost of $476,887 and thus our objective is satisfied. Table 21 clearly illustrates the difference in the total mass and total cost of the single-rotor system and the proposed solution of the three-rotor system.

Bending stresses at the tower base using bending moment are calculated by Eq. (5.45).

$$\sigma_b = \frac{M_b y}{I} = \frac{(64551.65\ x\ 10^{-3}) x (\frac{6}{2})}{(\frac{\pi}{32} x (6^4 - 5.9649^4))} = 65.6\ MPa \qquad (5.45)$$

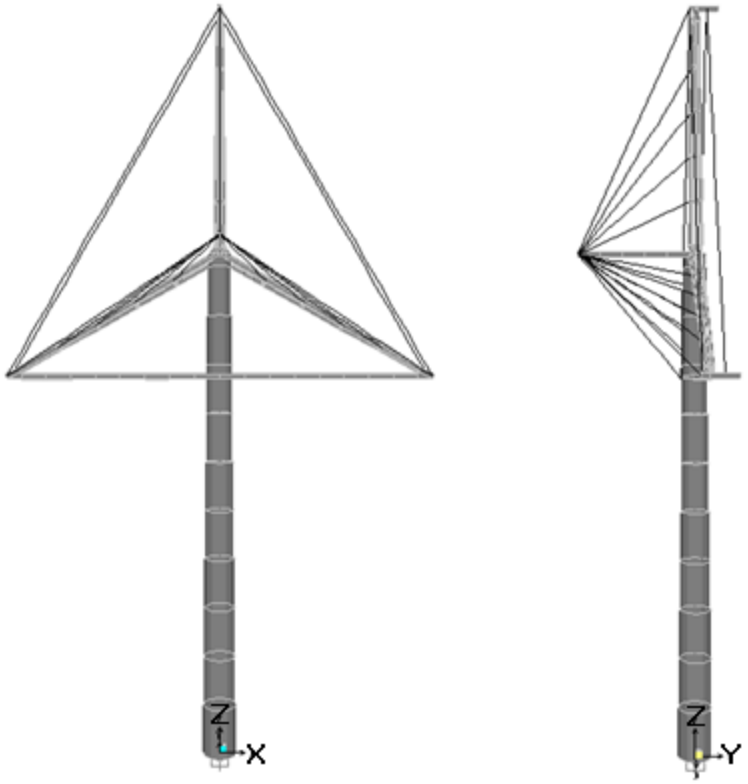

Figure 34. Final Design Solution- Three-Rotor System

Table 21. Comparison of the proposed three-rotor system with the single-rotor system

SYSTEM	Total Mass (kg)	Total Cost ($)
Single-rotor system	601,429	3,809,250
Three-rotor system without support structure	562,598	3,332,363
Three-rotor system (proposed solution)	**677,489**	**3,631,077**

This shows that the stresses are within the limit of the minimum specified yield strength of steel, which is 344 MPa.

Comparing the above results in Table 21 with the final three-rotor MRWT values obtained in the work by Verma [32], i.e. a mass of 735,200 kg and cost of $3,730,150, this MRWT is lighter and even costs less. This could be attributed to the different cost of steel considered as well as differences in certain component values.

CHAPTER 6

THREE-ROTOR ANALYSIS – ANALYSIS OF SPECIAL CASES

While the three-rotor model was developed and analyzed in the previous chapter, this chapter discusses some additional analysis namely, the following cases:

1. Two-bladed Three-rotor model with and without gearbox
2. Three-rotor model with no or zero thrust and torque loads
3. Three-rotor model - Order of Assembly of the components of the support structure.
4. Comparison between each turbine of the Three-rotor model with the WindPACT 1.5 MW turbine.

6.1. Two-Bladed case

One of the objectives of this thesis is the reduction of the total cost of a MRWT system. While trying to achieve cost reduction to the extent possible, a special case of a three-rotor system involving two bladed rotors is considered.

When the number of blades of a HAWT is changed from three to two, the optimum tip speed ratio (T.S.R.) λ changes, so that the aerodynamic properties including the blade dimensions remain constant.

6.1.1 Determination of optimum T.S.R. for two-bladed turbine

The NREL 5 MW turbine, having a three-bladed rotor, has an optimum T.S.R. of 7.55 at the peak power coefficient as per Jonkman et al. [7]. The design code WT_Perf [19] is used for obtaining the optimum T.S.R for an equivalent two-bladed rotor. The WT_Perf input file is

created for the NREL 5 MW three-bladed turbine with the following parameters. The airfoil data is also taken from reference [7].

Table 22. WT_Perf Input parameters for the 3-bladed 5 MW rotor

Parameter	**Value**
Rotor radius	63 m
Hub radius	1.5 m
Precone	2.5 deg
Tilt	5 deg
Hub height	90 m
Blade pitch variation	-7 to 7 deg
T.S.R. variation	4 to 10
Rotor speed	12.1 rpm

The result is a graph as shown in Figure 35 called the C_p-λ curve, which is different for different blade pitch angles. The maximum value of λ is the optimum T.S.R. at C_p = 0.4855 is 7.5, which matches the value from Jonkman et al. as mentioned above.

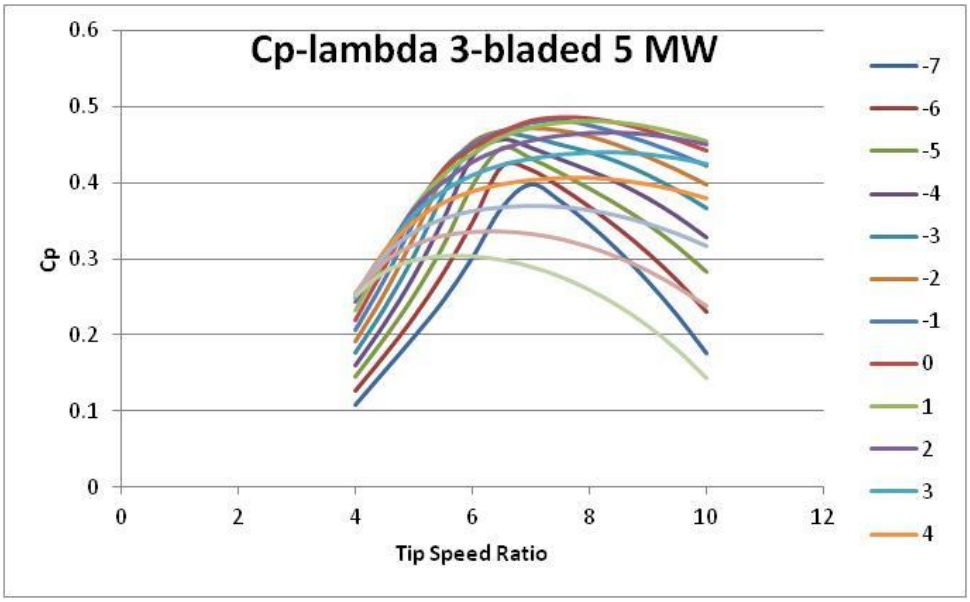

Figure 35. C_p-λ curves for three-bladed NREL 5 MW

Keeping all the above inputs the same, the number of blades is changed from 3 blades to 2 blades of the same size. The result is now as shown in Figure 36 and the optimum T.S.R. for Cp = 0.466 is 9.

Therefore, we study a two-bladed case having a T.S.R. equal to 9, with and without a gearbox. The number of blades is also changed from 3 to 2 and the 5 MW design is downscaled to 1.67 MW in the scaling model by selecting three rotors.

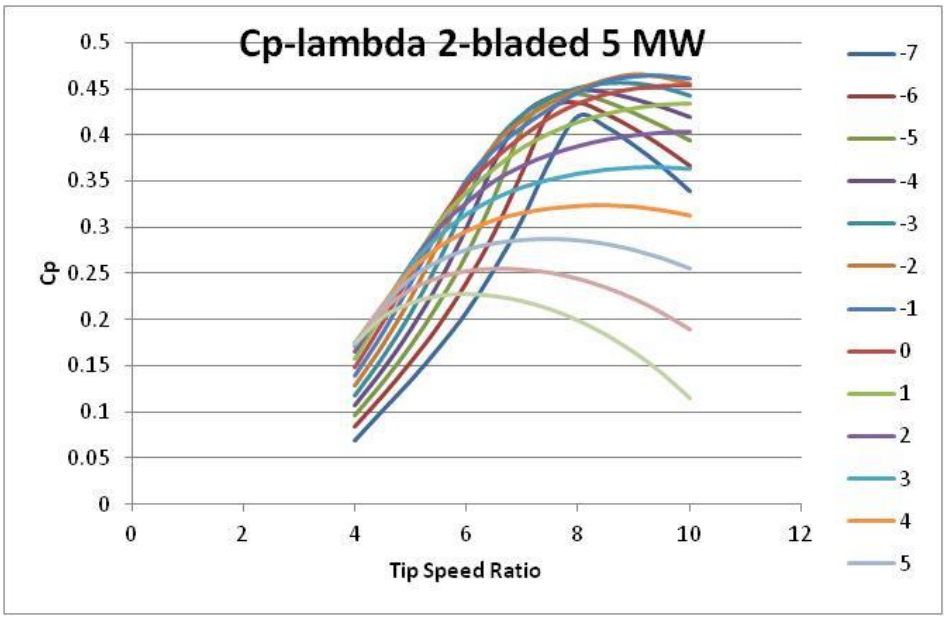

Figure 36. C_p-λ curves for two-bladed 5 MW

6.1.2. Two-Bladed case with gearbox

Initially for a three-bladed 5 MW turbine, the T.S.R. is given by the relation below.

$$T.S.R. = \frac{Tip\ Speed}{Wind\ speed} = \frac{\Omega R}{U} \tag{6.1}$$

$$7 = \frac{\left(\frac{2\pi}{60} * 12.1\right) * 63}{11.4} \tag{6.2}$$

For a three-bladed 1.67 MW turbine used in the three-rotor model, the T.S.R. is the shown in Eq. (6.3). Notice that the rotational speed is now 21 rpm.

$$7 = \frac{\left(\frac{2\pi}{60} * 21\right) * 36.37}{11.4} \tag{6.3}$$

For a two-bladed 1.67 MW turbine in the three-rotor model, as per WT_Perf, the T.S.R. becomes 9 as per section 5.1.1.

$$9 = \frac{\left(\frac{2\pi}{60} * 26.94\right) * 36.37}{11.4} \quad (6.4)$$

The rotational speed changes from 21 rpm to 26.94 rpm. Based on the WT_Perf results and the above equation, the inputs to the Baseline scaling model for a two-bladed three-rotor gearbox case are:

1. The number of blades B = 2.
2. The number of rotors is three.
3. The tip speed ratio is 9. With a wind speed of 11.4 m/s, the new tip speed is 102.6 m/s.
4. The rated rotor RPM is 26.94 rpm.
5. The turbine has a gearbox. (Direct drive = False)

With these modified inputs to the scaling model, we get the following mass and cost results.

Table 23. Two-bladed three-rotor 5 MW with T.S.R. 9 and gearbox

BASELINE	**1-Rotor 5 MW**		**3-Rotor 5 MW, 1.67 MW each**			
	B=3, λ=7.5		B=3, λ=7.5		**B=2, λ=9**	
Components	**Mass(kg)**	**Cost($)**	**Mass(kg)**	**Cost($)**	**Mass(kg)**	**Cost($)**
Blades	76,843	778,421	46,466	470,696	30,977	313,798
Hub	30,116	127,995	31,817	135,222	31,817	135,222
Nose Cone	1,810	10,085	2,476	13,791	2,476	13,791
Pitch System	14,423	183,551	11,613	147,798	8,950	113,903
Low speed shaft	16,526	115,670	10,147	71,020	10,147	71,020
Main bearing	5,400	95,050	2,334	41,086	2,334	41,086
Variable speed electronics	-	395,000	-	395,000	-	395,000
Yaw system	13,152	113,896	17,098	120,896	17,098	120,896
Brake & coupling	994	9,946	995	9,946	995	9,946
Electrical system	-	200,000	-	200,000	-	200,000
Hydraulic & Cooling system	400	60,000	400	60,000	400	60,000
Nacelle Cover	6,154	61,535	6,923	69,234	6,923	69,234
Gearbox	39,688	661,203	34,086	567,876	28,220	470,152
Generator	16,690	324,960	18,178	353,918	18,178	353,918
Mainframe, Platform & Railing	31,773	150,748	32,605	154,690	32,605	154,690
Tower	347,460	521,190	347,460	521,190	347,460	521,190
TOTAL	**601,429**	**3,809,250**	**562,598**	**3,332,363**	**538,580**	**3,043,846**

The three-bladed 1.67 MW case yields a mass reduction of 38,831 kg (6.46%) and a cost reduction of $476,887 (12.5%). With a two-bladed gearbox case, a mass reduction of 62,849 kg (10.45%) and a cost reduction of $765,404 (20.1%) would be possible. This is without considering the mass and the cost of the support structure.

There may be a need to consider the fact that hubs on two-bladed turbines could be more expensive than those for three-bladed machines and that factor although not determined here, needs to be taken into account.

6.1.3. Two-Bladed case without gearbox (direct drive)

Now a two-bladed case with a direct-drive generator is considered. The scaling model inputs are the same as in section 5.1.2 except that the turbine has no gearbox (Direct Drive = True).

Table 24. Two-bladed three-rotor 5 MW with T.S.R. 9 with direct-drive

BASELINE	**1-Rotor 5 MW**		**3-Rotor 5 MW, 1.67 MW each**			
	B=3, λ=7.5		B=3, λ=7.5		**B=2, λ=9, Direct Drive**	
Components	**Mass(kg)**	**Cost($)**	**Mass(kg)**	**Cost($)**	**Mass(kg)**	**Cost($)**
Blades	76,843	778,421	46,466	470,696	30,977	313,798
Hub	30,116	127,995	31,817	135,222	31,817	135,222
Nose Cone	1,810	10,085	2,476	13,791	2,476	13,791
Pitch System	14,423	183,551	11,613	147,798	8,950	113,903
Low speed shaft	16,526	115,670	10,147	71,020	10,147	71,020
Main bearing	5,400	95,050	2,334	41,086	2,334	41,086
Variable speed electronics	-	395,000	-	395,000	-	395,000
Yaw system	13,152	113,896	17,098	120,896	17,098	120,896
Brake & coupling	994	9,946	995	9,946	995	9,946
Electrical system	-	200,000	-	200,000	-	200,000
Hydraulic & Cooling system	400	60,000	400	60,000	400	60,000
Nacelle Cover	6,154	61,535	6,923	69,234	6,923	69,234
Gearbox	39,688	661,203	34,086	567,876	0	0
Generator	16,690	324,960	18,178	353,918	98,214	1,012,582
Mainframe, Platform & Railing	31,773	150,748	32,605	154,690	17,930	56,540
Tower	347,460	521,190	347,460	521,190	347,460	521,190
TOTAL	**601,429**	**3,809,250**	**562,598**	**3,332,363**	**575,721**	**3,134,208**

The three-bladed 1.67 MW case yields a mass reduction of 38,831 kg (6.46%) and a cost reduction of $476,887 (12.5%) compared to the single-rotor three-bladed 5 MW. With a two-bladed direct-drive case, a mass reduction of 25,708 kg (4.27%) and a cost reduction of $198,155 (5.2%) would be possible. This is without considering the mass and the cost of the support structure.

The gearbox case is preferred over the direct-drive case since the cost reduction is greater. This would be attributed to the high cost of the direct-drive generator, in the latter case, which depends on the rotor torque, even though there is no gearbox cost.

6.1.4. Overall comparison of different systems

Table 25 compares the two and three-bladed systems with the gearbox and direct-drive cases on a total system basis including the support structure. The two-bladed gearbox case seems to be the best in terms of achievable cost reduction.

Table 25. Total system comparison – two and three-bladed systems

Values		**Gearbox**		**Direct Drive**	
3-bladed 1-rotor	**Mass (kg)**	601,429	(0%)	634,085	(+5.43%)
	Cost ($)	3,809,250	(0%)	3,865,976	(+0.42%)
3-bladed 3-rotor	**Mass (kg)**	677,489	(+12.65%)	708,764	(+17.85%)
	Cost ($)	3,631,077	(-4.68%)	3,623,715	(-4.87%)
2-bladed TSR 9 3-rotor	**Mass (kg)**	653,471	(+8.65%)	690,612	(+14.83%)
	Cost ($)	3,342,560	(-12.25%)	3,432,922	(-9.88%)

6.2. Zero Thrust and Zero Torque case

When the three-rotor system is being installed or when the blades are pitched out of the wind, the thrust and torque loads due to the wind do not act on the blades. At this point, the cables which are pre-tensioned might undergo deflection in the opposite direction. Therefore, it becomes essential to analyze the case of zero thrust and zero torque. This case is analyzed in SAP2000 by setting the thrust and torque loads on each of the three-rotors to zero.

Following are the results for deflection and stress.

1. Maximum Deflection = 0.1488 m
2. Minimum Deflection = -0.2922 m
3. All stress ratios within 0.95 (stress criterion satisfied)
4. All slenderness ratios within 200 (buckling criterion satisfied)

6.3. Order of Assembly and Loads

The support structure is assembled in stages and two options are considered. The tower and support frames would be the first step in either case. This would be followed by the cables or the RNAs of the three turbines. Ultimately, the blades would be pitched into the wind.

The weight of the cables for the three-rotor model, 7,620 kg is much less than the weight of all the RNAs, 212,507 kg. Therefore, the RNAs are assembled first and then the cables. This would prevent any deflection in the cables which might result while attaching the RNAs.

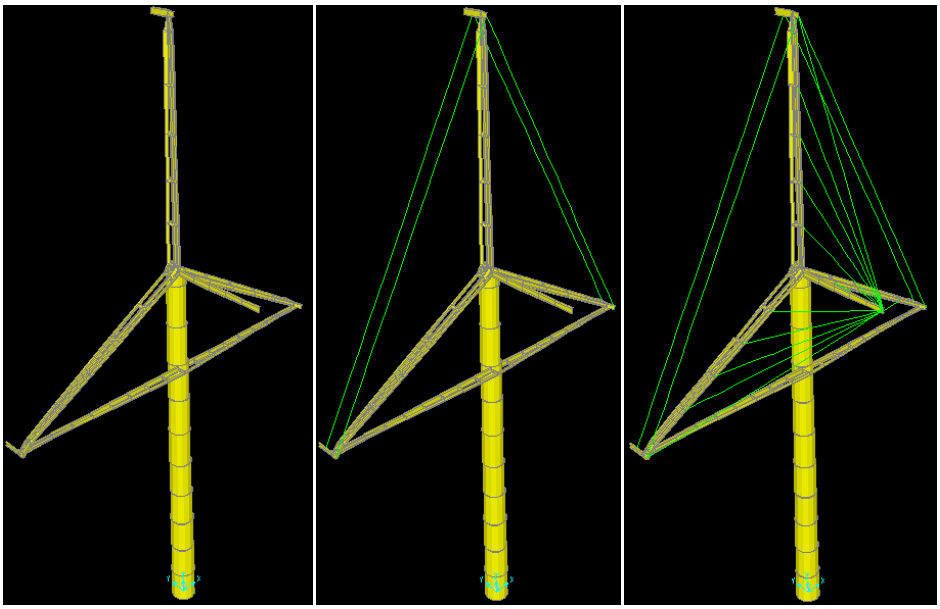

Figure 37. Order of Assembly – Structure, RNAs and Cables

Therefore, the order of assembly and loads for a three-rotor model in SAP2000 is as follows.

1. Tower
2. Support Structure
3. RNAs
4. Cable #2, #3 then #1, one by one each.
5. Thrust and Torque loads (Pitch blades into the wind)

Figure 37 shows the sequence in which the components of the structure are assembled. In the first figure, the tower, the support structure and the RNAs have been attached. In the next figure cables of type #2 and #3 are attached and finally in the last figure, cables of type #1 have been attached.

Table 26 shows this order being followed for assembly and the SAP2000 results for each step. The maximum and the minimum deflections for the entire system are noted along with the maximum angular deflection. Initially, a large angular deflection is observed at the tips of the lower rotors, which decreases as the cables are attached. The deflection, stress and buckling criteria as mentioned in section 4.8 are satisfied at each stage.

6.4. Comparison with the 1.5 MW WindPACT Turbine

In order to verify that the accuracy of the baseline scaling relations is within an acceptable limit, the 1.67 MW turbine model is compared with another turbine design namely, the 1.5 MW WindPACT Turbine. Even though the rated power is slightly different, the mass and cost values of the components are expected to be within 10%.

Table 26. Order of Assembly and Results for Each Step

Assembly Stage	Deflection	Angular Deflection	Stress Criterion Fulfilled	Buckling Criterion Fulfilled
1) Tower & Support Structure, RNAs	Max= 0.306 m, Min = -0.389 m	4˚- 5˚	Yes	Yes
2) Cable 2 #1	Max = 0.317 m, Min = -0.385 m	4˚ - 5˚	Yes	Yes
3) Cable 2 #2	Max = 0.256 m, Min = -0.335 m	3.5˚ – 4˚	Yes	Yes
4) Cable 3 #1	Max = 0.258 m, Min = -0.336 m	3˚ – 4˚	Yes	Yes
5) Cable 3 #2	Max = 0.191 m, Min = -0.226 m	2˚ – 3˚	Yes	Yes
6) Cable 1 #1	Max= 0.163 m, Min = -0.213 m	2˚ – 3˚	Yes	Yes
7) Cable 1 #2	Max= 0.163 m, Min = -0.213 m	2˚ – 3˚	Yes	Yes
8) Cable 1 #3	Max= 0.163 m, Min = -0.213 m	2˚ – 3˚	Yes	Yes
9) Cable 1 #4	Max= 0.163 m, Min = -0.213 m	2˚ – 3˚	Yes	Yes
10) Cable 1 #5	Max= 0.163 m, Min = -0.213 m	2˚ – 3˚	Yes	Yes
11) Cable 1 #6	Max= 0.164 m, Min = -0.213 m	2˚ – 3˚	Yes	Yes
12) Cable 1 #7	Max= 0.165 m, Min = -0.213 m	2˚ – 3˚	Yes	Yes
13) Cable 1 #8	Max= 0.166 m, Min = -0.213 m	2˚ – 3˚	Yes	Yes
14) Cable 1 #9	Max= 0.167 m, Min = -0.213 m	2˚ – 3˚	Yes	Yes
15) Cable 1 #10	Max= 0.168 m, Min = -0.213 m	2˚ – 3˚	Yes	Yes
16) Cable 1 #11	Max= 0.149 m, Min = -0.213 m	2˚ – 2.5˚	Yes	Yes
17) Cable 1 #12	Max= 0.131 m, Min = -0.213 m	2˚ – 2.5˚	Yes	Yes
18) Cable 1 #13	Max= 0.105 m, Min = -0.213 m	2˚ – 2.5˚	Yes	Yes
19) Cable 1 #14	Max= 0.080 m, Min = -0.213 m	2˚ – 2.5˚	Yes	Yes
20) Cable 1 #15	Max= 0.075 m, Min = -0.213 m	1.5˚ – 2˚	Yes	Yes
21) Torque & Thrust	Max= 0.986 m, Min = -0.534 m	1.5˚ – 2˚	Yes	Yes

As previously stated, each of the rotors of the three-rotor 5 MW model (1.67 MW each) is downscaled from the 5 MW baseline model. The rotor diameters for the 1.67 MW model and the 1.5 MW WindPACT Turbine are 72.74 m and 70 m respectively. Table 27 compares all the components of both the above systems except the tower, since the 5 MW baseline tower is different from the 1.5 MW WindPACT turbine tower.

The mass and the cost values for the 1.67 MW model in Table 27 are obtained by dividing the values of the three-rotor model in Table 12 by a factor of 3, except for the yaw bearing.

The values for the yaw bearing is downscaled from the 5 MW model and is different from the one used to support the three-rotor model.

Table 27. Comparison Between 1.67 MW Model and the 1.5 MW WindPACT Turbine

BASELINE	**Each 1.67 MW turbine of the Three rotor Model**		**1.5 MW WindPACT**	
Components	**Mass(kg)**	**Cost($)**	**Mass(kg)**	**Cost($)**
Rotor	15,489	156,899	12,690	152,000
Hub	10,606	45,074	12,516	48,000
Nose Cone	825	4,597	775	4,000
Pitch System	3,871	49,266	3,588	36,000
Low speed shaft	3,382	23,670	3,025	20,000
Main bearing	778	13,695	679	12,000
Variable speed electronics	-	131,667	-	81,000
Yaw system	2,130	18,447	1,875	12,000
Brake & coupling	332	3,315	-	3,000
Electrical system	-	66,667	-	60,000
Hydraulic & Cooling system	133	20,000	120	7,000
Nacelle Cover	2,308	23,078	2,351	36,000
Gearbox	11,362	189,292	10,603	161,000
Generator	6,059	117,973	5,421	78,000
Mainframe, Platform & Railing	10,868	51,563	15,057	66,000
TOTAL	**68,143**	**865,937**	**68,700**	**776,000**

The 1.5 MW WindPACT turbine data is found from sources [6], [11] and [14]. Since both set of values have the same order of magnitude and are approximately within 10% of the WindPACT values, it can be concluded that the baseline scaling relations are reasonably accurate and suitable for analysis.

The low speed shaft cost equation from reference [6] is supposed to be $0.1D^{2.887}$ instead of $0.01D^{2.887}$ so as to be the same order of magnitude as the cost of the low speed shaft of the WindPACT 1.5 MW or of the NREL 5 MW turbine.

6.5. Comparison with the 20 MW UpWind Project

The scaling done till now was with multiple small rotors and then comparing those systems with large single rotors. Consider now a different case in which multiple large rotors namely 5 MW rotors are compared with an even larger rotor namely the 20 MW. This UpWind 20 MW project funded by the EU [4] is also in a conceptual design phase and the rotor and nacelle masses [36] are obtained by upscaling the 5 MW. As shown in Table 28, the 20 MW upscaled system using baseline scaling matches with the one in ref. [36]. Also, the Multi-rotor system offers advantages in terms of mass even at a higher level of rated power. The tradeoffs would be associated with the added complexity of the support structure.

Table 28. Comparison of a 20 MW Multi-rotor system with the UpWind project

Mass (kg)	**Multi-Rotor 20 MW (4 X 5MW)**	**Upscaled 20 MW**	**Upwind 20 MW (upscaled) [36]**
Blades	307,372	579,894	
Hub	120,464	190,086	
Nose Cone	7,240	4,142	
TOTAL ROTOR	**435,076**	**774,122**	**770,000**
Pitch System	57,692	100,935	
Low speed shaft	66,104	122,330	
Main bearing	21,600	61,712	
Variable speed electronics	-	-	
Yaw system	52,608	130,799	
Brake & coupling	3,976	3,976	
Electrical system	-	-	
Hydraulic & Cooling system	1,600	1,600	
Nacelle Cover	24,616	23,459	
Gearbox	158,752	192,356	
Generator	66,760	59,944	
Mainframe, Platform & Railing	127,092	109,351	
TOTAL NACELLE	**580,800**	**806,462**	**880,000**

CHAPTER 7

DYNAMIC ANALYSIS

There has only been a static analysis of the three-rotor model performed in Chapter 4 and 5 i.e. at the rated wind speed conditions. In order to prove that the design is safe for all other conditions including turbulent wind, a dynamic analysis is carried out.

7.1. Recompiled FAST with Controller

For obtaining accurate results for the dynamics, an appropriate dynamic wind turbine controller is required. Therefore, the FAST design code is either recompiled with the controller file or a previously recompiled FAST version that is readily available is used. In this analysis, a FAST v7.01 that has been recompiled with the 'BladedDLLInterface' controller is used. The controller is defined according to the NREL 5 MW baseline turbine. Subroutines such as UserYawCtrl, PtchCont, UserVSCont in the FAST file are turned ON. The BladedDLLInterface allows the user to control pitch, HSS brake torque, electrical generator torque and/or nacelle yaw with a single master controller even if the user does not use the Bladed code or does not work with DLLs [29].

7.2. Dynamic Analysis

The following six cases for the dynamic analysis are evaluated.

1. Steady wind – 3 m/s, 7 m/s, 11.4 m/s, 18 m/s, 25 m/s
2. Time History Analysis – Continuously varying wind speeds
3. Modal Analysis and Campbell diagram
4. Drag Forces

5. Turbulent Wind – NTM Model
6. Extreme Condition – 50-year EOG

7.2.1. Steady Wind

The first case considered is that of several constant wind speed conditions. The five wind speeds analyzed are the cut-in [3 m/s], below rated [7 m/s], rated wind [11.4 m/s], above rated [18 m/s] and cut-out [25 m/s] speeds.

The input files with these wind speed conditions are defined and successively used in the FAST code for the NREL 5 MW baseline turbine. The FAST results, namely thrust and torque loads, are downscaled for each of the 1.67 MW turbines of the three-rotor model, keeping in mind the following points.

1. Thrust load for the 1.67 MW turbine downscales by 1/3 of its value for the 5 MW turbine.
2. Torque load for the 1.67 MW turbine downscales by $1/3\sqrt{3}$ of that for the 5 MW turbine.

The other loads are constant and these include the weights of the nacelle, the hub and the rotor as well as the self-weight of the frames and cables. Ultimately, these loads are applied to the SAP2000 three-rotor model to obtain the deflection and stress results shown in Table 29.

The SAP2000 results satisfy the design criteria. Also the thrust and torque loads follow a similar trend as that given in [7] for the NREL 5 MW baseline turbine as shown in Figure 38.

Table 29. Steady Wind Conditions - Results

Wind Speed	FAST Results for 5 MW		FAST Results for 1.67MW (scaled)		SAP2000 Results		
	Thrust (kN)	Torque (kNm)	Thrust (kN)	Torque (kNm)	Max Deflection (m)	Position of max deflection	Stress & Buckling Ratios
3 m/s Cut-in	78.08	56.21	26.03	10.82	0.115	Right hand rotor (from upwind)	Within limits
7 m/s	304.2	1441	101.40	277.32	0.378	Top-rotor (y-defl)	Within limits
11.4 m/s Rated	667.8	4169	222.6	802.32	0.803	Top-rotor (y-defl)	Within limits
18 m/s	349	4179	116.33	804.25	0.458	Top-rotor (y-defl)	Within limits
25 m/s Cut-out	271.5	4178	90.5	804.06	0.3	Top-rotor (y-defl)	Within limits

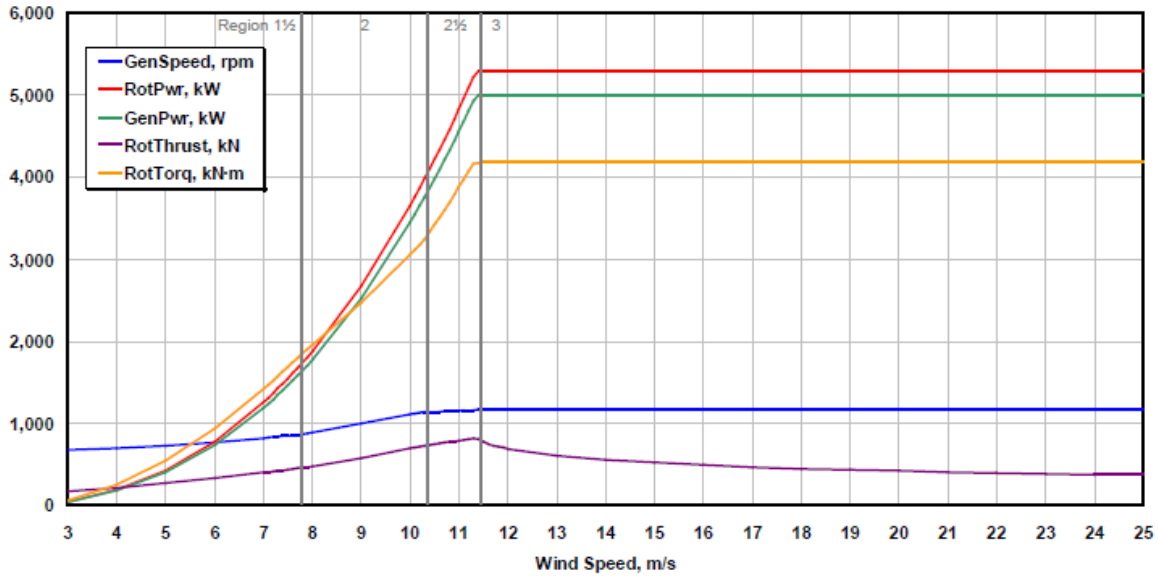

Figure 38. NREL 5 MW Baseline turbine – Steady Wind Results [7]

7.2.2. Time History Analysis

The time history analysis is the more general form of the steady wind case, as the three-rotor model is analyzed for all constant wind speeds from the cut-in [3 m/s] to cut-out [25 m/s]

wind speeds. These wind speeds are simulated in FAST to obtain the thrust and torque loads, which are in turn used in the SAP2000 model to obtain the deflection and stress results.

In SAP2000, 'Time history' load cases and load functions are defined using the 'Function' tab in the Define menu. The time series is then referred to in the load case definition. The modal damping ratio is chosen at 5% or 0.05.

Wind shear could have been considered to obtain different wind speeds at different rotor hub heights. But the controller adjusts the thrust coefficient as per the speed to maintain the same thrust load. So, wind shear is neglected and the thrust load is the same for all three rotors.

The NREL 5 MW single-rotor model is first implemented in FAST for time history analysis. The wind speed varies from 3 m/s to 25 m/s in steps of 0.05 m/s. With a time step of 1 second, the total simulation time becomes 440 seconds for this wind speed data. The thrust and torque loads are then obtained as shown in Figure 39 and 40 which are used as inputs in the SAP2000 model.

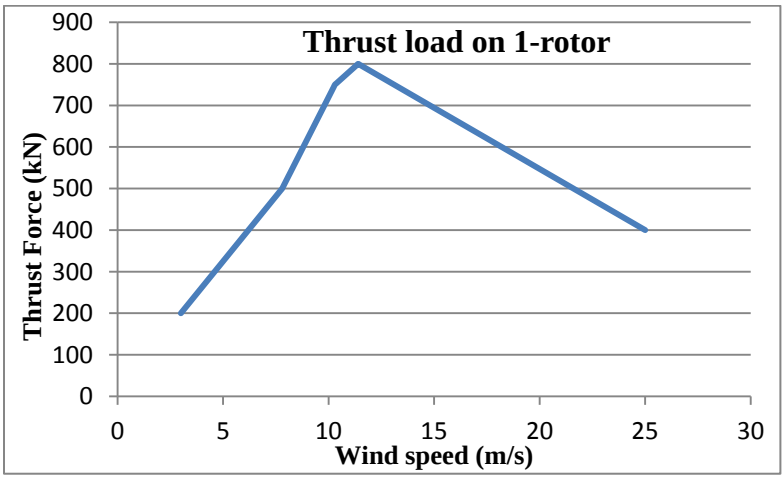

Figure 39. Thrust load on a Single-rotor NREL 5 MW model

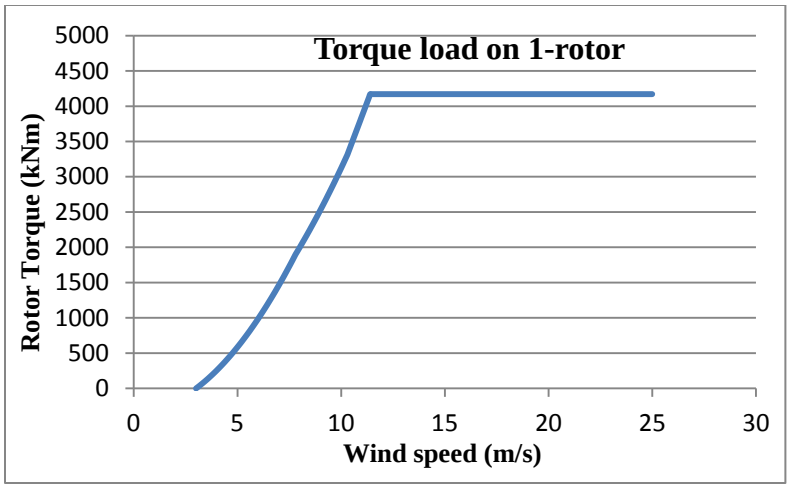

Figure 40. Torque load on a Single-Rotor NREL 5 MW model

The thrust and torque loads for the 1.67 MW model as shown in Figure 41 and 42 are then obtained by scaling down the 5 MW results. These loads are used as inputs in the SAP2000 model. The results for the single-rotor and the three-rotor 5 MW model are summarized in Table 30.

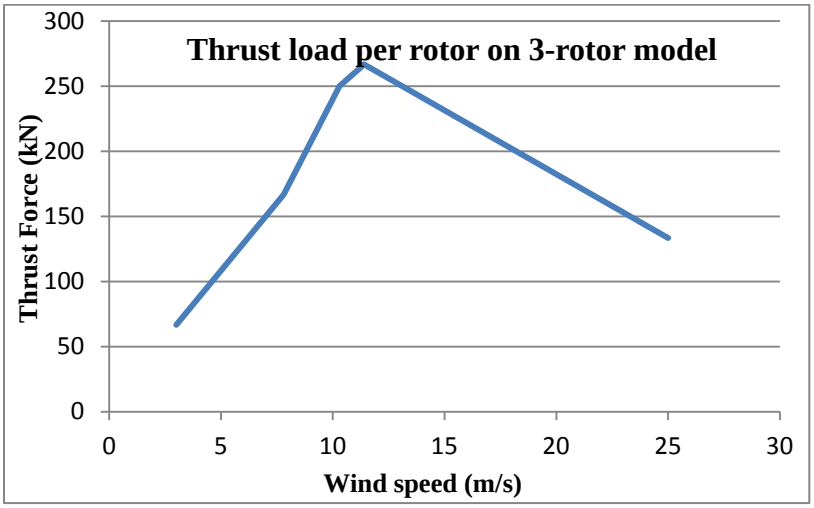

Figure 41. Thrust load per rotor for the Three-Rotor 5 MW model

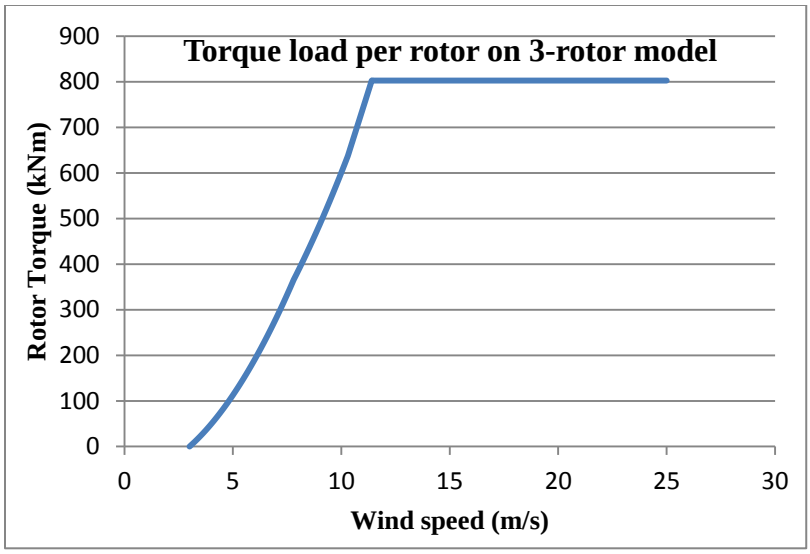

Figure 42. Torque load per rotor for the Three-Rotor 5 MW model

Table 30. Time History Results

Criteria	**Single-Rotor 5 MW**	**Three-Rotor 5 MW**	
Max Deflection	0.453 m	(y-deflection & downwind)	
		Top Rotor	0.879 m (maximum)
		Left Rotor	0.448 m
		Right Rotor	0.453 m
		Tower Top	0.455 m
Min Deflection	-0.026 m	-0.064 m	
Stress ratios < 0.95	Yes	Yes	
Slenderness ratios < 200	Yes	Yes	

The deflection at the point where it is maximum is plotted with respect to time for the two models as shown in Figures 43 and 44. The results are all within limits of the design criteria of deflection, stress and buckling.

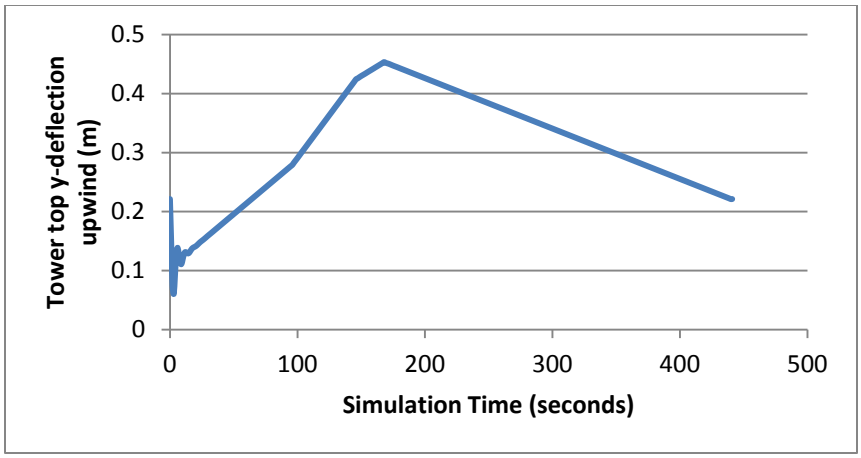

Figure 43. Deflection at pt. of maximum deflection – Single-Rotor 5 MW Time history

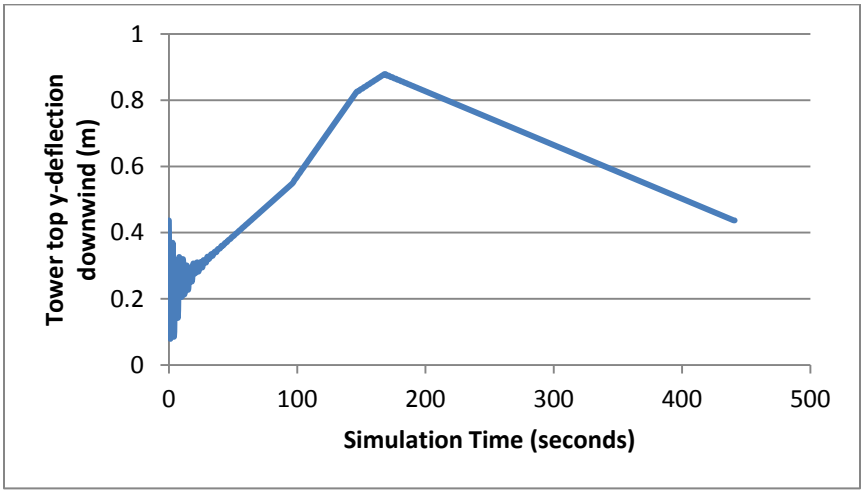

Figure 44. Deflection at pt. of maximum deflection – Three-Rotor 5 MW Time history

The point of maximum deflection is found to be near the top rotor on the upwind side.

7.2.3. Modal Analysis

Modal analysis of the three-rotor model is necessary in order to determine the natural frequency of the support structure and the blade and rotor rotation frequencies, and to prevent any resonance conditions at the critical rotor speeds that may affect the stability of the structure. The NWTC Design code Modes is used to evaluate these natural frequencies. The

critical rotor speeds of the system, which are to be avoided for safe operation, are then obtained by plotting the Campbell diagram [5].

Modal analysis is done in SAP2000 by either choosing Eigen vectors or Ritz vectors. Ritz vector analysis yields more accurate mode shapes as Ritz vectors are generated by taking into account the spatial distribution of dynamic loading [27]. As the structure being analyzed involves a great deal of complexity, Ritz vectors would be more suitable for determining the mode frequencies.

The analysis starts with the Modes input file. The data for the NREL 5 MW single-rotor model [7] is used to initially analyze the single-rotor model. The natural frequencies of the first 5 mode shapes obtained from Modes are compared with the 5 modal frequencies obtained from the Modal analysis of the SAP2000 model as shown in Table 31. The mode shapes are shown in Figure 45.

Table 31. Single-rotor model tower natural frequencies from Modes and from SAP2000

Tower Mode	Freq from Modes	Freq from SAP2000	Mode type
1	0.898 Hz	0.835 Hz	Fore-aft
2	4.430 Hz	4.343 Hz	Fore-aft
3	11.733 Hz	26.720 Hz	Twisting
4	24.745 Hz	33.667 Hz	Twisting
5	74.515 Hz	81.008 Hz	Side-side

The natural frequencies from Modes and those from SAP2000, especially for the first 2 mode shapes are approximately the same.

Now, with the similar method, the natural frequencies of the three-rotor model i.e. the structure which includes the tower and the support structure are obtained from SAP2000. These are as shown in Table 32. The mode shapes are shown in Figure 46.

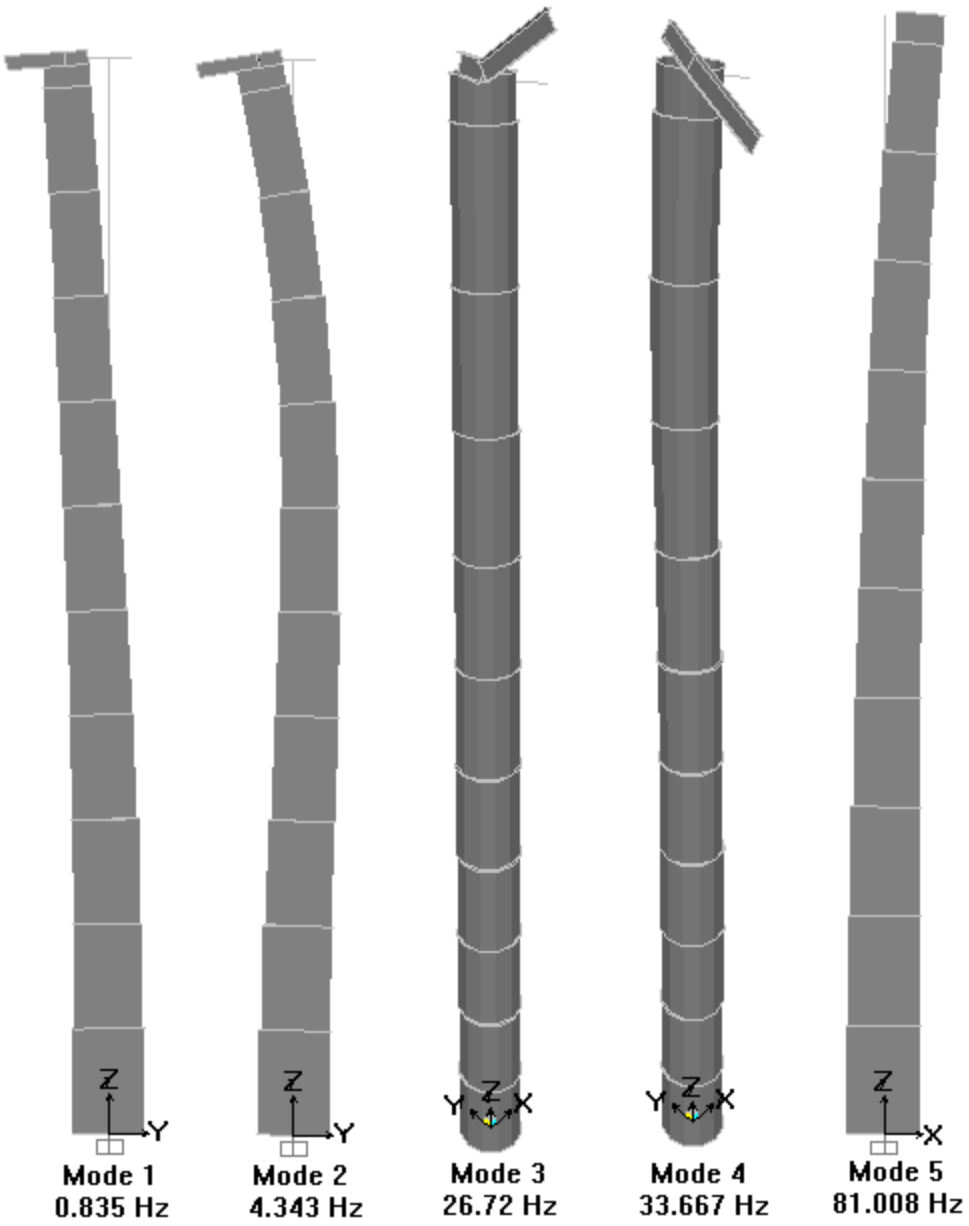

Figure 45. Mode shapes for the single-rotor model

Table 32. Three-rotor model structure natural frequencies from SAP2000

Structure Mode	Natural Frequency	Mode type
1	0.266 Hz	Fore-aft
2	1.531 Hz	Twisting
3	2.876 Hz	Side-side
4	3.195 Hz	Twisting
5	4.388 Hz	Twisting

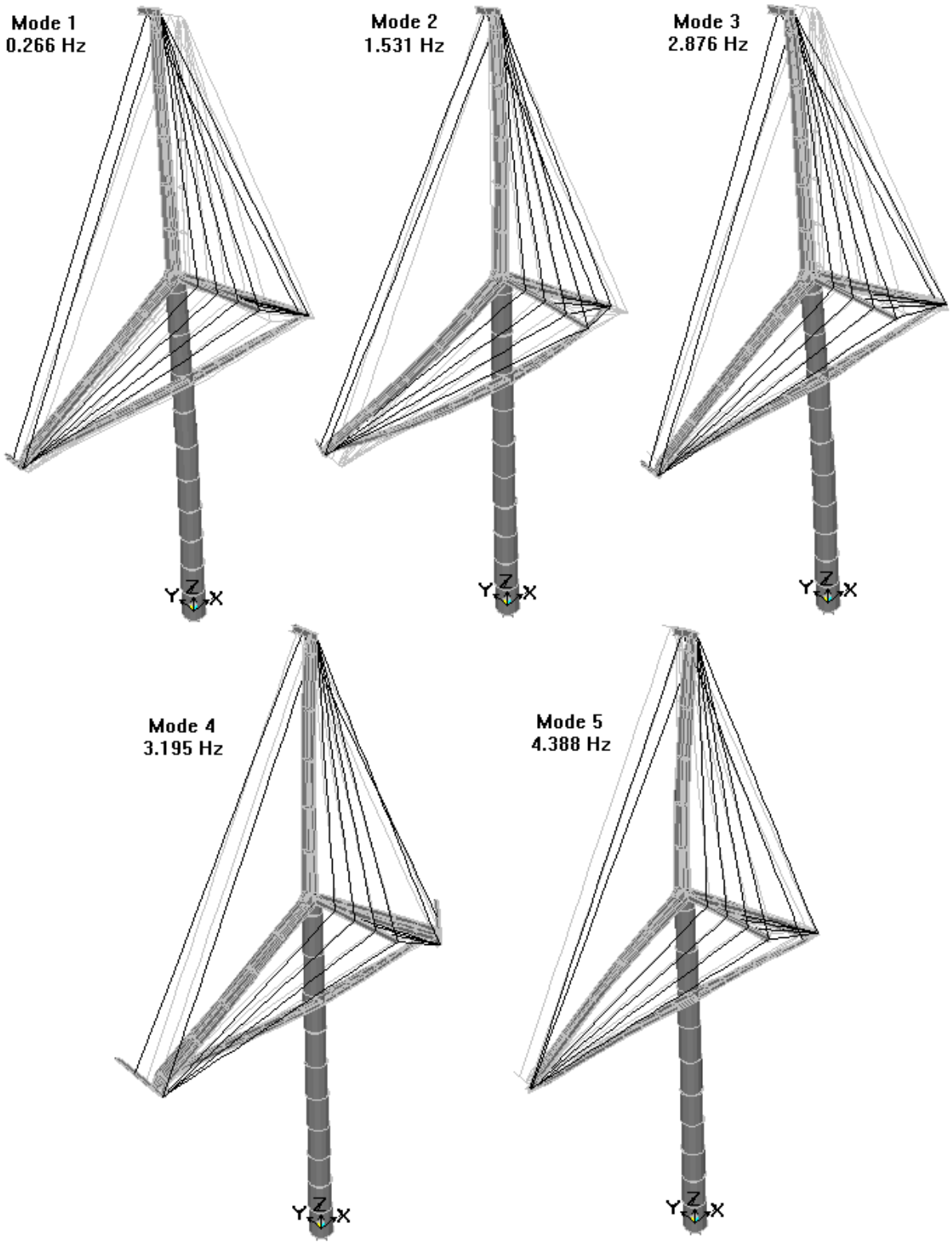

Figure 46. Mode shapes for the Three-rotor model

7.2.3.1 Campbell Diagram

In order to plot the Campbell diagram for the three-rotor model, the blade aerodynamic properties of the NREL 5 MW single-rotor model are downscaled to obtain the blade aerodynamic properties of the 1.67 MW blade used in the three-rotor model.

Table 33 uses the blade aerodynamic properties as obtained from [7] to calculate the mass and stiffness of each airfoil section.

Table 33. NREL 5 MW blade aerodynamic properties used in Modes [7]

NREL 5MW Baseline (Fingersh et al.)									
Node	**RNodes**	**AeroTwst**	**DRNodes**	**Chord**	**Airfoils**	**r/R**	**mass/len**	**flap stiff**	**edge stiff**
	(m)	**(°)**	**(m)**	**(m)**					
						0	678.935	18,110,000,000	18,113,600,000
1	2.8667	13.308	2.73	3.542	Cylinder1	0.044	740.55	17,455,900,000	19,497,800,000
2	5.6	13.308	2.73	3.854	Cylinder1	0.089	450.275	7,229,720,000	10,220,600,000
3	8.3333	13.308	2.73	4.167	Cylinder2	0.133	382.062	4,980,060,000	6,884,440,000
4	11.75	13.308	4.1	4.557	DU40_A17	0.199	406.186	3,386,520,000	7,081,700,000
5	15.85	11.48	4.1	4.652	DU35_A17	0.267	346.538	2,271,990,000	4,808,020,000
6	19.95	10.162	4.1	4.458	DU35_A17	0.333	330.004	1,828,250,000	4,244,070,000
7	24.05	9.011	4.1	4.249	DU30_A17	0.399	313.82	1,361,930,000	3,750,760,000
8	28.15	7.795	4.1	4.007	DU25_A17	0.467	287.12	875,800,000	3,139,070,000
9	32.25	6.544	4.1	3.748	DU25_A17	0.533	253.207	534,720,000	2,554,870,000
10	36.35	5.361	4.1	3.502	DU21_A17	0.599	220.638	314,540,000	1,828,730,000
11	40.45	4.188	4.1	3.256	DU21_A17	0.667	179.404	175,880,000	1,323,360,000
12	44.55	3.125	4.1	3.01	NACA64_A17	0.733	154.41	107,260,000	1,020,160,000
13	48.65	2.319	4.1	2.764	NACA64_A17	0.799	129.55	76,310,000	709,610,000
14	52.75	1.526	4.1	2.518	NACA64_A17	0.867	98.776	49,480,000	454,870,000
15	56.1667	0.863	2.73	2.313	NACA64_A17	0.911	72.906	30,410,000	304,730,000
16	58.9	0.37	2.73	2.086	NACA64_A17	0.956	55.914	16,000,000	137,880,000
17	61.6333	0.106	2.73	1.419	NACA64_A17	0.999	10.319	170,000	5,010,000
	Blade Length		61.5						

The following points are taken into account while downscaling the blade section-wise properties.

1. The tip speed ratio (T.S.R.) is constant.
2. The number of blades, airfoils and the blade material are the same.
3. Geometric similarity is maintained to the extent possible.

The scale factor is given by the following.

$$Scale\ Factor = \frac{r}{R} = \frac{36.37}{63} = 0.577 \tag{7.1}$$

Table 34. 1.67 MW blade properties downscaled from NREL 5 MW used in Modes

1.67 MW Downscaled Design									
Node	**RNodes**	**AeroTwst**	**DRNodes**	**Chord**	**Airfoils**	**r/R**	**mass/len**	**flap stiff**	**edge stiff**
	(m)	**(°)**	**(m)**	**(m)**					
						0.000	226.222	2010626487	2011026170
1	1.655	13.308	1.5778	2.045	Cylinder1	0.044	246.752	1938006344	2164704203
2	3.233	13.308	1.5778	2.225	Cylinder1	0.089	150.032	802665186	1134721650
3	4.810	13.308	1.5778	2.405	Cylinder2	0.133	127.304	552901190	764331166
4	6.782	13.308	2.3667	2.630	DU40_A17	0.200	135.342	375981602	786231562
5	9.149	11.48	2.3667	2.685	DU35_A17	0.267	115.467	252243140	533800793
6	11.516	10.162	2.3667	2.574	DU35_A17	0.333	109.958	202977795	471189374
7	13.883	9.011	2.3667	2.453	DU30_A17	0.400	104.565	151205551	416420619
8	16.249	7.795	2.3667	2.313	DU25_A17	0.467	95.669	97233941	348508961
9	18.616	6.544	2.3667	2.164	DU25_A17	0.533	84.369	59366217	283649326
10	20.983	5.361	2.3667	2.022	DU21_A17	0.600	73.517	34921174	203031086
11	23.349	4.188	2.3667	1.879	DU21_A17	0.667	59.778	19526725	146923394
12	25.716	3.125	2.3667	1.738	NACA64_A17	0.733	51.450	11908327	113261221
13	28.083	2.319	2.3667	1.596	NACA64_A17	0.800	43.166	8472165	78783029
14	30.449	1.526	2.3667	1.454	NACA64_A17	0.867	32.912	5493418	50501031
15	32.421	0.863	1.5778	1.335	NACA64_A17	0.911	24.292	3376209	33832038
16	33.999	0.37	1.5778	1.204	NACA64_A17	0.956	18.631	1776368	15307851
17	35.577	0.106	1.5778	0.819	NACA64_A17	1.000	3.438	18874	556225
	Blade Length		35.5						

If 'R' is the radius of the rotor in general, the following parameters depend on the R in the following way.

1. Chord varies as R^1
2. Mass density varies as R^2
3. Flap wise/Edgewise stiff vary as R^4
4. Assume blade pitch = 1°

With these dependencies, the 1.67 MW downscaled design is as shown in Table 34.

Modes is run separately for the rotor and the tower of the NREL 5 MW single-rotor model. In case of the three-rotor model, only the rotor can be analyzed as the tower is integrated with

the support structure. Although Modes cannot directly simulate a three-rotor system, the Campbell diagram would consist of the modes of the structure as obtained in SAP2000 in addition to the blade modes obtained from Modes code.

For the rotor, the 1P or once per revolution and 3P or thrice per revolution frequencies corresponding to the rotor and blade rotation [5] are obtained at each rotational speed (RPM). At or below rated wind speed, the RPM varies linearly with the wind speed and above rated, it is constant. The RPM is found from the equation (6.2) where the wind speed U varies from 0 to 25 m/s.

$$\lambda = \frac{\Omega R}{U} \tag{7.2}$$

$$\Omega = \frac{\lambda U}{R} \tag{7.3}$$

$$\Omega = \frac{7*U}{36.37} \tag{7.4}$$

For each of the Ω values (RPM), the frequencies from Modes and SAP2000 of the different components are obtained and plotted. This forms the Campbell diagram.

The Campbell diagram therefore consists of the following frequencies plotted with respect to the RPM as per [5].

1. The first 5 frequencies of the Blade flapwise mode shapes [from Modes]
2. The first 5 frequencies of the Blade edgewise mode shapes [from Modes]
3. The first 5 natural frequencies of the three-rotor model structure (support structure & tower) [from SAP2000]
4. 1P – once per revolution frequencies corresponding of the rotor rotation [from Modes]

5. 3P – thrice per revolution frequencies corresponding to the blade passing frequencies [from Modes].

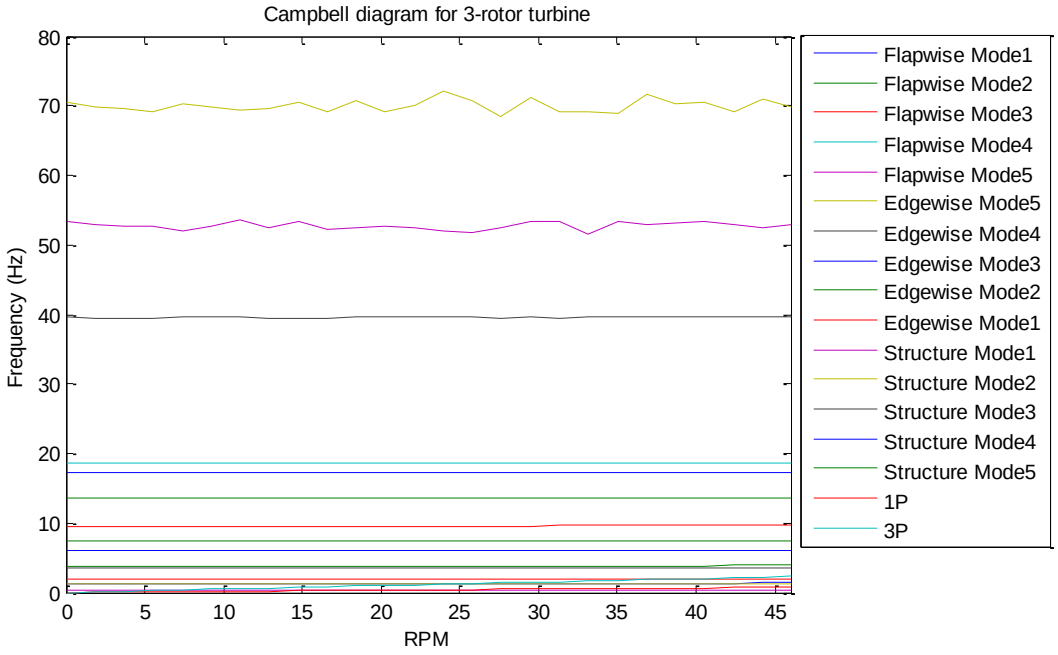

Figure 47. Campbell diagram for the three-rotor model

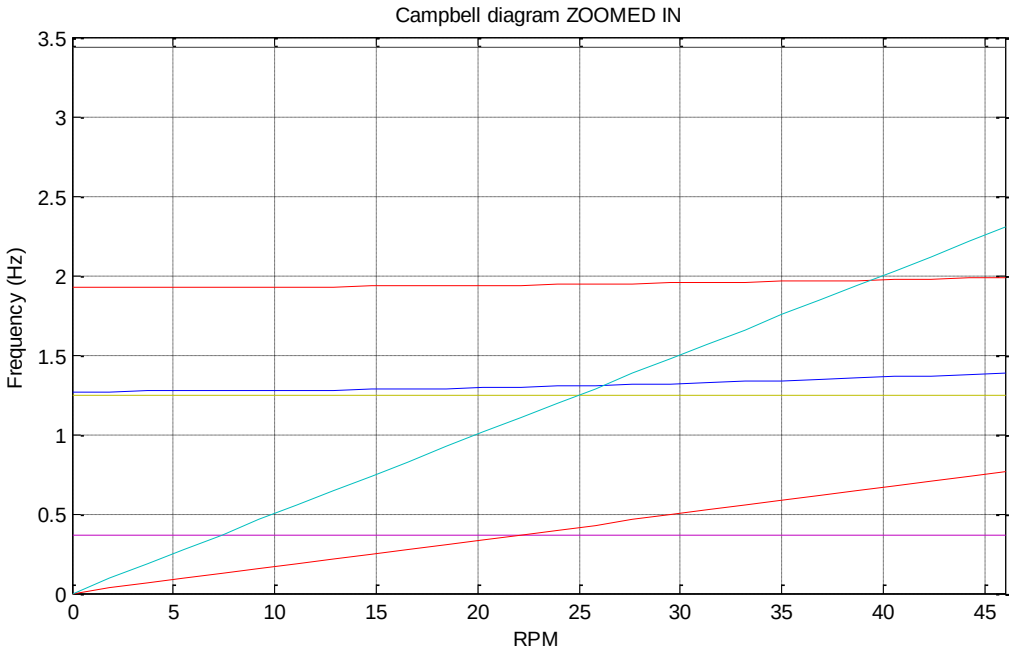

Figure 48. Campbell diagram showing Critical Rotor Speeds

The Campbell diagram is shown in Figure 47. The points of intersection of the frequency lines, if any, with the 1P and 3P lines are the critical rotor speeds to be avoided.

Figure 48 provides a closer (zoomed in) view of the Campbell diagram to show the critical speeds – 7.5 rpm, 22 rpm, 25 rpm, 25.5 rpm and 39.5 rpm. Since the rated rotor speed is 21 rpm for a three-rotor model, the controller does not exceed this rotor speed which means that the only critical speed is 7.5 rpm which should be avoided to prevent resonance. Also, in the Campbell diagram, there are two modes – Structure Mode 2 and Flapwise Mode 1 in Figure 48 which appear to be very near to each other. This can be problematic for the structure and with design changes can be avoided.

7.2.4. Drag Forces

The effect of aerodynamic drag forces due to the wind acting on the tower and the support structure is studied. The coefficient of drag (C_d) is determined from external sources as given below for calculation.

1. (C_d) = 0.6 for wind turbine towers. [20]
2. (C_d) = 1.0 for wires and cables. [21]
3. (C_d) = 1.3 for steel frames with an average aspect ratio (b/h) of 10. [35] The steel frames have a rectangular section facing the wind.

Using these values, the drag force per unit length is calculated as per the Eq. (7.5).

$$Drag\ force\ per\ unit\ length = \frac{1}{2}\rho A C_D U^2 \tag{7.5}$$

Where ρ = Air density = 1.225 kg/m^3

A = Drag area

U = Wind speed (assumed rated) = 11.4 m/s

For the tower, the drag area is the projected area of the tower section in the wind direction and is equal to the length times the diameter of the tower section. Similarly, cable drag area is equal to the length times the diameter of the cable. The steel frames vary considerably in terms of their sections and so an average drag area is assumed.

In SAP2000, a new load case called 'Drag' is defined. As the drag force is a uniformly distributed load (udl), the Distributed frame load option from the Assign menu is selected.

For the first tower section, the drag force per unit length is calculated as below.

$$\frac{1}{2} * 1.225 * (8.76 * 6) * 0.6 * 11.4^2 * \frac{1}{8.76x1000} = 0.287\ kN/m \qquad (7.6)$$

Table 35 calculates the tower drag force per unit length for all the sections. These values are of the order of 0.3 kN/m or less.

Table 35. Tower drag force per unit length for each section

Section location (z-axis)	Outer Diameter (m)	Drag Force per unit length (kN/m)
0 m – 8.76 m	6	0.287
8.76 m – 17.52 m	5.787	0.276
17.52 m – 26.28 m	5.574	0.266
26.28 m – 35.04 m	5.361	0.256
35.04 m – 43.8 m	5.148	0.246
43.8 m – 52.56 m	4.935	0.236
52.56 m – 61.32 m	4.722	0.226
61.32 m – 70.08 m	4.509	0.215
70.08 m – 78.84 m	4.296	0.205
78.84 m – 87.6 m	4.083	0.195
87.6 m – 90 m	3.87	0.185

Similarly for the cables, the calculations are as below.

$$\frac{1}{2}x1.225x\ (0.026)x1.0\ x11.4^2x\frac{1}{1000} = 0.00207\ kN/m \qquad (7.7)$$

Table 36 shows the values for all the cables.

Table 36. Cable drag force per unit length

Cable Type	Cable diameter (mm)	Drag Force per unit length (kN/m)
1	0.026	0.00207
2	0.065	0.00518
3	0.050	0.00398

The drag force per unit length for the support structure, considering the average drag area of all the sections, is chosen as 0.1157 kN/m

This analysis is only for rated wind speed and the change in deflection and stress is found to be negligible. For higher wind speeds, the drag effects are higher. Although these are not analyzed in this thesis, they need to be considered.

7.2.5. Turbulent Wind

This section deals with simulation of turbulent wind conditions and so uses the TurbSim design code [22] created by NWTC. TurbSim can produce full-field wind speed data given the turbulence intensity (T.I.), the mean wind speed and random seeds for variation.

Table 37. Basic parameters for wind turbine classes [25]

Wind Turbine Class		I	II	III
Vref	(m/s)	50	42.5	37.5
A	Iref (-)	0.16		
B	Iref (-)	0.14		
C	Iref (-)	0.12		

Assuming a Normal Turbulence Model (NTM) for the wind profile, the standard deviation σ_x is given by the IEC 61400-1 standard [25].

$$\sigma_x = I_{ref}(0.75 * U_{hub} + 5.6) \tag{7.8}$$

While the hub height wind speed U_{hub} is 15 m/s [25], assuming Class 1A wind speed, the T.I. is I_{ref} is 16% as given in Table 37. So, σ_x equals 2.696. Now, the equation for different mean

wind speeds U_{hub} changes to the one below. Different turbulence intensities for different values of U_{hub} are obtained as shown in Table 38.

$$2.696 = I(0.75 * U_{hub} + 5.6) \quad (7.9)$$

Table 38. Turbulence Intensities for NTM

Mean Wind speed (m/s) U_{hub}	**Turbulence Intensity (T.I.) I_{ref}**	
4	0.313	31.3%
6	0.267	26.7%
8	0.232	23.2%
10	0.206	20.6%
12	0.185	18.5%
14	0.167	16.7%
16	0.153	15.3%
18	0.141	14.1%
20	0.131	13.1%
22	0.122	12.2%
24	0.114	11.4%

7.2.5.1. TurbSim

Following are the inputs to the TurbSim file.

1. In TurbSim, the values of T.I. from Table 37 defined for the variable *IECTurbc* at mean wind speed *Uref* for the 11 different wind speeds. *IECWindType* is NTM. *IECStandard* is 1ed-3 (IEC 61400-1 Third Edition).
2. Random seeds are obtained by using the rand function in MATLAB. There are 66 different random seeds in all.
3. *GridHeight* and *GridWidth* equal 138.6 m which is 10% larger than the rotor diameter, 126 m as per [22].
4. *NumGrid_Z* and *NumGrid_Y* equal the ratio of *GridHeight* to *MeanChord.* The mean chord for a 1.67 MW blade is 3.418. As the value of *NumGrid_Z* of 39 requires a very large computation time, a value of 13 is finally chosen.

5. The recommended *TimeStep* equals 0.05 sec and the *AnalysisTime* is 600 sec which is the minimum suggested as per [22]. *UsableTime* is also 600 sec.
6. *HubHt* equals *RefHt* equals 90 m.
7. *TurbModel* is IECKAI. A Kaimal spectrum is assumed.

Figures 49-51 show the first three turbulent HH (hub height) wind speed files obtained from the full-field wind output files. These have a mean wind speed of 4 m/s and three different random seeds. Similarly, for wind speeds from 4 to 24 m/s in steps of 2 m/s, three wind files with three different random seeds are generated. Figures 52-55 show only one turbulent wind file associated with one random seed for 6, 8, 10 and 24 m/s respectively.

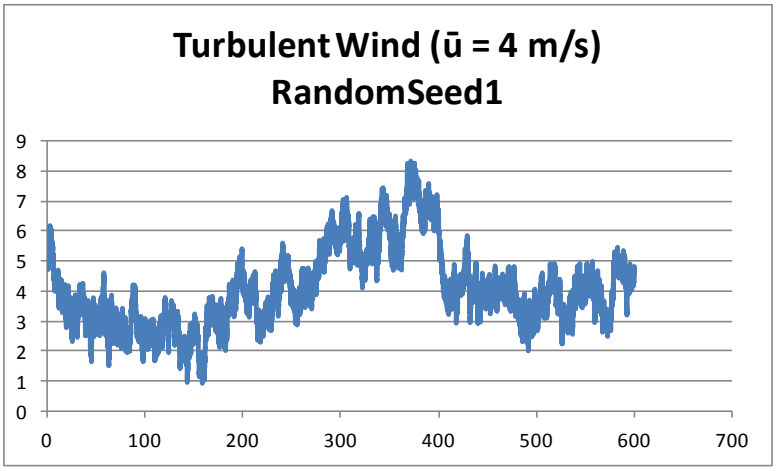

Figure 49. Turbulent wind 4 m/s mean speed, NTM and first random seed

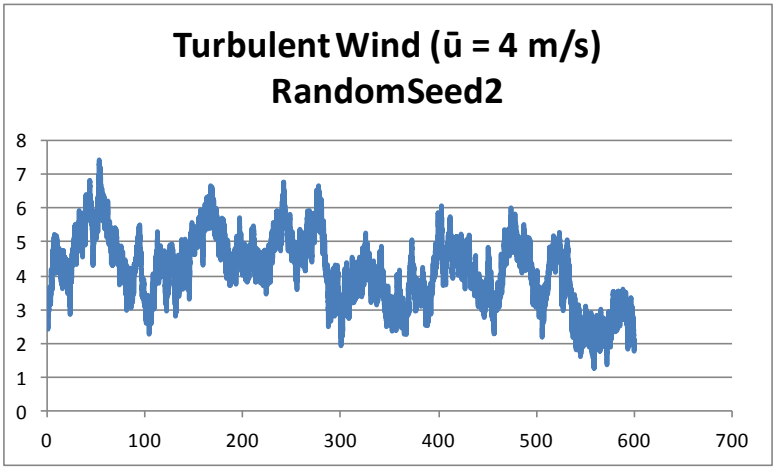

Figure 50. Turbulent wind 4 m/s mean speed, NTM and second random seed

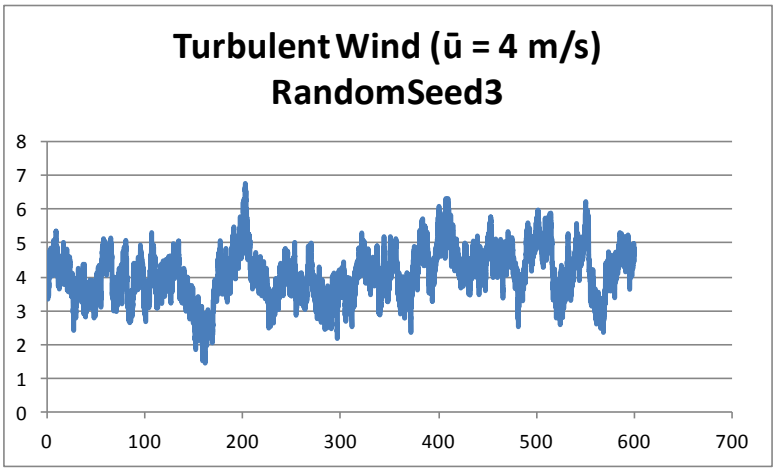

Figure 51. Turbulent wind 4 m/s mean speed, NTM and first random seed

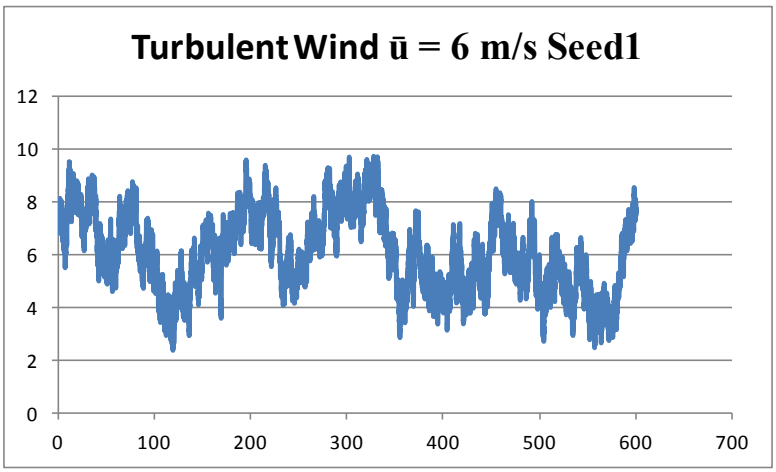

Figure 52. Turbulent wind 6 m/s mean speed, NTM and first random seed

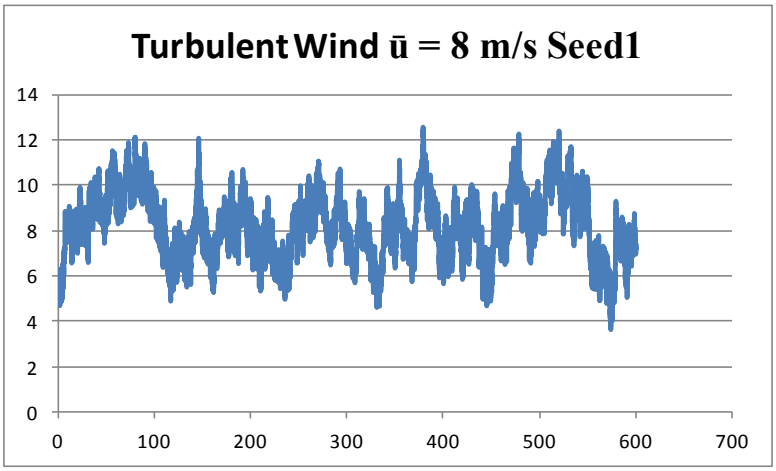

Figure 53. Turbulent wind 8 m/s mean speed, NTM and first random seed

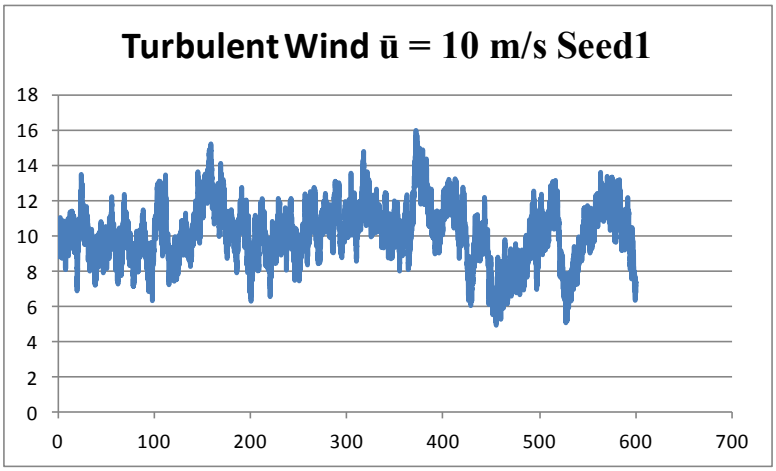

Figure 54. Turbulent wind 10 m/s mean speed, NTM and first random seed

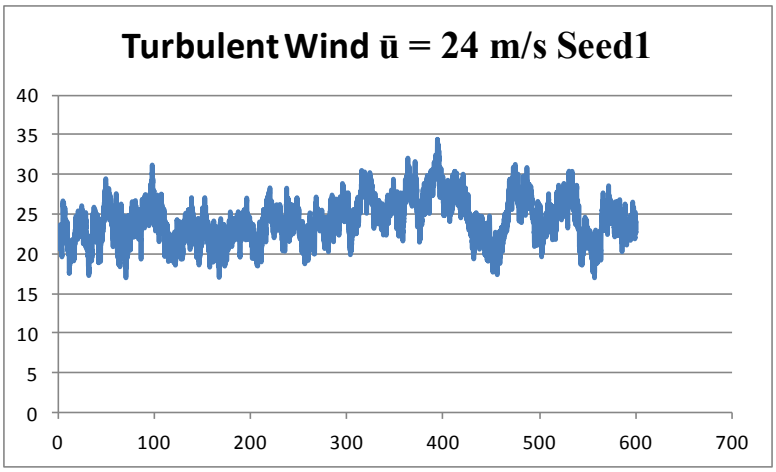

Figure 55. Turbulent wind 24 m/s mean speed, NTM and first random seed

7.2.5.2. FAST

After the turbulent wind files are generated (33 in all), each of them is simulated in FAST for the NREL 5 MW single-rotor model, which has been recompiled (BladedDLLInterface controller and Discon.dll). The time step is 0.02 sec (least possible without errors) and total runtime is 600 sec. The subroutines UserYawCont, PitchCntrl, UserVSCont are ON. The outputs are rotor torque and thrust loads as shown in Figures 56 and 57 for 4 m/s mean wind. These outputs are scaled down by $1/3\sqrt{3}$ and 1/3 respectively to obtain rotor torque and thrust for the 1.67 MW rotor used in the three-rotor model as shown in Figures 58 and 59.

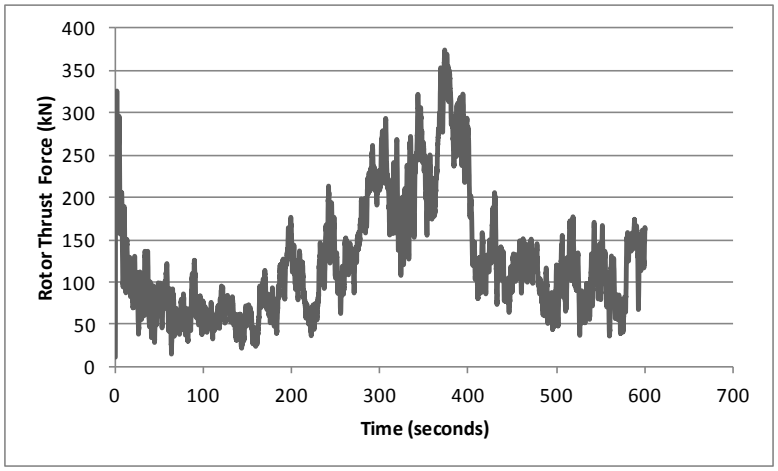

Figure 56. Thrust Force for NREL 5 MW single-rotor for 4 m/s

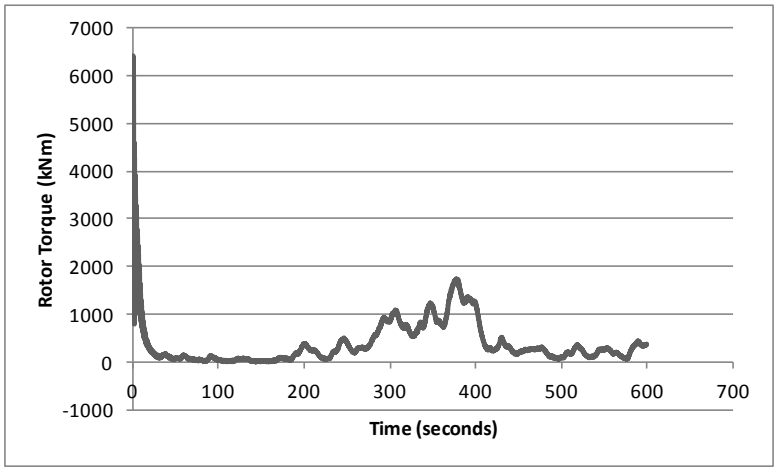

Figure 57. Rotor Torque for NREL 5 MW single-rotor for 4 m/s

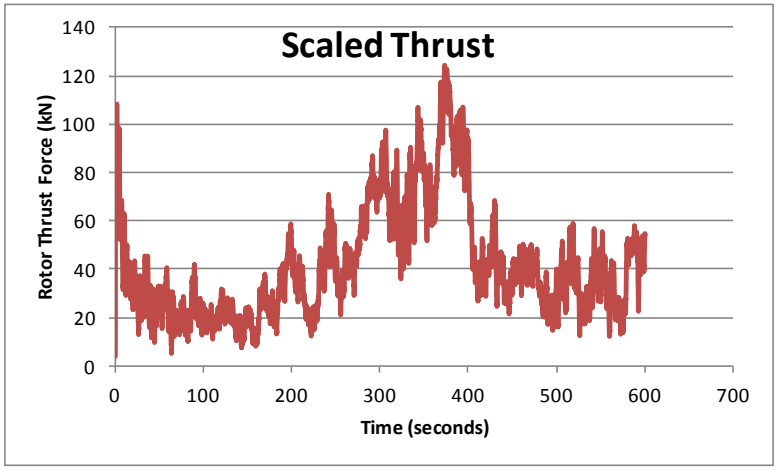

Figure 58. Thrust Force for 1.67 MW rotor for three-rotor model for 4 m/s

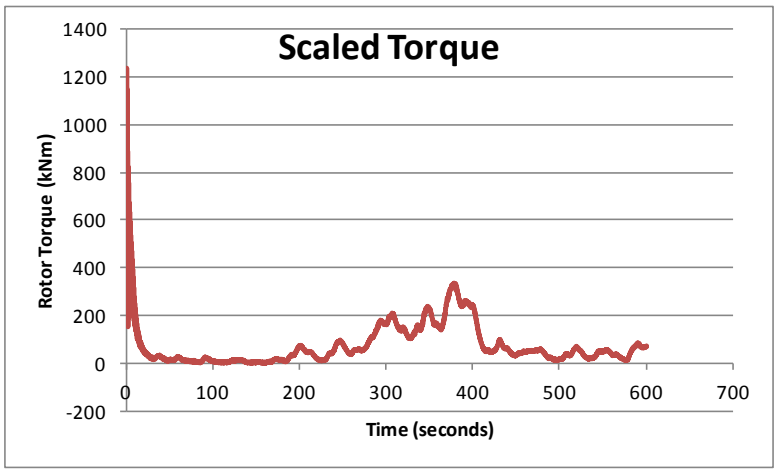

Figure 59. Rotor Torque for 1.67 MW rotor for three-rotor model for 4 m/s

Similarly, the thrust and torque loads for the three-rotor model for the remaining wind speeds are also obtained (33 files in all) from FAST. The correlation coefficients of the load data sets 1, 2, and 3 corresponding to the three random seeds are calculated in MATLAB as shown in Table 39. Since the data is mostly 0% correlated i.e. not correlated, three different load sets (thrust and torque) are applied in SAP2000 to each of the three rotors of the three-rotor model.

Table 39. Correlation Coefficients for Load Data sets for the three-rotor model

Wind (m/s)	Correlation Coeff (Thrust)			Correlation Coeff (Torque)		
	1-2	2-3	1-3	1-2	2-3	1-3
4	-0.221	-0.145	0.116	0.289	0.595	0.546
6	-0.063	-0.076	-0.304	0.041	0.067	-0.205
8	-0.097	0.101	-0.090	-0.022	0.174	-0.044
10	-0.174	0.080	0.011	-0.070	-0.020	-0.110
12	-0.142	0.019	-0.092	0.309	-0.064	0.110
14	0.095	-0.078	0.087	0.223	0.016	0.108
16	0.077	-0.061	0.076	0.082	0.053	0.169
18	0.033	0.057	0.028	0.120	0.114	0.080
20	0.118	0.192	0.039	0.162	0.221	0.073
22	0.195	0.217	0.098	0.160	0.173	0.069
24	0.216	0.303	0.313	0.223	0.282	0.234

7.2.5.3. SAP2000

The load results from FAST for the 11 wind speeds are then applied to each of the three rotors of the three-rotor model in SAP2000. The new load patterns defined with the time-history load type are Thrust1, Thrust2, Thrust3, Torque1, Torque2 and Torque3. The other loads i.e. the weight of the hub, blades and nacelle and the self-weight of the frames and cables are constant.

SAP2000 results for these 11 wind speed cases for the three-rotor model are given in Table 40. All the design criteria i.e. deflection, stress and buckling are satisfied.

Table 40. SAP2000 results for Turbulent Wind (11 mean wind speeds)

Wind speed	Deflection (y-deflection & downwind)				Stress & Buckling Ratios
	Top Rotor	Left Rotor	Right Rotor	Tower Top	
4 m/s	0.353 m	0.323 m	0.275 m	0.155 m	Within limits
6 m/s	0.444 m	0.323 m	0.379 m	0.219 m	Within limits
8 m/s	0.703 m	0.490 m	0.477 m	0.354 m	Within limits
10 m/s	0.893 m	0.599 m	0.597 m	0.439 m	Within limits
12 m/s	0.913 m	0.622 m	0.669 m	0.452 m	Within limits
14 m/s	1.078 m	0.653 m	0.664 m	0.551 m	Within limits
16 m/s	0.961 m	0.651 m	0.649 m	0.514 m	Within limits
18 m/s	1.079 m	0.689 m	0.620 m	0.566 m	Within limits
20 m/s	1.061 m	0.592 m	0.538 m	0.585 m	Within limits
22 m/s	1.416 m	0.661 m	0.579 m	0.726 m	Within limits
24 m/s	1.316 m	0.606 m	0.714 m	0.712 m	Within limits

Figures 60-64 show the deflection plots with respect to time for 4, 6, 8, 10 and 24 m/s mean wind speeds. The transient data at the start is neglected and only the steady-state maximum is considered as also seen in Table 40 above. The point of maximum deflection is found to be near the top rotor on the upwind side.

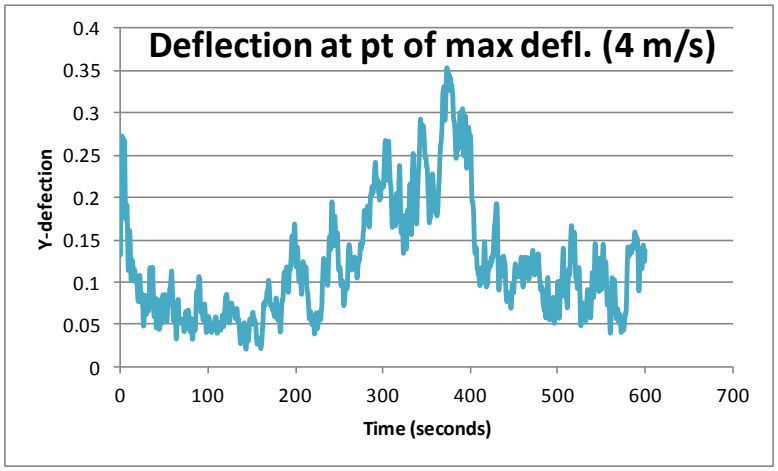

Figure 60. Deflection at max deflection pt. in the three-rotor model (4 m/s mean wind)

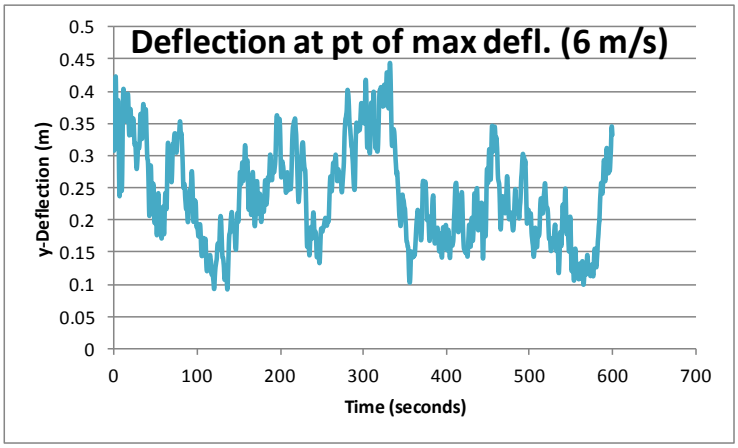

Figure 61. Deflection at max deflection pt. in the three-rotor model (6 m/s mean wind)

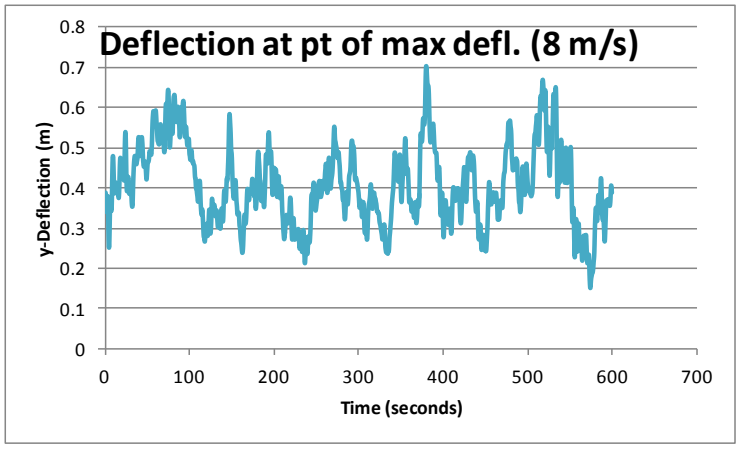

Figure 62. Deflection at max deflection pt. in the three-rotor model (8 m/s mean wind)

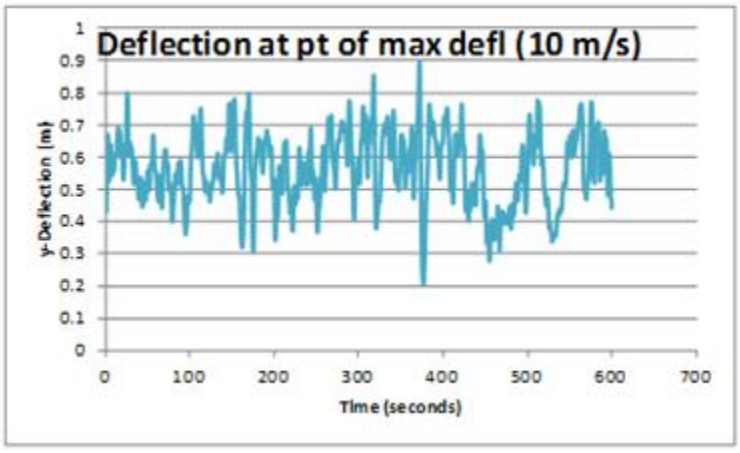

Figure 63. Deflection at max deflection pt. in the three-rotor model (10 m/s mean wind)

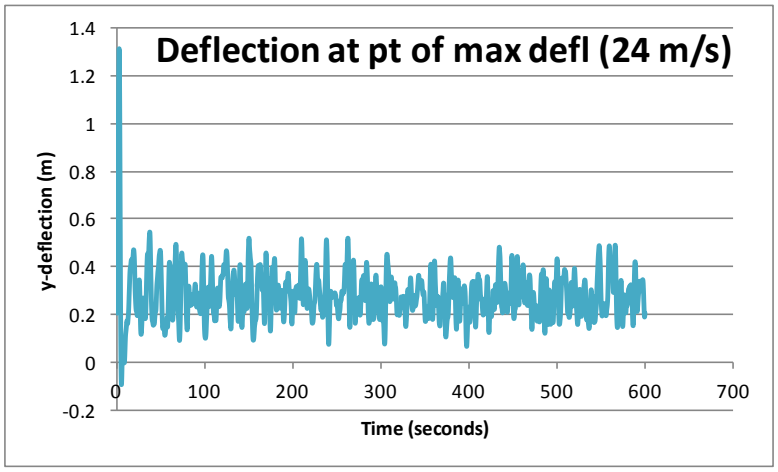

Figure 64. Deflection at max deflection pt. in the three-rotor model (24 m/s mean wind)

The analysis is repeated with perfectly correlated loads i.e. the same thrust and the same torque loads are applied to all the three rotors. The results are as shown in Table 41. The deflection is nearly the same for the side rotors and is maximum at the top rotors.

Table 41. SAP2000 results for Turbulent Wind – Perfectly Correlated Case

Wind speed	Deflection (y-deflection & downwind)				Stress & Buckling Ratios
	Top Rotor	Left Rotor	Right Rotor	Tower Top	
4 m/s	0.366 m	0.246 m	0.246 m	0.214 m	Within limits
6 m/s	0.485 m	0.238 m	0.238 m	0.259 m	Within limits
8 m/s	0.776 m	0.363 m	0.366 m	0.404 m	Within limits
10 m/s	0.968 m	0.440 m	0.442 m	0.501 m	Within limits
12 m/s	0.974 m	0.441 m	0.444 m	0.504 m	Within limits
14 m/s	1.123 m	0.499 m	0.502 m	0.580 m	Within limits
16 m/s	1.058 m	0.475 m	0.477 m	0.546 m	Within limits
18 m/s	1.089 m	0.486 m	0.488 m	0.563 m	Within limits
20 m/s	1.036 m	0.465 m	0.468 m	0.537 m	Within limits
22 m/s	1.430 m	0.621 m	0.624 m	0.735 m	Within limits
24 m/s	1.275 m	0.558 m	0.561 m	0.657 m	Within limits

7.2.6. Extreme Conditions

The IEC Design condition [25] for the 50-year Extreme operating gust (EOG) is simulated in SAP2000. The steps for simulating the EOG are given below.

1. From Table 37, assuming wind turbine class 1A,

   V_{ref} = 50 m/s, I_{ref} = 0.16 at V_{hub} = 15 m/s.

2. Assuming NTM, $\sigma_1 = I_{ref}(0.75V_{hub} + 5.6)$ = σ_1 = 2.696.

3. Turbulence scale parameter Λ = 42 m for z >=60 m. Rotor diameter D = 126 m

4. Extreme wind speed

$$V_{e1(z)} = 0.8V_{e50(z)} = 0.8 * \left(1.4 * V_{ref} * \left(\frac{z}{z_{hub}}\right)^{0.11}\right) = 56\ m/s \quad (7.10)$$

5. Hub height gust magnitude

$$V_{gust} = \min\{1.35(V_{e1} - V_{hub}); 3.3(\frac{\sigma_1}{1+\left(0.1*\frac{D}{\Lambda}\right)})\} \quad (7.11)$$

$$V_{gust} = \min\{41.85; 6.844\} = 6.844\ m/s \quad (7.12)$$

6. Wind speed at hub height

$$V(z) = V_{hub}(\frac{z}{z_{hub}})^{\alpha} = 25 * (1)^{0.2} = 25\ m/s \quad (7.13)$$

7. Wind gust profile for $0 \leq t \leq T$, T = 10.5 sec,

$$V(z,t) = V(z) - 0.3 * V_{gust} * \sin\left(\frac{3\pi t}{T}\right) * [1 - \cos(\frac{2\pi t}{T})] \quad (7.14)$$

$$V(z,t) = 25 - 2.532 * \sin(0.898t) * [1 - \cos(0.598t)] \quad (7.15)$$

Otherwise,

$$V(z,t) = V(z) \quad (7.16)$$

$$V(z,t) = 25\ m/s \quad (7.17)$$

8. Defining the above function in MATLAB as shown in Figure 65.

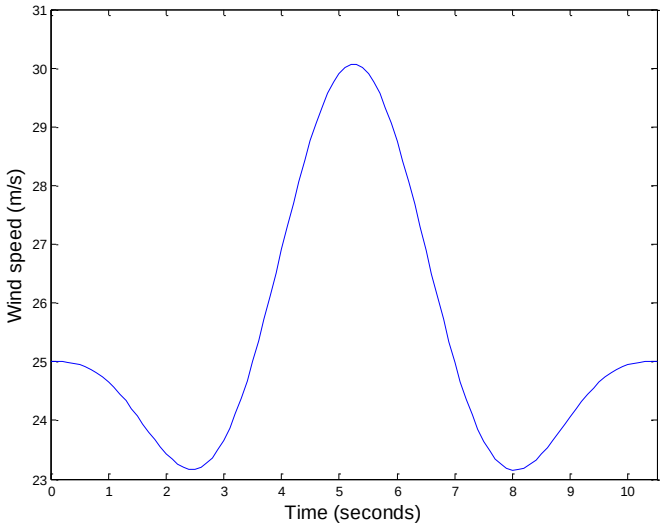

Figure 65. 50-year EOG in MATLAB

9. The data points for this gust function are then copied to a HH wind file in FAST where the total runtime is 300 seconds and the gust is introduced 200 seconds after the start for 10.5 seconds duration as shown in Figure 66.

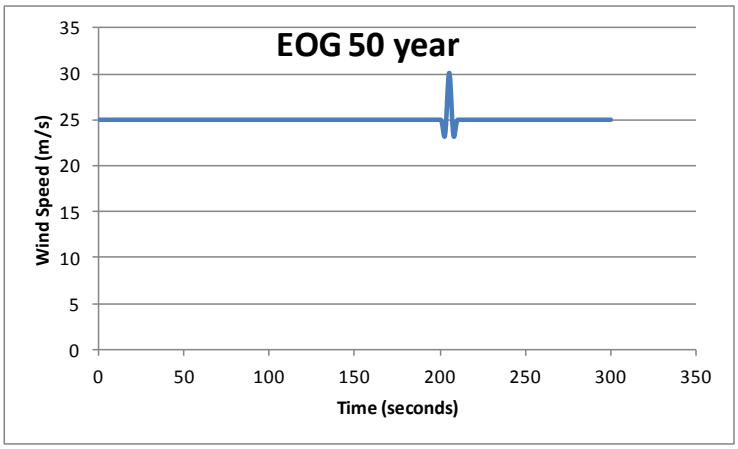

Figure 66. 50-year EOG hub height (HH) wind file

10. This file is implemented in FAST for the NREL 5 MW single-rotor model and the results are then downscaled to those for the 1.67 MW rotors used in the three-rotor model. Figures 67 and 68 show the FAST results. Clearly,

    1) The maximum thrust (steady-state value) is 624.7 kN.

    2) The maximum rotor torque (steady-state value) is 4905 kNm.

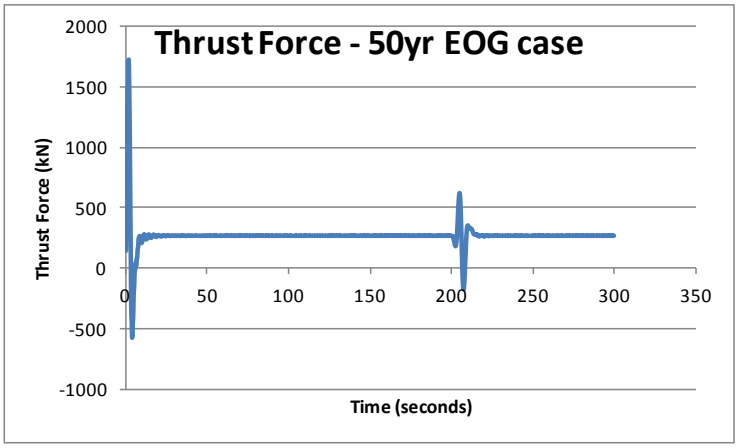

Figure 67. Thrust Force for 50-year EOG case for single-rotor model

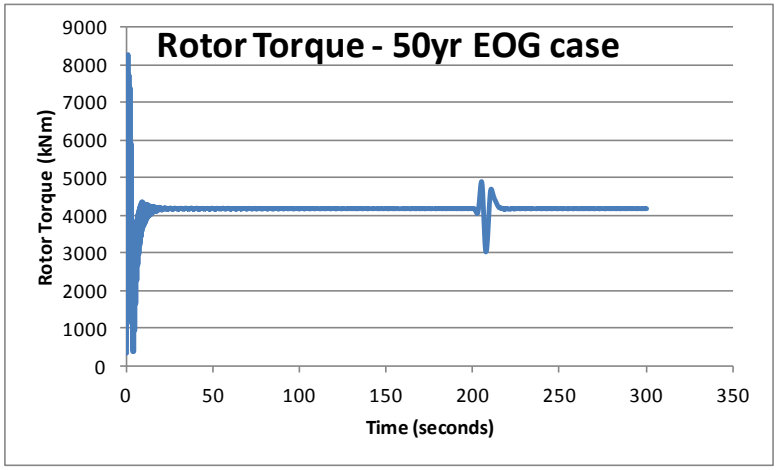

Figure 68. Rotor Torque for 50-year EOG case for single-rotor model

11. Figures 69 and 70 show the SAP2000 downscaled results for the 1.67 MW rotor of the three-rotor model.

    1) The maximum thrust (steady-state value) is 208.2 kN.

    2) The maximum rotor torque (steady-state value) is 943.97 kNm.

12. The SAP2000 result is shown in Figure 69 for the maximum deflection point. The maximum deflection is 0.616 m. The position of this point is the top rotor (downwind). Also, the stress and buckling criteria are satisfied. In each of the above cases, the transients are removed by ignoring the first 50 second results in the simulation.

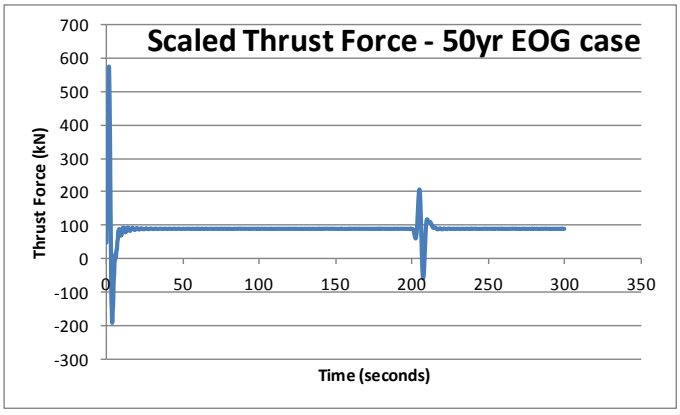

Figure 69. Thrust Force for 50-year EOG case for each rotor of the three-rotor model

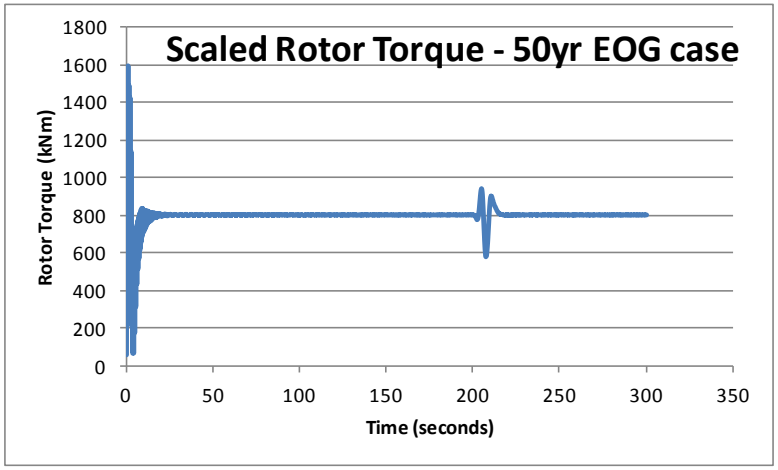

Figure 70. Rotor Torque for 50-year EOG case for each rotor of the three-rotor model

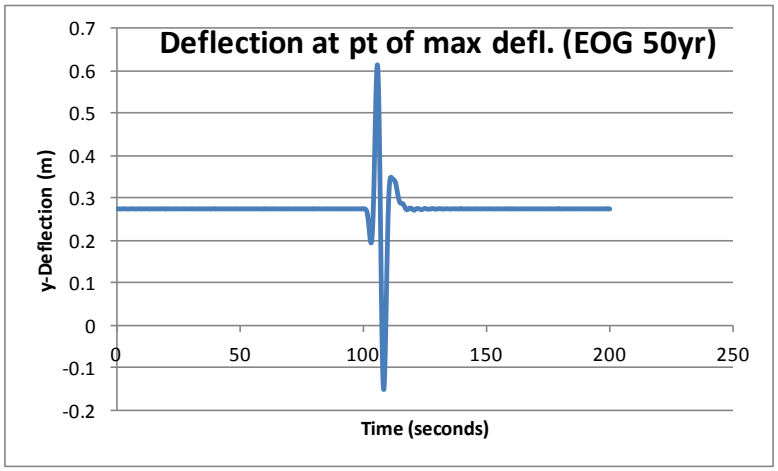

Figure 71. SAP2000 deflection for 50-year EOG at maximum deflection point

CHAPTER 8

SEVEN-ROTOR MODEL

In chapter 4, a three-rotor model was developed using the baseline scaling model followed by the structural analysis. This chapter uses a similar approach to develop and analyze a seven-rotor 5 MW model with each rotor producing 0.71 MW or 710 kW.

8.1. Baseline Seven-Rotor Model

The number of rotors in the baseline model is changed to seven rotors. This model has a three-stage gearbox and uses the same tower used in the single-rotor model. The tower is not downscaled since it has to withstand the same loads. The mass and cost values for a seven-rotor model are shown in Table 42. The single-rotor baseline model is also shown for comparison.

Table 42. Seven-rotor model and equivalent single-rotor model

BASELINE	**Single rotor 5 MW**		**Seven rotor 5 MW, 0.71 MW**	
Components	**Mass(kg)**	**Cost($)**	**Mass(kg)**	**Cost($)**
Rotor	76,843	778,421	31,524	319,333
Hub	30,116	127,995	49,786	211,593
Pitch System	14,423	183,551	13,874	176,563
Nose Cone	1,810	10,085	2,524	14,057
Low speed shaft	16,526	115,670	6,965	48,750
Main bearing	5,400	95,050	1,214	21,358
Variable speed electronics	-	395,000	-	395,000
Yaw system	13,152	113,896	17,098	120,896
Brake & coupling	994	9,946	995	9,946
Electrical system	-	200,000	-	200,000
Hydraulic & Cooling system	400	60,000	400	60,000
Nacelle Cover	6,154	61,535	8,463	84,633
Gearbox	39,688	661,203	30,312	504,997
Generator	16,690	324,960	19,414	378,002
Mainframe, Platform &	31,773	150,748	33,261	157,801
Tower	347,460	521,190	347,460	521,190
TOTAL	**601,429**	**3,809,250**	**563,290**	**3,224,119**

The mass and cost of the 2 yaw bearings for the seven-rotor model are discussed in section 5.5.6. The main yaw bearing at the rotor centroid (hub height of 90 m) is the same as the single-rotor model, whereas the second yaw bearing only provides stability to the yawing motion and only supports a fraction of the weight.

The reduction in total mass of 38,139 kg and total cost of $585,131 is due to the square-cube law discussed in section 1.2. The cost reduction is attributed to the following individual reductions.

Table 43. Contribution of Cost Reduction per Component for Seven-Rotor Model

Component	**Cost Reduction**	**Percentage Contribution**
Rotor	$459,088	60.18%
Pitch system	$6,988	0.92%
Low speed shaft	$66,920	8.77%
Main bearing	$73,692	9.66%
Gearbox	$156,206	20.48%
Total	**$762,894**	**100%**

Most other components either do not contribute to or cause a significant effect on the cost. This is of course, without considering the additional mass of the support structure.

8.2. Arrangement of Rotors

Some general considerations for the arrangement of rotors include:

1. While designing a multi-rotor system with *n* rotors, the center of their collective swept area should correspond to the hub height of the NREL 5 MW single-rotor turbine which is 90 m [7], since we are comparing rotor scenarios producing the same power and therefore having the same average elevation.
2. For multi-rotor offshore turbines, the wave height should be used to determine the limit of the lowest rotor location. A distance of 15 m, which is half the blade tip

clearance of 30 m, for the NREL 5 MW single-rotor turbine [7] is chosen for the MRWT rotor configuration.

3. The rotors should be symmetric to an extent that the stresses due to gravity are minimized.

8.2.1. Rotor Spacing

Referring to section 4.3.1, the spacing between the rotors for this thesis is chosen as 5% of rotor diameter, so t = 1.05 which is used in the next section.

8.2.2. Rotor Locations

With the criteria from sections 7.1 through 7.2, the rotor coordinates for a seven-rotor system are calculated. In this configuration, the rotor tips are sufficiently far away from the mean sea level (M.S.L.). These values are shown in Eq. (8.1) and (8.2).

$$\textit{Height of lower rotors} = 46.7 \text{ m} \tag{8.1}$$

$$\textit{Distance between lower rotor tip and M.S.L.} = 46.7 \text{ m} - 23.81 \text{ m} = 22.89 \text{ m} \tag{8.2}$$

This distance of 22.89 m is greater than 15 m as per [7] and hence acceptable. The rotor spacing is selected as 5% of the rotor diameter which is 47.62 m.

$$Rotor\ spacing = 0.05 * \ 47.62 = 2.381\ m \tag{8.3}$$

The distance between the rotors is given by Eq. (8.4)

$$s = 47.62 + 2.381 = 50.001\ m \tag{8.4}$$

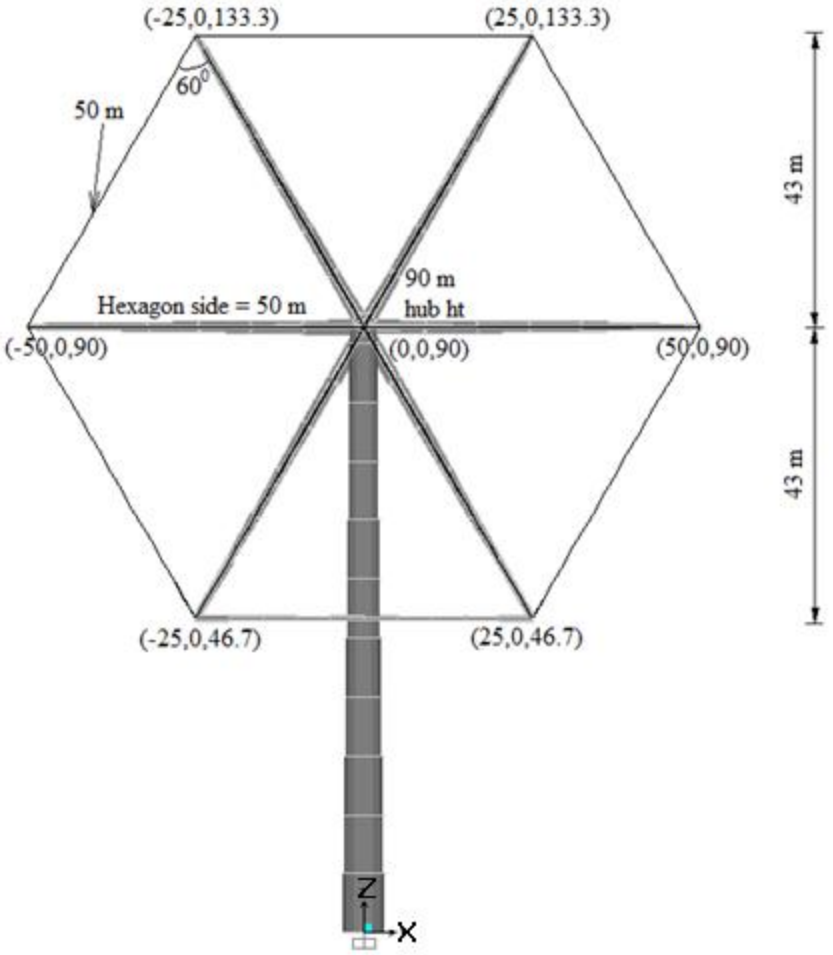

Figure 72. Calculation of rotor locations – Seven-rotor model

The rotor arrangement is a hexagon with 50 m long sides. From the geometry shown in Figure 72, the co-ordinates of the rotor centers are:

$$\textit{Top left rotor} = (-25,\ 0,\ 133.3)\ \text{m} \tag{8.5}$$

$$\textit{Top right rotor} = (25,\ 0,\ 133.3)\ \text{m} \tag{8.6}$$

$$\textit{Centre left rotor} = (-50,\ 0,\ 90)\ \text{m} \tag{8.7}$$

$$\textit{Centre mid rotor} = (0,\ 0,\ 90)\ \text{m} \tag{8.8}$$

$$\textit{Centre right rotor} = (50,\ 0,\ 90)\ \text{m} \tag{8.9}$$

$$\textit{Lower left rotor} = (-25,\ 0,\ 46.7)\ \text{m} \tag{8.10}$$

$$\textit{Lower right rotor} = (25,\ 0,\ 46.7)\ \text{m} \tag{8.11}$$

In the single-rotor model, there were two frames near the rotor location – one joining a point 2.4 m above the tower top to the C.M. of the hub located upwind and, the other joining the former point to the C.M. of the nacelle located downwind. The lengths of these frames as per Chapter 3 are 5 m upwind and 1.9 m downwind, respectively.

In the seven-rotor model, there are two frames at each of the seven rotor locations. The lengths of these frames are downscaled because the hub and the nacelle masses are also downscaled. This explanation is similar to section 4.3.2.

As mass is a product of density and volume, and the volume is proportional to the cube of length dimensions, these CM lengths are downscaled as the cube root of the masses.

$$New\ Hub\ CM\ dist = 5 * \left(\frac{1\ hub\ mass\ (3-rotor)}{hub\ mass\ (1-rotor)}\right)^{\frac{1}{3}} = 5 * \left(\frac{3066}{56780}\right)^{\frac{1}{3}} = 1.889\ m \quad (8.12)$$

$$New\ Nacelle\ CM = 1.9 * \left(\frac{1\ nacelle\ mass\ (3-rotor)}{nacelle\ mass\ (1-rotor)}\right)^{\frac{1}{3}} = 1.9 * \left(\frac{12959}{240000}\right)^{\frac{1}{3}} = 0.718\ m \quad (8.13)$$

The maximum chord of the 0.71 MW turbine blade obtained by downscaling the 5 MW turbine blade (chord = 4.652 m [7]) is 1.758 m. Chord varies as per R^1.

$$\frac{c_1}{c_2} = \frac{R_1}{R_2} \quad (8.14)$$

$$\frac{4.652}{c_2} = \frac{63}{23.81} \quad (8.15)$$

$$c_2 = 1.758\ m \quad (8.16)$$

The chord length affects the clearance between the blades and the cables used in the structure. Also, the tower diameter at the lower rotor locations i.e. at 46.7 m from the ground is 4.94 m. So, to avoid contact between cables and the blades, the total clearance is found.

$$Total\ clearance = \left(\frac{4.935}{2}\right) + \left(\frac{1.758}{2}\right) + \left(\frac{1}{2}\right) = 3.85\ m. \quad (8.17)$$

The new distance of the hub C.M. is therefore, increased to 3.85 m. The new distance of nacelle C.M. is increased to 1 m to make the design safer.

Finally, since a downwind rotor is used for the seven-rotor case, the lengths of these frames in the seven-rotor model are 3.85 m downwind for the hub C.M., and 1 m upwind for the nacelle C.M.

8.3. Support Structure Considerations and Model Geometry

The support structure design for a seven-rotor model is similar to that for a three-rotor model and therefore, section 4.4 should be consulted for preliminary considerations.

After calculating the rotor co-ordinates and the distances to the C.M.s, the rest of the model is constructed in SAP2000. The seven-rotor model also uses downwind rotors similar to the three-rotor model. Section 4.5 should be referred to for the model geometry.

The structure is made of steel and consists of frames and cables. The spars or group of frames used in the structure as shown in Figure 25 are also used in the seven-rotor model.

In the course of achieving the final design, several different I-beam sections are tested for the frames. Different "Auto-select" lists are used by the SAP2000 optimization code to minimize deflection and stresses. Some other considerations for designing frames are already provided in Section 4.5.2.

The spars connect the rotors to the tower at the rotor centroid and follow the same procedure as outlined for the three-rotor model in Section 4.5.3. The only exceptions for the seven-rotor model are as follows:

1. The spar is rotated by 60° five times with the axis of rotation parallel to y-axis using the "Replicate" command and the "Radial" option. Six spars are thus created. The spars are attached to each other at the rotor centroid after rotating.
2. The number of spar sections is arbitrarily decided as 6. If several frames undergo buckling then the number of sections should be increased.

The dimensions of the spar for the final design are shown in the Table 44. The isosceles triangle referred to in the table is shown in Figure 29. The spar section number is 1 near the rotor and increases towards the tower.

Table 44. Dimensions of triangle for spar sections for the seven-rotor model

Spar section number	Dimensions of Triangle (Isosceles)	
	Base	Height
1	0.4 m	0.8 m
2	0.6 m	1 m
3	0.8 m	1.2 m
4	1 m	1.4 m
5	1.2 m	1.6 m
6	1.4 m	1.8 m
7	1.6 m	2 m

8.3.1. Cables

Cables are used with downwind rotors, by connecting them to a jib located upwind. The load carrying capacity of cables can be controlled by increasing the pre-tension applied to them.

Most of the cable design steps are the same as those for the three-rotor system and section 4.5.4 provides additional details. Three different cable types are used in the support structure

depending on the loads they support. The design steps to calculate the pre-tension T in the cable, cross section area A of the cable, and its material density ρ are explained in the following sections.

8.3.1.1. Cables of Type 1

These cables are located upwind and they resist the thrust force on each rotor. With design iterations, it is found to be a better option to attach more than one cable of type 1 to the jib.

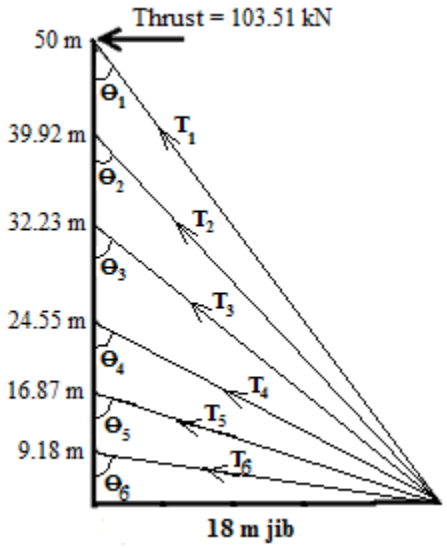

Figure 73. Cables of Type 1 (upwind)

The magnitude of the thrust force on one rotor is 103.51 kN. There are six cables of type 1, attached to the top spar from a horizontal jib located upwind as shown in Figure 73. The cables oppose the thrust force, as shown in Equation 8.18.

$$Thrust = \sum T \sin\theta \tag{8.18}$$

To simplify the analysis, assume $T_1 = T_2 = T_3 = T_4 = T_5 = T_6 = T$

$$103.51\ kN = T \sum \sin\theta \tag{8.19}$$

Calculating the angle θ_1 from the geometry,

$$\theta_1 = \tan^{-1}\frac{18}{50} = 19.8° \tag{8.20}$$

Similarly, finding the other angles, the pre-tension T is equal to the value in Eq. (8.21).

$$\boldsymbol{T = 33.27\ kN} \tag{8.21}$$

Now, the allowable stress σ^* in the cable, related to the yield stress σ_y of the cable material, is used to find the cross-sectional area A of the cable. The safety factor is denoted by *s.f.*

$$\sigma^* = \frac{\sigma_y}{s.f.} = \frac{T}{A} \tag{8.22}$$

$$\sigma^* = \frac{379.2\ MPa}{2} = \frac{33.27\ kN}{A} \tag{8.23}$$

$$A = 175.47\ mm^2 \tag{8.24}$$

Choosing a cable of diameter d = 21 mm from the catalogue [23],

$$\boldsymbol{A \cong 281\ mm^2} \tag{8.25}$$

The cable is made of multi-strand steel cords wrapped together. The effective density is thus calculated from the mass per unit length *m/l* obtained from [23] and the area *A*.

$$\rho = \frac{m/l}{A} = \frac{2.4\ kg/m}{2.81{*}10^{-4}\ m^2} \tag{8.26}$$

$$\boldsymbol{\rho = 8540.92\ kg/m^3} \tag{8.27}$$

8.3.1.2. Cables of Type 2

These cables are located upwind and they support the weight of the nacelle associated with each rotor. The nacelle load per rotor is 166.15 kN. One of the two cables of type 2 is as shown in Figure 74.

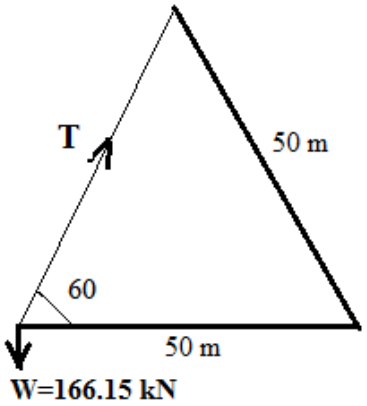

Figure 74. Cable of Type 2 (upwind)

There are five cables of this type, each joining the nacelle C.M. of one rotor to the nacelle C.M. another rotor. As the opposing load is *W* equal to 166.15 kN, and θ = 60˚.

$$W = T \sin\theta \tag{8.28}$$

$$166.15\ kN = T \sin 60° \tag{8.29}$$

$$\boldsymbol{T = 191.85\ kN} \tag{8.30}$$

Following the same procedure as cables of type 1,

$$\sigma^* = \frac{\sigma_y}{s.f.} = \frac{T}{A} \tag{8.31}$$

$$\sigma^* = \frac{379.2\ MPa}{2} = \frac{191.85\ kN}{A} \tag{8.32}$$

$$A = 1011\ mm^2 \tag{8.33}$$

Choosing a cable of diameter *d* = 40 mm from the catalogue [23],

$$\boldsymbol{A \cong 1060\ mm^2} \tag{8.34}$$

$$\rho = \frac{m/l}{A} = \frac{8.9\ kg/m}{1.06{*}10^{-3}\ m^2} \tag{8.35}$$

$$\boldsymbol{\rho = 8396.23\ kg/m^3} \tag{8.36}$$

As the design criteria are not satisfied with this cable size, the cable diameter should be increased to ***d* = 60 mm.**

8.3.1.3. Cables of Type 3

These cables are located downwind and they support the weight of the rotor and the hub. The sum total of these loads per rotor is 73.31 + 44.18 = 117.49 kN. One of the two cables of type 3 is as shown in Figure 75.

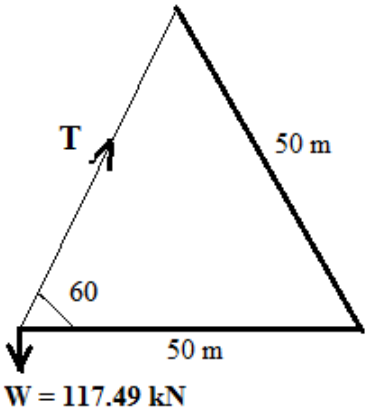

Figure 75. Cable of Type 3 (downwind)

These are two cables of this type each joining the C.M. of one rotor to the C.M. of another rotor. As the opposing load is *W* equal to 117.49 kN, and θ = 60˚.

$$W = T \sin\theta \tag{8.37}$$

$$117.49\ kN = T \sin 60° \tag{8.38}$$

$$\boldsymbol{T = 135.67\ kN} \tag{8.39}$$

Following the same procedure as cables of type 1,

$$\sigma^* = \frac{\sigma_y}{s.f.} = \frac{T}{A} \tag{8.40}$$

$$\sigma^* = \frac{379.2\ MPa}{2} = \frac{135.67\ kN}{A} \tag{8.41}$$

$$A = 715.56\ mm^2 \tag{8.42}$$

Choosing a cable of diameter *d* = 35 mm from the catalogue [23],

$$\boldsymbol{A \cong 808\, mm^2} \tag{8.43}$$

$$\rho = \frac{m/l}{A} = \frac{6.8\ kg/m}{8.08{*}10^{-4}\ m^2} \tag{8.44}$$

$$\boldsymbol{\rho = 8415.84\ kg/m^3} \tag{8.45}$$

The density of each cable type is fed into the material properties of the cables in SAP2000 along with the modulus of elasticity of 160 GPa and the effective yield strength of 379 MPa. The cross-section area is fed into the section properties and the pre-tension values are used to define the individual cables in the model. A cable can also be defined by its length before and after deformation, which is calculated from the pre-tension. The self-weight of each of the cables is applied as a load.

8.3.2. Yaw bearing System, Lower link and Jib

The yaw bearing system for the seven-rotor system is exactly the same as that discussed for the three-rotor system in Section 4.5.6 with the exception that the lower yaw bearing is located at a height of 47.6 m instead of 67.95 m. The same follows for the lower link and the jib, with only some minor changes based on the shape of the support structure of the seven-rotor model.

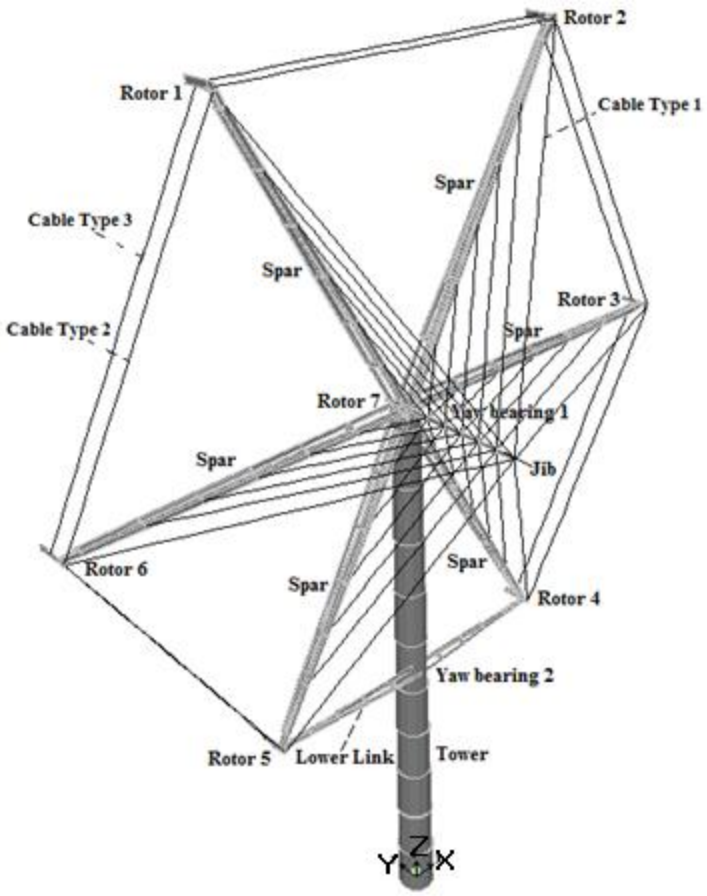

Figure 76. Model Geometry

After modeling all the components, the final structure before the analysis is as shown in Figure 76.

8.4. Model Loads

Table 45 is similar to the table for single-rotor loads (Table 11), except that since the rotor is downwind, the position of upwind loads are downwind and vice versa. Also, the point loads are located near each of the seven rotors. Although the rotors face different wind speeds due to wind shear, in this analysis it is assumed that the thrust force is the same i.e. 103.51 kN for all the seven rotors. The self-weight is also applied to cables similar to frames.

Table 45. Loads for a Seven Rotor Model

Load pattern	Type	Position	Value	Direction
Weight of the nacelle	Point Load at 7 points	Nacelle CM upwind	166.15 kN	Z axis downwards
Weight of the hub	Point Load at 7 points	Hub CM downwind	44.18 kN	Z axis downwards
Weight of the rotor blades	Point Load at 7 points	Hub CM downwind	73.31 kN	Z axis downwards
Self-weight of the tower	Distributed Load	Along tower	3408.58 kN (total)	Z axis downwards
Thrust force due to wind	Point Load at 7 points	Hub CM downwind	103.51 kN	Y axis downwind
Aerodynamic Torque	Point Load at 7 points	Nacelle CM upwind	225.22 kNm	@ Y axis CCW
Self-weight of frames and cables	Distributed Load	Along frames and cables	Value varies with elements	Z axis downwards

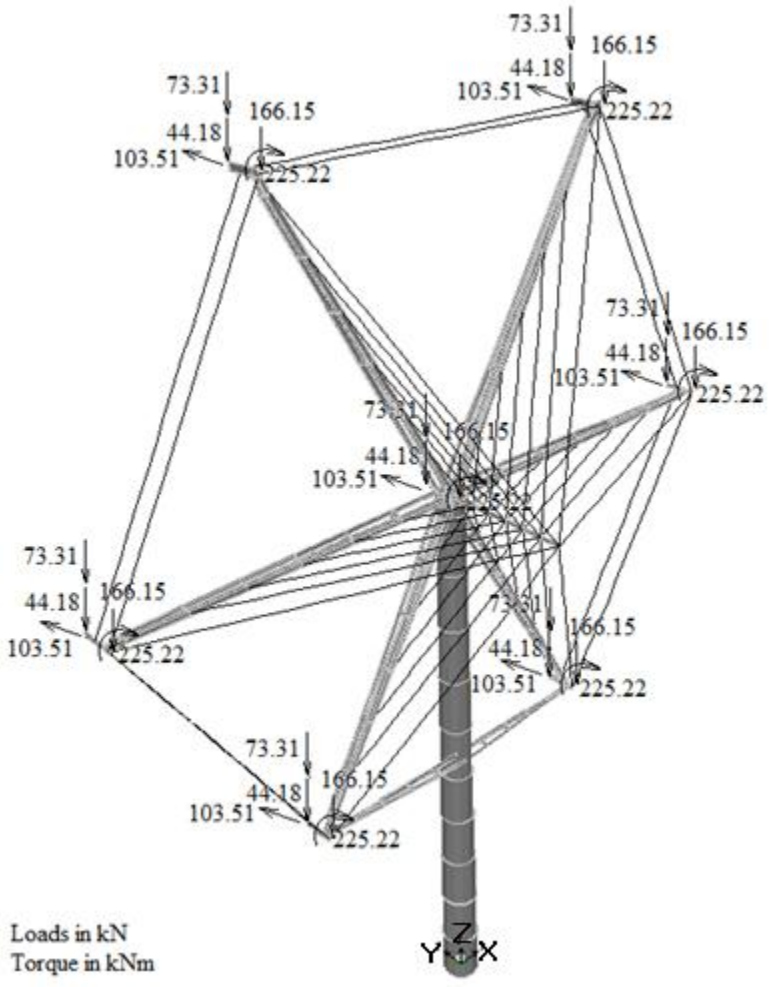

Figure 77. Loads for a Three Rotor Model

Apart from the static load case, the modal and buckling load cases are defined similarly to a single rotor model and the analysis is performed. The design process is iterated to satisfy some design constraints discussed in the next section.

8.5. Model Optimization Methods

The model is optimized subject to the constraints below:

1. The maximum deflection of all nodes of the entire structure should be less than 1 m.
2. All the elements of the support structure should satisfy the stress and buckling criteria i.e. stress ratio < 0.95 and slenderness ratio < 200. This is defined in the SAP2000 Design Code which is AISC-LRFD93.
3. The mass of the support structure should be less than 38,139 kg. This requirement is flexible, however, the cost constraint is more important than mass.
4. The cost of the support structure should be less than $585,131.

The model optimization methods are similar to those discussed in Section 5.8. Although mass and deflection are reduced below the limit, the number of overstressed and buckled members turns out to be high. So to make the structure stiffer, the priority is given to the cost limit instead of the mass limit.

8.6. Model Solutions

The solution obtained for the seven-rotor system is just one of several solutions that could be obtained for designing a support structure subject to the required constraints. The results for the final optimized structure for a configuration of 6 cables of type 1 attached from each spar to the jib are given in Table 46. Figure 78 provides a front and side view of the final design. Similar to Section 5.8., the cost of fabricated steel considered here, is $2600/ton.

Table 46. Seven-rotor Model Results

Design Criterion	Results		
Deflection (downwind side & y-direction)	Rotor 1 (Top left)	1.218 m	
	Rotor 2 (Top right)	1.221 m (maximum)	
	Rotor 3 (Center right)	0.740 m	
	Rotor 4 (Lower right)	0.256 m	
	Rotor 5 (Lower left)	0.244 m	
	Rotor 6 (Center left)	0.723 m	
	Rotor 7 (Center/Tower top)	0.421 m	
Stress	Stress ratio of all components < 0.95		
Buckling	Slenderness ratio of all components < 200		
Mass and cost of the support structure	**Component**	**Mass (kg)**	**Cost ($)**
	Jib	1,516	3,942
	Cable 1	2,656	6,906
	Cable 2	5,125	13,325
	Cable 3	1,700	4,420
	Spars & Lower link	172,541	448,607
	Total	**183,538**	**477,198**

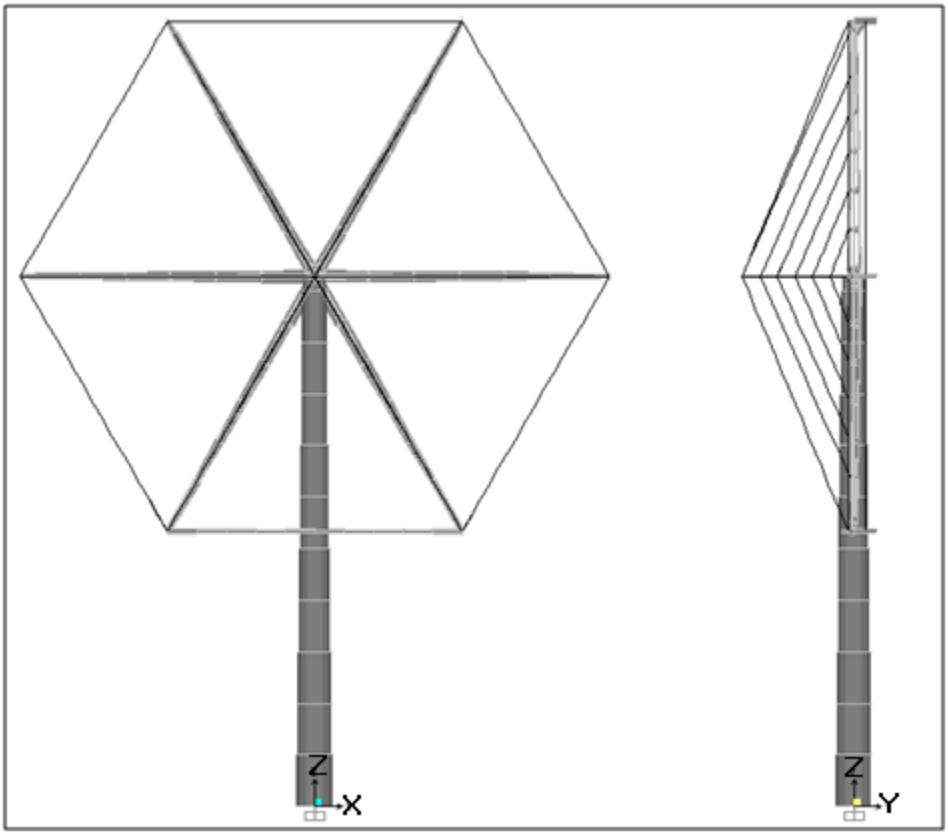

Figure 78. Final Design Solution- Seven-Rotor System

The total mass in Table 47 is greater than the target mass of 38,139 kg. On the other hand, the total cost is less than the target cost of $585,131 and thus our objective is satisfied. Table 47 clearly illustrates the difference in the total mass and total cost of the single-rotor system and the proposed solution of the seven-rotor system.

Table 47. Comparison of the proposed seven-rotor system with the single-rotor system

SYSTEM	Total Mass (kg)	Total Cost ($)
Single-rotor system	601,429	3,809,250
Seven-rotor system without support structure	563,290	3,224,119
Seven-rotor system (proposed solution)	**746,828**	**3,701,317**

Bending stresses at the tower base using the bending moments are calculated by Eq. (8.46).

$$\sigma_b = \frac{M_b y}{I} = \frac{(64918.9\, x\, 10^{-3}) x (\frac{6}{2})}{(\frac{\pi}{32} x (6^4 - 5.9649^4))} = 65.99\, MPa \qquad (8.46)$$

This shows that the stresses are within the limit of the minimum specified yield strength of steel, which is 344 MPa.

8.7. Comparison with the Vestas V47 660 kW Turbine

In order to verify that the accuracy of the baseline scaling relations is within an acceptable limit, the 0.71 MW turbine model is compared with an actual turbine in the industry namely, the Vestas V47 660 kW turbine [26]. Even though the rated power is slightly different, the mass values of the components are expected to be within 10%.

Table 48 initially shows the values of the total mass of the seven-rotor system components and then the values for each rotor is obtained by dividing by 7 except the yaw bearing. Reference [26] only provides two values, the rotor mass and the nacelle mass. Although the rotor mass is on a higher side and nacelle mass is on a lower side, the total mass of the 0.71

MW rotor compares well with the Vestas turbine. Thus, it can be concluded that the baseline scaling relations are reasonably accurate and suitable for analysis.

Table 48. Comparison between 1.67 MW model and the 1.5 MW WindPACT Turbine

BASELINE	**Seven rotor 5 MW**	**Each 0.71 MW turbine of the Seven rotor model**	**Vestas V47 660kW**
Components	**Mass(kg)**	**Mass(kg)**	**Mass(kg)**
Rotor	31,524	4,503	
Hub	49,786	7,112	
Nose Cone	2,524	361	
Total Rotor		**11,976**	**7,200**
Pitch System	13,874	1,982	
Low speed shaft	6,965	995	
Main bearing	1,214	173	
Variable speed electronics	-	-	
Yaw system	**15,752**	**524**	
Brake & coupling	995	142	
Electrical system	-	-	
Hydraulic & Cooling system	400	57	
Nacelle Cover	8,463	1,209	
Gearbox	30,312	4,330	
Generator	19,414	2,774	
Mainframe, Ptfm & Railing	33,261	4,752	
Total Nacelle		**16,938**	**20,400**
TOTAL		**28,914**	**27,600**

CHAPTER 9

CONCLUSION

The three-rotor and seven-rotor models developed in this thesis are an important milestone in the analysis of MRWTs, making use of the baseline scaling model, which was found to be the best fit for the latest empirical data for wind turbines. This study is also a step forward in the scaling analysis and preliminary structural analysis done by Verma [32]. A few concluding remarks are provided below.

1. MRWTs offer several advantages that may or may not be offset by the support structure required to hold the rotors in place. This work however, has shown that it is possible to obtain a MRWT system with a total cost significantly less than that of a single-rotor conventional system. This was true for the three-rotor case but not for the seven-rotor model, as the difference in the latter case was not significant.

2. A method of developing MRWT support structures has been outlined in this thesis. This method is systematic and consistent for both the cases considered – three and seven rotors. Also, it uses support members such as steel frames and cables which are commonly used in the construction industry. This makes the implementation of MRWTs more feasible.

3. Although the total mass of MRWT systems including the support structure exceeds that of the single-rotor system, the total cost of MRWT systems is less. This is of prime advantage for MRWTs to be developed on a commercial scale.

4. The baseline scaling model is a very important tool used to find the parameters of MRWTs. It is validated each time by comparing with similar turbines like the 1.5MW WindPACT and the Vestas V47. The baseline model is accurate since the individual turbines used in the MRWTs compare well with the above two turbines.

5. The rotor is the most important contributor in reduction of cost – 57% for the three-rotor model and 60% for the seven-rotor model, followed by the gearbox, main bearing, pitch system and low speed shaft. The other components cost approximately the same as that in case of a single-rotor model.

6. At all stages of the design, such as the static and the dynamic analysis, the MRWT structural models satisfy the deflection, stress and buckling criteria and hence are acceptable. The model has been analyzed for steady, turbulent and extreme wind conditions. As a future work, a multi-rotor prototype should be tested in a wind tunnel for these criteria and conditions.

7. Drag forces do affect the MRWT structure in terms of design life and can be significant especially at high wind conditions. Therefore, drag should not be neglected.

8. In all the analysis results, the maximum deflection point in the support structure is found to be at the topmost rotor at the downwind side.

9. The yaw system introduced is very fundamental and a detailed design is necessary to complete the analysis. As previously discussed, the purpose of the upper yaw bearing is for supporting the weight of the components and that of the lower yaw bearing is only to guide the lower rotors. This approach is consistent with that followed in [32].

10. A two-bladed case is analyzed by considering its aerodynamic similarity with the three-bladed case i.e. using the optimum tip speed ratio. After comparing a combination of systems, the two-bladed case with the gearbox is found to be the most economical.

11. The three-rotor structure is found to be safe even with the blades pitched out of the wind i.e. with zero thrust and torque loads on the rotor. Also, during assembly, it is appropriate to first have the RNAs fixed to the structure followed by the cables.

12. The modal analysis identifies the critical rotor speeds to be avoided to prevent resonance. Again, these results should be validated by testing.

13. Several design features that will complete this analysis should be considered. For example the cost of welding or bolting frames and the surface finish costs needs to be included. In SAP2000, the cables were directly attached to the frames. The cost of turnbuckles or similar equipment required to attach the cables to the structure also should be used.

14. Although the seven-rotor model has a maximum deflection which is slightly higher than the design value, the rest of the criteria are met. With further design improvements, the deflection can be reduced.

15. Looking at the big picture and comparing the single-rotor and MRWT models, the three-rotor model is the most economical as shown in Table 49. This table could extend further to include different number of rotors when the scaling analysis and the support structure design for each is completed. The flowchart showing the design and analysis steps is shown in Figure 79.

Table 49. Comparison between 1-rotor, 3-rotor and 7-rotor scaling models

BASELINE	1-Rotor 5 MW		3-Rotor 5 MW, 1.67 MW		7-Rotor 5 MW, 0.71	
Components	**Mass(kg)**	**Cost($)**	**Mass(kg)**	**Cost($)**	**Mass(kg)**	**Cost($)**
Rotor	76,843	778,421	46,466	470,696	31,524	319,333
Hub	30,116	127,995	31,817	135,222	49,786	211,593
Nose Cone	1,810	10,085	2,476	13,791	2,524	14,057
Pitch System	14,423	183,551	11,613	147,798	13,874	176,563
Low speed shaft	16,526	115,670	10,147	71,020	6,965	48,750
Main bearing	5,400	95,050	2,334	41,086	1,214	21,358
Variable speed electronics	-	395,000	-	395,000	-	395,000
Yaw system	13,152	113,896	17,098	120,896	17,098	120,896
Brake & coupling	994	9,946	995	9,946	995	9,946
Electrical system	-	200,000	-	200,000	-	200,000
Hydraulic & Cooling	400	60,000	400	60,000	400	60,000
Nacelle Cover	6,154	61,535	6,923	69,234	8,463	84,633
Gearbox	39,688	661,203	34,086	567,876	30,312	504,997
Generator	16,690	324,960	18,178	353,918	19,414	378,002
Mainframe, Ptfm &	31,773	150,748	32,605	154,690	33,261	157,801
Tower	347,460	521,190	347,460	521,190	347,460	521,190
Support Structure	-	-	114,891	298,714	183,538	477,198
TOTAL	**601,429**	**3,809,250**	**677,489**	**3,631,077**	**746,828**	**3,701,317**

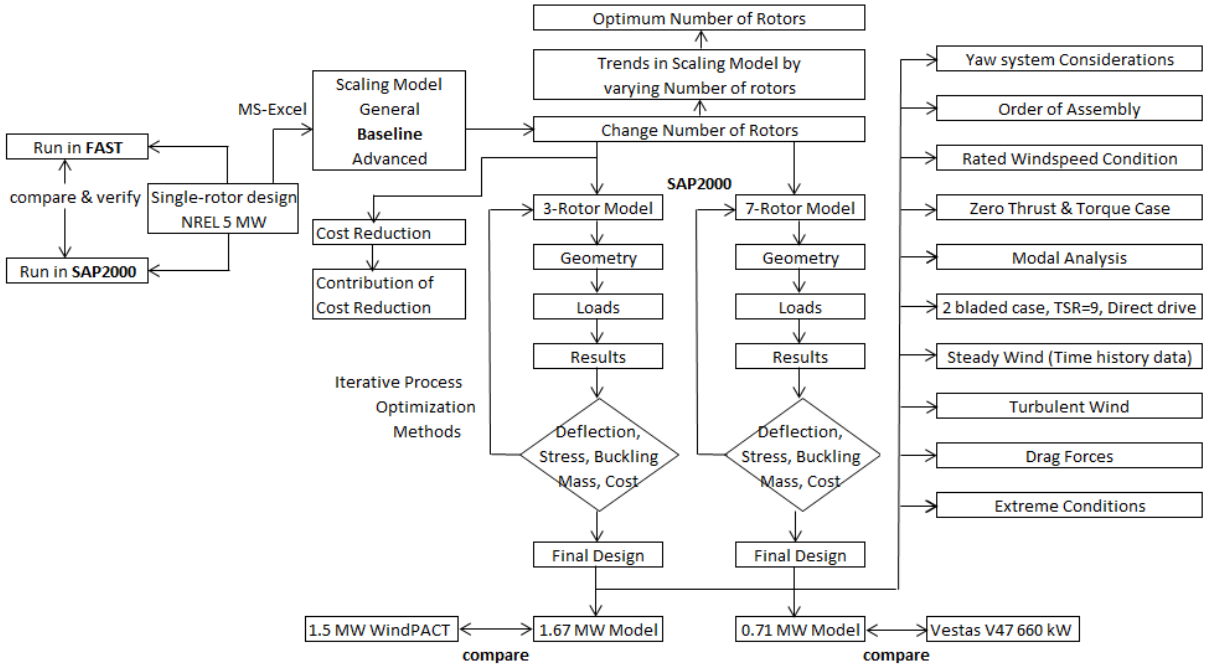

Figure 79. Thesis Flowchart

BIBLIOGRAPHY

[1] Anonymous. *Worldwide electricity production from renewable energy sources: Stats and Figures series: Fourteenth inventory – Edition 2012*, http://www.energies-renouvelables.org/ observ-er/html/inventaire/pdf/14e-inventaire-Chap02.pdf.

[2] Fried L., *Global Wind Energy Statistics 2011- GWEC, http://gwec.net/wp-content/uploads/ 2012/06/GWEC_-_Global_Wind_Statistics_2011.pdf*, February 2012.

[3] Vries E., *Enercon E-126 7.5 MW still world's biggest,* Wind Power Monthly, News Article, August 2012.

[4] Peeringa J., Brood R., Ceyhan O., Engels W., Winkel G., *Upwind 20 MW Wind Turbine Pre-Design, Blade design and control.*

[5] Manwell J.F., McGowan J.G., Rogers A.L., *Wind Energy Explained: Theory, Design and Application (2nd ed.)*, John Wiley & Sons, 2009.

[6] Fingersh L., Hand M., Laxson A., *Wind Turbine Design Cost and Scaling Model*, Technical Report, National Renewable Energy Laboratory, Golden, CO, December 2006

[7] Jonkman J., Butterfield S., Musial W., Scott G., *Definition of a 5-MW Reference Wind Turbine for Offshore Development*, Technical Report, National Renewable Energy Laboratory, Golden, CO, February 2009.

[8] Smulders P.T., Orbons S., Moes C., *Aerodynamic Interaction Between Two Wind Rotors Set Next To Each Other In One Plane*, European Wind Energy Conference, Hamburg, October 1984.

[9] Ransom D., Moore J.J., Heronemus-Pate M., Performance of Wind Turbines in a Closely Spaced Array, *Renewable Energy World Magazine: North America*, May/June 2010, Volume 2:3, pp 32-36.

[10] Jamieson P., Branney M., *Multi-Rotors; A Solution to 20 MW and Beyond?*, Energy Procedia, Vol. 24, 2012, pp 52-59.

[11] Laxson A., *WindPACT Turbine Design Scaling Studies Technical Area 3 – Self Erecting Tower and Nacelle Feasibility*, National Renewable Energy Laboratory (NREL) Subcontract Report, May 2001.

[12] Heronemus W.E., *Vertical Array Wind Turbine*, U.S. Patent Number 6,749,399 B2, June 15, 2004.

[13] Echavarria E., Hahn B., Bussel G.J.W., Tomiyama T., *Reliability of Wind Turbine Technology through time,* Journal of Solar Energy Engineering, Vol.130, August 2008.

[14] Malcolm D.J., Hansen A.C., *WindPACT Turbine Rotor Design Study*, National Renewable Energy Laboratory (NREL) Subcontract Report

[15] Jamieson P., *Innovation in Wind Turbine Design*, First edition, John Wiley & Sons, 2011.

[16] Slew bearing price quote *http://www.seekpart.com/power-transmission/gears/other-gears/slewing+gear+slewing+bearing.html*

[17] Thomas P.H., *Aerogenerator Tower,* U.S. Patent Number 2,511,023, June 13, 1950.

[18] Stoddard W., *The Life and Work of Bill Heronemus, wind engineering pioneer,* Wind Engineering Volume 26, Issue 5, pp 335-341, 2002.

[19] Buhl M.L. Jr., *WT_Perf User's Guide,* National Wind Technology Center, NREL, Golden, CO, December 2004

[20] Nicholson J.C., Arora J.S., "*Design of wind turbine tower and foundation systems: Optimization approach",* Master's Thesis, University of Iowa, 2011.

[21] Wikipedia article, 'Drag coefficient', http://en.wikipedia.org/wiki/Drag_coefficient

[22] Jonkman B.J., *Turbsim User's Guide v1.5,* Technical Report, National Renewable Energy Laboratory, Golden, CO, September 2009

[23] *Structural Cables,* Product Catalogue, Ronstan Tensile Architecture, 2008.

[24] *Steel Data and Fabrication Capabilities,* Steel Driven Construction, Agate Inc., 2011.

[25] International Standard, *IEC 61400-1 Wind Turbines Part 1: Design Requirements,* Third Edition, 2005-08.

[26] *Vestas V47-660 kW with OptiTip and OptiSlip*, Product Document, Vestas Wind Systems A/S Denmark, May 2000.

[27] *SAP2000 Basic Analysis Reference Manual – Linear and Non-linear Static and Dynamic Analysis and Design of Three-Dimensional Structures*, Version 14, Computers & Structures Inc., Berkeley, CA, April 2009.

[28] *CSI Analysis Reference Manual – For SAP2000, ETABS, SAFE and CSiBridge*, Computers & Structures Inc., Berkeley, CA, August 2010.

[29] Jonkman J.M., Buhl M.L. Jr., *FAST User's Guide,* Technical Report, National Renewable Energy Laboratory, Golden, CO, August 2005

[30] Wikipedia article 'I-beam' http://en.wikipedia.org/wiki/I-beam

[31] *Structural Steel: An Industrial Overview,* American Institute for Steel Construction (AISC), September 2012.

[32] Verma P. "*Multi-Rotor Wind Turbine Design & Cost Scaling*", Master's Thesis, University of Massachusetts Amherst, Mechanical Engineering, 2013

[33] *Kaydon Infinite Bearing Solutions*, Slewing Ring Bearings Catalog 390, Kaydon corporation Issue 11, www.kaydonbearings.com

[34] J. V. Nielsen. Danmarks Vindkrafthistoriske Samling (Danish Wind Historical Collection), http://www.vindhistorie.dk/Faktablade/Faktablad_2a.pdf, 2001

[35] Wilcox D.C., *Basic Fluid Mechanics*, Third Edition, 2007.

[36] Fichaux N., Beurskens J., Jensen P. H., Wilkes J., *UpWind: Design limits and solutions for very large wind turbines*, *March 2011*, SUPPORTED BY: The Sixth Framework Programme for Research and Development of the European Commission (FP6)